UNIVERSITI TEKNOLOGI MARA

HYBRID IMAGE ENHANCEMENT WITH MULTI-STAGE DEEPLABV3+ SEGMENTATION FRAMEWORK FOR SCAR DETECTION IN LGE-CMRI IMAGES

NUR ‘ULYA NASUHA BINTI ZAKARIA

MSc

July 2026

UNIVERSITI TEKNOLOGI MARA

HYBRID IMAGE ENHANCEMENT WITH MULTI-STAGE DEEPLABV3+ SEGMENTATION FRAMEWORK FOR SCAR DETECTION IN LGE-CMRI IMAGES

NUR ‘ULYA NASUHA BINTI ZAKARIA

Thesis submitted in fulfilment
of the requirements for the degree of
Master of Science
(Electrical Engineering)

Faculty of Electrical Engineering

July 2026

CONFIRMATION BY PANEL OF EXAMINERS

I certify that a Panel of Examiners has met on 5^{th} June 2026 to conduct the final examination of Nur ‘Ulya Nasuha Binti Zakaria on her Masters of Science thesis entitled “Hybrid Image Enhancement with Multi-Stage DeepLabV3+ Segmentation Framework for Scar Detection in LGE-CMRI Images” in accordance with Universiti Teknologi MARA Act 1976 (Akta 173). The Panel of Examiners recommends that the student be awarded the relevant degree. The Panel of Examiners was as follows:

Zainal Hisham Che Soh, PhD
Associate Professor
Faculty of Electrical Engineering
Universiti Teknologi MARA
(Chairman)

Saiful Zaimy Yahaya, PhD
Senior Lecturer
Faculty of Electrical Engineering
Universiti Teknologi MARA
(Internal Examiner)

Nor Hazlyna Harun, PhD
Senior Lecturer
School of Computing
Universiti Utara Malayia
(External Examiner)

PROFESSOR DR HJH ZURAEDA IBRAHIM
Dean
Institute of Postgraduates Studies
Universiti Teknologi MARA
Date : 9 July 2026

AUTHOR'S DECLARATION

I declare that the work in this thesis was carried out in accordance with the regulations of Universiti Teknologi MARA. It is original and is the results of my own work, unless otherwise indicated or acknowledged as referenced work. This thesis has not been submitted to any other academic institution or non-academic institution for any degree or qualification.

I, hereby, acknowledge that I have been supplied with the Academic Rules and Regulations for Postgraduate, Universiti Teknologi MARA, regulating the conduct of my study and research.

Name of Student	:	Nur 'Ulya Nasuha Binti Zakaria
Student I.D. No.	:	2024674728
Programme	:	Master of Science (Electrical Engineering) – EE750
Faculty	:	Electrical Engineering
Thesis Title	:	Hybrid Image Enhancement with Multi-Stage DeepLabV3+ Segmentation Framework for Scar Detection in LGE-CMRI Images
Signature of Student	:	……………………………………………..
Date	:	July 2026

ABSTRACT

Accurate myocardial scar segmentation from Late Gadolinium-Enhanced Cardiac Magnetic Resonance Imaging (LGE-CMRI) is essential for the assessment of myocardial infarction and treatment planning; however, it remains a challenging task due to low contrast between tissues, intensity inhomogeneity, blurry images, variation cardiac anatomy and size and complexity of scar regions. To address these limitations, this study proposed a comprehensive framework for automated myocardial structure and scar segmentation, beginning with the acquisition of LGE-CMRI datasets under approved ethical approval to ensure compliance with patient confidentiality and research governance requirements. Following data collection, image pre-processing was conducted, consisting of image augmentation and image labelling, where augmentation strategies were applied to increase dataset variability and improve model robustness, while precise manual labelling established reliable ground truth masks for the left ventricle, cavity, myocardium, and scar regions. After pre-processing, the images underwent image enhancement, incorporating both contrast improvement and image sharpening to increase visibility of subtle myocardial tissues and enhance structural boundaries without compromising anatomical integrity. Building upon this stage, a new Hybrid Contrast Enhancement–Image Sharpening (Hybrid CE-IS) approach was implemented to further refine intensity transitions and structural clarity, thereby generating more discriminative features for segmentation. The enhanced images were subsequently processed using a multi-stage DeepLabV3+ segmentation framework, where the first stage captured the anatomical structures of the left ventricle and cavity, the second stage refined myocardial tissue representation, and the third stage focused on precise delineation of small and irregular scar regions. To maximize segmentation effectiveness, a proposed Hybrid Image Enhancement–Image Segmentation (Hybrid IE-IS) strategy integrated the outputs of the Hybrid CE-IS with the multi-stage segmentation architecture, enabling improved feature extraction and spatial consistency across all myocardial structures. Performance evaluation demonstrated that the hybrid IE-IS framework achieved mean Dice Similarity Coefficient values of 98.22% for the left ventricle, 97.78% for the cavity, 85.15% for the myocardium, and 70.88% for myocardial scar, with corresponding Intersection over Union values of 91.67%, 93.75%, 75.68%, and 62.37%, and mean accuracy values of 96.57%, 95.85%, 83.54%, and 65.21%, respectively. In comparison, the multi-stage framework without hybrid enhancement achieved mean Dice values of 96.98%, 95.48%, 83.32%, and 68.49% for the respective regions, indicating that the hybrid enhancement contributed improvements of approximately 1–3% across all targets. These findings confirm that integrating structured data augmentation, hybrid image enhancement, and a progressive multi-stage segmentation strategy effectively improves feature representation and segmentation reliability, offering a robust and clinically applicable approach for automated myocardial scar analysis and decision support in cardiac assessment.

ACKNOWLEDGEMENT

Alhamdulillah, Subhanallah, Allahuakbar.

First and foremost, I wish to thank Allah the Merciful and the All-Knowing for granting me the strength and perseverance to successfully complete this long and challenging MSc journey. Without His guidance and blessings, this work would not have been possible.

My deepest gratitude sincerely to my supervisor, Assoc. Prof. Dr Muhammad Khusairi Osman, and co-supervisor Prof. Ir. Ts. Dr. Hjh Siti Noraini Sulaiman and Prof. Ir. Dr. Nor Ashidi Mat Isa and Dr. Dayang Suhaida Awang Damit for the continuous guidance, invaluable advice, and constructive feedback provided throughout this research. Their expertise, encouragement, and support were instrumental in shaping the direction of this study and ensuring the successful completion of this thesis.

I also wish to extend my appreciation to Advance Medical and Dentist Institute (AMDI) for providing the facilities, knowledge and LGE-CMRI datasets used in this study. The availability of these data was essential for conducting experimental evaluations and validating the proposed image enhancement and multi-stage deep learning segmentation framework.

I am deeply grateful to my parents, Zakaria Hussain and as well as my family members, Azri Nasli, Khairun Nida Zakaria, Muhammad Ayman Danieyal Zakaria, Muhammad Emran Zikrey Zakaria, and my adoring niece, Aisyah Sofiyah Azri, for their unwavering support, patience, prayers and for being my constant source of motivation throughout my academic journey. Their love and sacrifices have been the foundation of every achievement I have accomplished. A special note of appreciation goes to my fiancé, Ahmad Habiburrahman Marzuqi, and his family for their prayers and encouragement. I am especially thankful to my fiancé for his presence during this meaningful chapter of my life and for sharing in the joy of reaching this milestone.

Finally, I would like to thank my friends and colleagues, Advanced Control System and Computing Research Group (ACSCRG), for their support, helpful discussions, and encouragement throughout the research process. And not to forget my side-by-side master partner Nur Najiha Kamarulzaman for always helping and cheering throughout this process of completing this journey. Their assistance and companionship contributed significantly to the successful completion of this thesis.

TABLE OF CONTENTS

LIST OF TABLES

LIST OF FIGURES

LIST OF ABBREVIATIONS

Abbreviations

ACDC	Automated Cardiac Diagnosis Challenge
AI	Artificial Intelligence
AMDI	Advance Medical and Dentist Institute
CAD	Coronary Artery Disease
CADs	Computer Aided Diagnosis
CLAHE	Contrast Limited Adaptive Histogram Equalization
CMR	Cardiac Magnetic Resonance
CNN	Convolutional Neural Network
CRMS	Contrast Root Mean Square
CT	Computed Tomography
CVD	Cardiovascular Disease
DL	Deep Learning
DSC	Dice Similarity Coefficient
ECG	Electrocardiography
EMIDEC	Automatic Evaluation of Myocardial Infarction from Delayed-Enhancement Cardiac MRI
FCN	Fully Connected Network
FN	False Negative
FP	False Positive

HE	Histogram Equalization
ICD	Implantable Cardioverter Defibrillator
IoU	Intersection over Union
LGE	Late Gadolinium Enhancement
LV	Left Ventricle
M&M	Multi-Centre, Multi-Vendor & Multi-Disease Cardiac Image Segmentation Challenge
MI	Myocardial Infraction
MICCAI	Medical Image Computing and Computer Assisted Intervention
ML	Machine Learning
MRI	Magnetic Resonance Imaging
MSE	Mean Squared Error
MSE	Mean Absolute Error
PET	Positron Emission Tomography
PSIR	Phase-Sensitive Inversion Recovery
PSNR	Peak Signal-to-Noise Ratio
ROI	Region of Interest
SPECT	Single-Photon Emission Computed Tomography
SSIM	Structural Similarity Index Measure
TN	True Negative
TP	True Positive

CHAPTER 1
INTRODUCTION

1.1 Research Background

Cardiovascular diseases (CVDs) remain the foremost cause of death worldwide, and myocardial infarction (MI), commonly known as a heart attack, was one of the most prevalent and life-threatening manifestations (Abbas et al., 2024; Jafari et al., 2022; Organization., 2021; Qi et al., 2024). When an MI occurs, the restriction of blood supply causes ischemia, which in turn results in necrosis of myocardial tissue. Over time, this damaged tissue heals as fibrotic scar tissue, leading to alterations in both the structural and electrical properties of the heart (Z. Chen et al., 2022; Sahu & Ray, 2022). These changes are clinically significant because myocardial scars not only compromise cardiac function but also create a substrate for arrhythmias and increase the risk of sudden cardiac death (D. Chen et al., 2022; Jafari et al., 2022). Hence, accurately detecting and characterizing myocardial scar tissue was critical for guiding treatment decisions, risk stratification, and long-term patient management (Ding et al., 2023; Rayed et al., 2024).

Traditionally, several imaging modalities such as electrocardiography (ECG), echocardiography, and computed tomography (CT) have been employed in the diagnosis and assessment of myocardial health (Avard et al., 2022; Chen et al., 2020; Zafar et al., 2023). While ECG provides functional information and echocardiography offers real-time imaging at low cost, both lack the sensitivity required for detailed visualization of scar tissue (Wallis et al., 2012). CT can provide anatomical insights, but its limited tissue contrast and radiation exposure reduce its suitability for repeated assessments (El-Taraboulsi et al., 2023; Jafari et al., 2022; Pradeep Kundur et al., 2025). In contrast, Late Gadolinium Enhancement Cardiac Magnetic Resonance Imaging (LGE-CMRI) has emerged as the gold standard due to its high spatial resolution and excellent soft tissue contrast, which enable clinicians to distinguish between healthy, ischemic, and scarred myocardium (Chen et al., 2023; Hasny et al., 2024; Schulz-Menger et al., 2020). Manual segmentation of scar regions is labour-intensive, subjective, and prone to inter-observer variability, particularly when scar borders are subtle or when image quality was degraded by noise and acquisition artifacts (Sinha et al., 2020).

Image enhancement and advanced computational methods play a critical role. LGE-CMRI scans are inherently susceptible to blurry, low contrast, and variability in acquisition settings, which can obscure fine structural details (Lepcha et al., 2022; Qiu et al., 2022). Image enhancement techniques help to overcome low-contrast and blurry image to highlight relevant features, thereby improving the visibility of cardiac structures (Bansal & Singh, 2020; Jiang et al., 2024). Clinicians also require precise segmentation of scarred tissue to quantify infarct size and assess the extent of damage. Conventional segmentation methods, such as thresholding or region growing, shows that complex cardiac images where scar tissue intensity overlaps with that of surrounding myocardium or blood pools was hard to segment (Hasny et al., 2024; Wu et al., 2021). Therefore, the need for more robust, intelligent approaches that can reliably handle variability across patients and imaging conditions.

Recent advances in deep learning, particularly convolutional neural networks (CNNs), have transformed the field of medical image analysis (Liu et al., 2021). These models can automatically learn hierarchical features from raw images, outperforming traditional handcrafted approaches in both classification and segmentation tasks (Sinha et al., 2020; Wu et al., 2021). Architectures such as DeepLabV3+ have proven effective in semantic segmentation by capturing both global contextual information and fine structural details (Liu et al., 2021). DeepLabV3+ was selected in this study because its encoder-decoder architecture, combined with Atrous Spatial Pyramid Pooling (ASPP), enables the extraction of multi-scale features while preserving object boundaries. This capability is particularly suitable for LGE-CMRI images, where myocardial scars exhibit irregular shapes, varying sizes, and low contrast with surrounding tissues. In cardiac imaging, deep learning has been increasingly applied for tasks such as chamber segmentation, functional assessment, and scar quantification. This drawback limits the performance of segmentation models, especially when dealing with noisy or low-contrast CMRI images (Hong & Zhang, 2023; Lepcha et al., 2022).

The research presented in this thesis directly addresses these challenges by proposing a multi-stage deep learning framework that integrates both image enhancement and segmentation for myocardial scar detection. In the first stage, image enhancement technique was employed to improve the clarity, contrast, and overall quality of LGE-CMRI, ensuring that subtle scar features are preserved and amplified.

In the second stage, a DeepLabV3+ segmentation model with a multi-stage refinement mechanism was developed to accurately delineate scarred regions. Unlike conventional pipelines, this dual-stage approach ensures that the segmentation model operates on optimized inputs, thereby reducing errors and improving accuracy. To validate the framework, both quantitative metrics such as Dice Similarity Coefficient (DSC), Peak Signal-to-Noise Ratio (PSNR), Structural Similarity Index Measure (SSIM), Mean Square Error (MSE) and accuracy, and qualitative evaluations through expert clinical review are employed, ensuring that the outcomes are not only statistically reliable but also clinically meaningful (Sharma & Kamra, 2023).

Ultimately, this study aims to bridge the gap between advanced image analysis research and clinical practice. By proposing the image enhancement and image segmentation of myocardial scars in LGE-CMRI, the proposed framework has the potential to reduce manual workload, minimize observer variability, and improve diagnostic consistency (Gautam et al., 2022). More importantly, it hopefully can support timely and precise clinical decisions, leading to better patient outcomes in myocardial infarction management. In this way, the research contributes not only to the field of medical image analysis but also to the broader objective of enhancing healthcare delivery through artificial intelligence.

1.2 Problem Statement

Early detection of myocardial infarction is crucial for reducing mortality, guiding appropriate treatment strategies, and improving long-term patient outcomes (Shaaf et al., 2023). Myocardial infarction results in irreversible damage to cardiac muscle tissue, leading to the formation of myocardial scars that impair cardiac function and increase the risk of heart failure and arrhythmia (Prabhakararao & Dandapat, 2020). Accurate detection and delineation of these scar regions are therefore essential for diagnosis, risk stratification, and treatment planning. LGE-CMRI has become the clinical reference standard for non-invasive myocardial scar assessment due to its ability to differentiate infarcted tissue from healthy myocardium (Wu et al., 2021). Despite its clinical importance, reliable analysis of myocardial scars from LGE-CMRI remains challenging and continues to rely heavily on manual interpretation by clinicians. This process was time-consuming, subjective, and prone to inter-observer variability, limiting its practicality in routine clinical settings (Sheikhjafari et al., 2023; G. Wang et al., 2023). One of the key difficulties lies in the inherently low contrast between scarred and healthy myocardial tissue, particularly in cases involving small, diffuse, or partially healed infarcts (Hasny et al., 2024). Although contrast agents enhance scar visibility, intensity differences are often subtle and inconsistent, making accurate delineation difficult even for experienced observers.

In addition, LGE-CMRI images are frequently affected by blurry appearance and low contrast image quality (Lepcha et al., 2022; Qiu et al., 2022), which may result from cardiac motion, breath-hold limitations, or spatial resolution constraints (Xing et al., 2023). These factors obscure fine myocardial details and weaken boundary definition, complicating the visual interpretation of scar regions. The problem is further aggravated by intensity inhomogeneity, where variations in signal intensity occur across the image due to -BI field inhomogeneity, surface coil sensitivity, or patient-specific factors. Such non-uniform intensity distribution causes similar tissues to appear differently, leading to fragmented or inaccurate scar representation.

Another significant challenge arises from inter-patient variability in cardiac anatomy, including differences in ventricular shape, myocardial thickness, and heart size (Rayed et al., 2024). These anatomical variations limit the generalisation capability of automated methods and often result in inconsistent segmentation performance across datasets (L. Wang et al., 2023). Furthermore, myocardial scar regions exhibit complex texture patterns, characterised by heterogeneous intensity, irregular shapes, and similarity to surrounding structures such as normal myocardium or papillary muscles (Almajmaie et al., 2022; Zhang et al., 2024). These characteristics increase the likelihood of misclassification and false detection, particularly when conventional or single-stage segmentation approaches are applied.

While deep learning has demonstrated strong potential in medical image analysis, many existing CMRI studies employ single-stage segmentation models that attempt to extract all structures simultaneously (Chen et al., 2023; S. Wang et al., 2023; Xing et al., 2023). Such approaches often struggle to cope with the combined challenges of low contrast, poor image quality, intensity inhomogeneity, anatomical variability, and complex cardiac textures (Fahmy et al., 2021; Rayed et al., 2024; Yu et al., 2022). Consequently, segmentation results may exhibit incomplete scar extraction, anatomically inconsistent boundaries, and reduced sensitivity to subtle infarct regions.

In brief, LGE-CMRI suffer low contrast, motion blurriness, intensity inhomogeneity and anatomical variability causing existing single-stage segmentation model to produce inaccurate and inconsistent scar boundaries (Jacobson et al., 2026). These limitations often lead to incomplete scar extraction, misclassification of nearby tissues and poor detection of subtle infarcts. Therefore, there is a need for a more robust method that can improve image quality and enhance segmentation reliability. It is expected that combining image enhancement with a multi-stage deep learning framework will improve performance and produce more anatomically consistent myocardial scar segmentation (Shi, 2025).

1.3 Research Objectives

The main aim of this study was to automate the enhancement and segmentation of scar from LGE-CMRI images using deep-learning approach. To achieve this aim, several specifics objectives are derived as follows:

a) To enhance CMRI images using proposed Hybrid Contrast Enhancement–Image Sharpening to improve the image quality and accuracy of image.
b) To develop a deep learning-based model with a multi-stage segmentation approach for accurate scar segmentation in CMRI images.
c) To evaluate the performance of the enhancement and segmentation model using qualitative and quantitative method.

1.4 Research Scope and Limitation

This research was subject to the following scope:

a) Focus on CMRI (LGE-CMR) Imaging

The scope of this research is confined to Late Gadolinium-Enhanced Cardiac Magnetic Resonance (LGE-CMR) images, which represent the gold standard for myocardial scar detection. The dataset was collected from Advance Medical and Dentist Institution (AMDI), Universiti Sains Malaysia (USM), covering the period 2020–2023. It includes 26 patients aged 18 years and above, with representation from both genders and with varying cardiac conditions, ranging from normal myocardium to scarred myocardium. This targeted scope ensures that the study remains clinically relevant and that the developed framework was tested on real-world medical data.

b) Deep Learning Model Selection

The study employs DeepLabV3+, a state-of-the-art semantic segmentation model, known for its effectiveness in capturing complex boundaries and structures in medical imaging. The model was adapted into a multi-stage pipeline, where enhancement and sharpening methods are integrated before segmentation to boost accuracy. This ensures methodological novelty while keeping the focus within a well-established deep learning architecture.

c) Platform for Development

All model development and implementation are carried out using MATLAB with the Deep Learning Toolbox, selected for its powerful medical image processing capabilities, integration with visualization tools, and ease of handling medical imaging datasets. The platform also provides reproducibility and reliability for academic research, making it an ideal choice for this study.

d) Performance Evaluation

The performance of both enhancement and segmentation models was evaluated using quantitative and qualitative measures. Quantitative metrics include Peak Signal-to-Noise Ratio (PSNR), Mean Squared Error (MSE), and Structural Similarity Index Measure (SSIM) for enhancement, as well as Dice Similarity Coefficient (DSC), for segmentation. In addition, qualitative validation of visual result was to ensure the outputs are consistent with clinical interpretations.

This research was subject to the following limitation:

a) Dataset Limitations

The dataset was limited in both size and diversity since it was based on AMDI USM available images and limited expert annotations. Real-world patient populations often involve a wider range of imaging conditions, scanner types, and disease variations. Therefore, the model may not fully generalize to all clinical scenarios.

b) Dependence on Expert Annotations

The segmentation model requires reliable ground-truth annotations for training and validation. Since manual labelling by cardiologists was time-consuming and resource-intensive, only a limited number of images can be annotated with precision. While augmentation strategies are applied to expand training data, they cannot fully replace diverse real-world annotations.

c) Computational and Resource Constraints

Training deep learning models such as DeepLabV3+ demands high computational resources, including GPUs with sufficient processing and memory capacity. While MATLAB provides a user-friendly environment, large-scale training may still face time and memory bottlenecks. This limits the model's scalability, particularly in clinical settings with restricted resources.

1.5 Significance of Study

This study holds significant importance in both academic research and clinical practice. By integrating image enhancement with a multi-stage segmentation framework using DeepLabV3+, the research demonstrates a novel approach to addressing the long-standing challenge of accurately detecting myocardial scar tissue in CMRI images. Manual interpretation of CMRI was often time-consuming and prone to inter-observer variability, which can lead to inconsistent diagnostic outcomes (G. Wang et al., 2023). The automated framework proposed in this study provides a more objective, reproducible, and consistent method of scar detection, thereby reducing dependency on subjective clinical judgment (Sheikhjafari et al., 2023).

Clinically, the accurate detection and quantification of myocardial scarring are essential for risk stratification, treatment planning, and prognosis in patients with myocardial infarction. Enhanced image clarity combined with precise segmentation ensures that scar regions are identified more reliably, enabling cardiologists to make informed decisions regarding interventions such as revascularization or implantable devices. This directly contributes to the goal of personalized medicine, where treatments are tailored to the unique cardiac profile of each patient.

From a research perspective, this study also contributes to the broader field of medical image processing by exploring the dual use of enhancement and segmentation in a unified pipeline. This approach addresses challenges of poor contrast, noise, and boundary ambiguity in MRI while pushing the application of deep learning toward more clinically relevant outcomes (Hong & Zhang, 2023). Finally, although currently evaluated in an offline setting, the framework establishes a strong foundation for future clinical integration into computer-aided diagnostic (CADs) systems, offering the potential to support cardiologists in real-time decision-making and improving efficiency in hospital imaging workflows (Sharma & Kamra, 2023).

1.6 Thesis Outline

This thesis is organized into five chapters. Chapter 1 introduces the research by presenting the background of the study, the problem statement, objectives, scope and limitations, and significance of the work. It establishes the foundation and highlights the importance of developing a deep learning-based framework for myocardial scar detection using LGE-CMRI images (Hong & Zhang, 2023).

Chapter 2 provides a comprehensive literature review on myocardial health issues, diagnostic modalities, and the role of imaging in myocardial scar detection. It critically discusses existing diagnostic techniques such as ECG, ultrasound, CT scan, and LGE-MRI, with emphasis on MRI as the gold standard (Zafar et al., 2023). The chapter also examines image processing methods, including enhancement, sharpening, filtering, and denoising, as well as segmentation approaches ranging from classical methods to deep learning. The review concludes by identifying existing research gaps that motivate the proposed study.

Chapter 3 describes the methodology adopted in this research. It outlines the research design, data collection process, and ethical considerations. This chapter explains preprocessing steps such as resizing, augmentation, and labelling, followed by detailed descriptions of enhancement and sharpening strategies. The proposed multi-stage segmentation framework using DeepLabV3+ was then presented, along with the evaluation metrics for both enhancement and segmentation, incorporating both quantitative and qualitative assessments.

Chapter 4 presents and discusses the experimental results. It begins with quantitative findings for enhancement, sharpening, and segmentation, followed by qualitative assessments of image quality and segmentation outcomes. Comparative analyses between single-stage and multi-stage approaches, as well as evaluations with and without enhancement, are provided. Expert validation was also included to ensure clinical reliability (Xing et al., 2023).

Finally, Chapter 5 concludes the study by summarizing the major findings, highlighting the contributions of the research, and discussing its implications for future medical imaging applications. Recommendations for further improvements and directions for future research are also proposed to advance the field of automated myocardial scar detection.

CHAPTER 2
LITERATURE REVIEW

2.1 Introduction

Cardiovascular diseases (CVDs) remain the leading cause of mortality worldwide, accounting for approximately 17.9 million deaths annually, representing 32% of all global deaths (Malaysia, 2023; Organization., 2021; Prabhakararao & Dandapat, 2020; Shaaf et al., 2023). Among cardiovascular conditions, myocardial infarction (MI), commonly known as heart attack, stands as one of the most critical and life-threatening events. Myocardial infarction occurs when blood flow to a portion of the heart muscle is blocked, typically by a blood clot in a coronary artery as shown in Figure 2.1, leading to tissue damage and the formation of myocardial scar tissue (Rajput et al., 2023). The extent and location of this scar tissue are crucial determinants of patient prognosis, risk of arrhythmias, heart failure development, and overall survival rates (Prabhakararao & Dandapat, 2020). The global burden of cardiovascular disease has been steadily increasing, driven by aging populations, urbanization, and the rising prevalence of risk factors such as hypertension, diabetes, obesity, and sedentary lifestyles (Abbas et al., 2024; Mustafa et al., 2022). Early and accurate detection of myocardial scar tissue was therefore not merely an academic exercise but a clinical imperative with profound implications for patient management, risk stratification, and therapeutic decision-making (Sahu & Ray, 2022; Xiong et al., 2022).

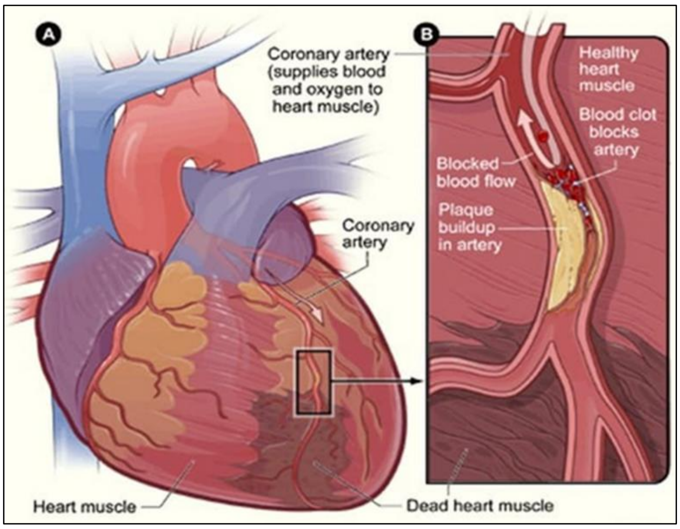

Figure 2.1 Example of Myocardial Blockage Causing Tissue Damage (National Heart & Blood)

The importance of early and accurate myocardial scar detection cannot be overstated in contemporary cardiology practice. Precise identification and quantification of scar tissue enable clinicians to stratify patients according to their risk of adverse cardiac events, guide decisions regarding implantable cardioverter-defibrillator (ICD) placement for primary prevention of sudden cardiac death, optimize medical therapy, and plan revascularization strategies (Karim et al., 2016) . Traditional clinical markers such as electrocardiography and biomarkers like troponin provide limited information about scar location, extent, and transmurally. Therefore, advanced imaging techniques that can directly visualize and quantify myocardial scar tissue have become indispensable tools in modern cardiovascular medicine (J. Zhang et al., 2023).

Medical imaging has revolutionized the diagnosis and management of cardiovascular diseases over the past several decades. Multiple imaging modalities are available for cardiac assessment, each with distinct advantages and limitations. Nuclear imaging techniques such as SPECT and PET offer functional information about myocardial perfusion and viability but have limited spatial resolution and involve radiation exposure (Avard et al., 2022; Liu et al., 2021). CT provides excellent anatomical detail of coronary arteries but has limited soft tissue contrast for myocardial tissue characterization (Smith et al., 2021). CMRI has emerged as the gold standard for myocardial scar detection and quantification due to its superior soft tissue contrast, high spatial resolution, absence of ionizing radiation, and ability to provide comprehensive anatomical and functional information in a single examination (Schulz-Menger et al., 2020).

The advent of deep learning has created a transformative era in medical imaging, offering great capabilities for automated image analysis, pattern recognition, and clinical decision support (Abbas et al., 2024). Deep learning, a subset of machine learning based on artificial neural networks with multiple layers, has demonstrated remarkable success in various computer vision tasks, including image classification, object detection, and semantic segmentation (Curiale et al., 2017; Liu et al., 2021; Zafar et al., 2023). In medical imaging, deep learning algorithms have achieved expert-level or even superhuman performance in several applications, such as diabetic retinopathy detection from fundus photographs, lung nodule detection in chest CT, and brain tumour segmentation from MRI (Chen et al., 2023). The key advantages of deep learning include the ability to automatically learn hierarchical feature representations from raw data without manual feature engineering, handle high-dimensional and complex data, and generalize to new cases when properly trained on diverse datasets (Almajmaie et al., 2022; Liu et al., 2021).

2.2 Traditional Cardiac Imaging Modalities

Traditional cardiac imaging modalities have played a foundational role in the diagnosis, assessment, and management of cardiovascular diseases for several decades. These techniques are routinely used in clinical practice to evaluate cardiac electrical activity, structural integrity, functional performance, and vascular conditions. Prior to the widespread adoption of advanced tissue-characterization imaging, clinicians relied heavily on indirect indicators of myocardial injury obtained from ECG, chest X-ray, echocardiography, and CT as shown in Fig 2.2. Li et al. reported that these modalities remain indispensable for early screening and acute clinical decision-making due to their availability, low cost, and rapid acquisition time (Li et al., 2024; Sahu & Ray, 2022). However, the same study highlighted that traditional imaging techniques are limited in their ability to directly visualize myocardial tissue composition, particularly in distinguishing viable myocardium from infarcted or fibrotic regions.

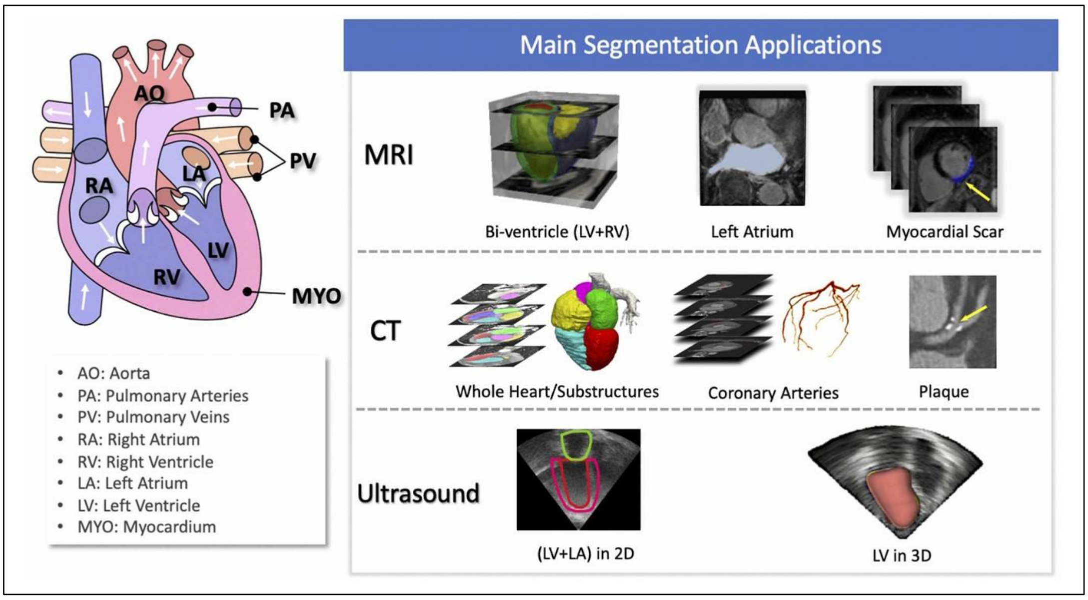

Figure 2.2 Example of Myocardial Infarctions Modalities Application (Chen et al., 2020)

Recent literature has increasingly emphasized that myocardial infarction is a complex pathological condition involving heterogeneous tissue remodelling rather than a purely functional abnormality. Furthermore, Mandoli et al. (Mandoli et al., 2021) showed that variability in operator expertise, image acquisition protocols, and patient-specific factors contributes to inconsistent interpretation across institutions. These limitations have prompted growing interest in advanced imaging approaches capable of providing more precise and reproducible myocardial tissue characterization.

2.2.1 Electrocardiography

Electrocardiography (ECG) is one of the most commonly used diagnostic tools for initial cardiac assessment due to its non-invasive nature, low cost, and rapid acquisition (Sahu & Ray, 2022; Zafar et al., 2023). It records the electrical activity of the heart generated during myocardial depolarization and repolarization using electrodes placed on the body surface. A standard 12-lead ECG provides multiple electrical views of the heart, allowing clinicians to evaluate cardiac rhythm, conduction abnormalities, and ischemic changes (Kolandaivelu et al., 2024). Figure 2.3 show the example of using ECG for detecting myocardial infarction according to the wave changes.

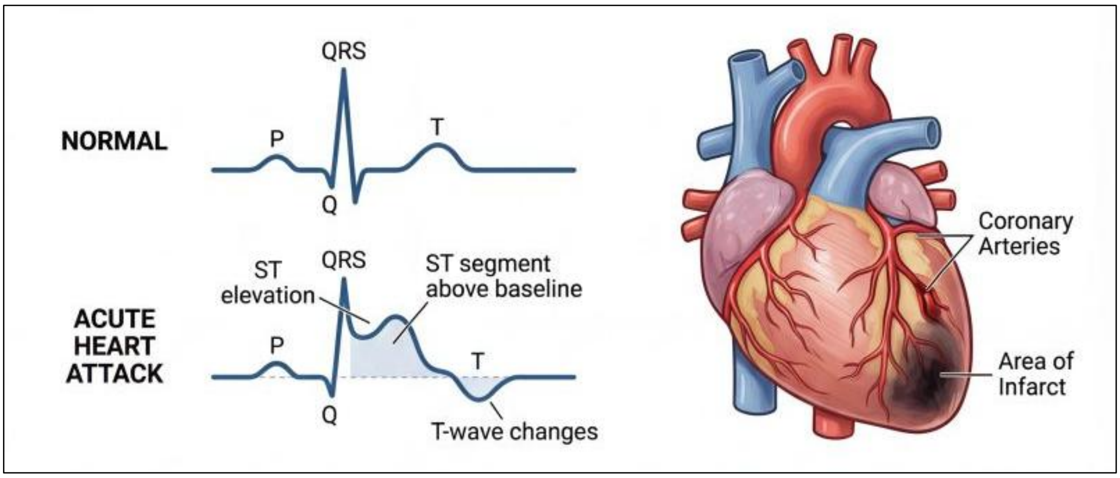

Figure 2.3 Example of ECG Pattern of Acute Myocardial Infarction (Brouki)

In MI, ECG plays a crucial role in early detection, particularly in acute settings. Changes such as ST-segment elevation or depression, T-wave inversion, and abnormal Q waves are commonly used indicators of myocardial ischemia or infarction (Safdar et al., 2024). Early ECG-based diagnosis enables timely clinical intervention and has been shown to improve patient outcomes in acute MI (Jian et al., 2021). However, ECG findings mainly reflect electrical disturbances rather than direct tissue damage.

Despite its clinical value, ECG has important limitations in myocardial scar assessment. Chronic or small scar regions may not produce distinct ECG changes, especially when the scars are diffuse or located in electrically silent regions of the myocardium. Furthermore, ECG lacks the ability to provide precise spatial localization, volumetric measurement, or tissue characterization of myocardial damage. Studies have reported limited correlation between ECG abnormalities and infarct size or scar extent measured using advanced imaging techniques.

Recent studies have explored the use of machine learning and deep learning to enhance ECG interpretation, however, these approaches remain indirect and do not offer anatomical visualization of myocardial scars (Jian et al., 2021). As a result, ECG is increasingly regarded as a complementary screening tool rather than a definitive modality for myocardial scar evaluation. These limitations highlight the need for advanced imaging techniques, such as cardiac magnetic resonance imaging, which provide direct visualization and quantitative assessment of myocardial scar tissue.

2.2.2 Echocardiography

Echocardiography is a non-invasive imaging modality that uses high-frequency ultrasound waves to generate real-time images of the heart (Chen et al., 2020). By transmitting ultrasound pulses and receiving their echoes from cardiac structures, echocardiography enables dynamic visualization of myocardial motion, chamber dimensions, valve function, and blood flow patterns (Jafari et al., 2022). In patients with myocardial infarction, echocardiography is extensively used to evaluate left ventricular systolic and diastolic function, regional wall motion abnormalities, and post-infarction mechanical complications, which collectively indicate impaired myocardial contractility resulting from ischemic or infarcted tissue (Mandoli et al., 2021). Figure 2.4 shows the example of echocardiography that shows a present of myocardial infraction. Due to its portability, real-time imaging capability, and absence of ionizing radiation, echocardiography is often the first-line imaging modality in both acute and chronic cardiac care.

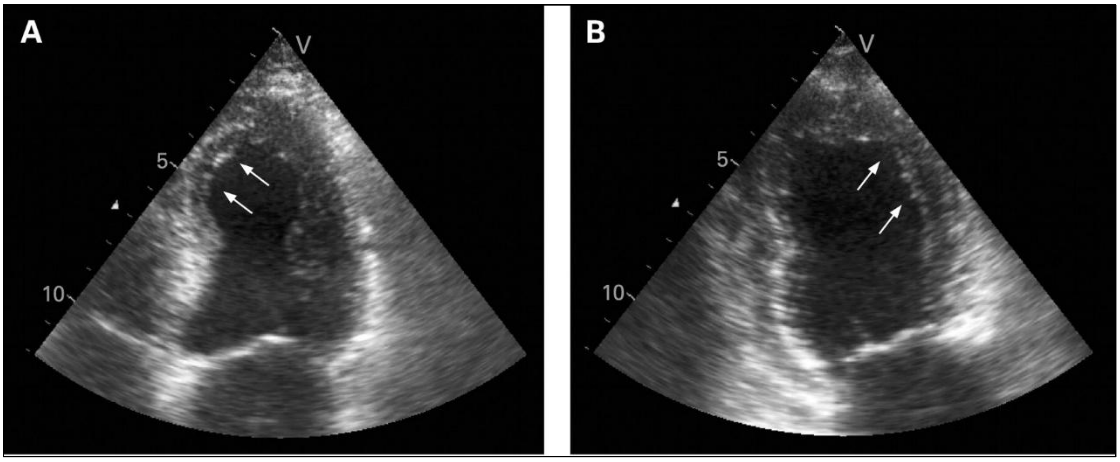

Figure 2.4 Example of Echocardiography Showing Myocardial Infarction (Michaelis et al., 2020)

Echocardiography is highly sensitive in detecting the functional consequences of myocardial infarction and plays a crucial role in post-infarction risk stratification (Mandoli et al., 2021; Prastaro et al., 2017). Despite these advantages, echocardiography assesses myocardial function rather than tissue composition. Degerli et al. showed that wall motion abnormalities may persist even after myocardial recovery or may be absent in small or subendocardial infarcts, leading to misinterpretation of infarct severity (Degerli et al., 2021; Wu et al., 2021). Advanced techniques such as speckle-tracking and strain imaging have been introduced to improve sensitivity, yet these approaches still provide indirect markers of myocardial injury.

2.2.3 Computed Tomography

Cardiac computed tomography, particularly coronary CT angiography (CCTA), has become an important non-invasive modality for evaluating coronary artery disease (Gautam et al., 2022). CT imaging uses X-ray beams and advanced reconstruction algorithms to produce high-resolution three-dimensional images of the heart and coronary vasculature. In clinical practice, CCTA is widely used to assess coronary stenosis, plaque morphology, and calcium burden, making it valuable for ruling out obstructive coronary artery disease in patients with chest pain (Z. Chen et al., 2022).

Recent advances in CT technology, including improved temporal resolution and dual-energy CT, have expanded its potential applications in myocardial tissue assessment. Delayed iodine enhancement CT has been explored as an alternative to LGE-CMRI for scar detection, as iodinated contrast agents exhibit delayed washout in fibrotic tissue (Smith et al., 2021). However, several studies have reported that CT-based scar imaging suffers from lower contrast resolution and higher noise levels compared to CMRI, limiting its reliability for accurate scar quantification. Ko et al. (2024) (Ko, 2024) showed that the soft tissue contrast of CT is inferior to that of CMRI, making differentiation between normal myocardium and scar tissue challenging. Although delayed iodine enhancement CT has been explored as an alternative to LGE-MRI, Maffei et al. (2022) (Jafari et al., 2022) reported that image noise, contrast variability, and radiation exposure limit its widespread clinical adoption. Radiation dose and contrast nephrotoxicity remain significant concerns associated with CT imaging. While CT excels in anatomical visualization of coronary arteries, its ability to characterize myocardial tissue remains inferior to CMRI.

2.2.4 Nuclear Cardiac Imaging

Nuclear imaging techniques such as SPECT and PET provide valuable insights into myocardial perfusion and metabolic activity. PET imaging, in particular, allows quantitative assessment of myocardial blood flow and viability, which is useful for guiding revascularization decisions. Di Carli et al. (Benz et al., 2021) demonstrated that

PET-derived flow measurements offer strong prognostic value in ischemic heart disease.

However, nuclear imaging suffers from limited spatial resolution, which restricts accurate delineation of myocardial scar boundaries (Almajmaie et al., 2022). Marquis et al. (2020) (Marquis et al., 2023) reported that partial volume effects and motion artifacts significantly affect scar size estimation, especially for small infarcts. Moreover, perfusion defects detected on nuclear imaging may reflect transient ischemia rather than irreversible myocardial injury, leading to potential misinterpretation. Recent systematic reviews conclude that while nuclear imaging is valuable for functional and metabolic assessment, it lacks the anatomical detail and tissue contrast required for precise myocardial scar characterization (Pradeep Kundur et al., 2025; J. Zhang et al., 2023).

Although ECG, echocardiography, CT, and nuclear cardiac imaging remain essential tools for the diagnosis and management of cardiovascular diseases, each modality presents limitations in the assessment of myocardial scar tissue. ECG and echocardiography primarily provide indirect information through electrical activity and functional abnormalities, while CT and nuclear imaging offer limited soft tissue characterization and scar delineation despite their advantages in anatomical and perfusion assessment. Consequently, accurate identification of myocardial scar extent and tissue composition remains challenging when relying solely on these conventional modalities. These limitations highlight the need for imaging techniques capable of providing direct visualization and detailed characterization of myocardial tissue. Compared with traditional cardiac imaging modalities, LGE-CMRI offers superior soft tissue contrast and enhanced visualization of infarcted myocardium, making it a more suitable modality for myocardial scar detection and subsequent image analysis applications.

2.3 Cardiac Magnetic Resonance Imaging

Cardiac magnetic resonance imaging, commonly known as cardiac MRI or CMRI, is a powerful medical imaging technology that allows doctors to see the heart in the best detail without using radiation or invasive procedures. CMRI uses strong magnetic fields and radio waves to create pictures of the heart (Chen et al., 2020). This makes it much safer for patients, especially those who need repeated imaging over time.

CMRI has become one of the most important tools in modern cardiology because it can show not only the structure of the heart but also how well it was working, how blood flows through it, and whether there was any damaged or scarred tissue.

2.3.1 Cardiac-Specific MRI Challenges

CMRI presents unique technical challenges compared to imaging of static organs due to the continuous motion of the heart throughout the cardiac cycle and the respiratory motion of the chest (Almajmaie et al., 2022). Without appropriate compensation strategies, these motions would result in severe image blurring and artifacts, rendering the images diagnostically unusable (Xing et al., 2023). ECG triggering was the fundamental technique used to synchronize image acquisition with the cardiac cycle. In prospective triggering, image acquisition was initiated at a specific point in the cardiac cycle, typically at the R-wave of the ECG, allowing imaging during a relatively quiescent phase such as diastole. In retrospective gating, data was continuously acquired throughout the cardiac cycle while recording the ECG, and images are reconstructed retrospectively for multiple cardiac phases, enabling cine imaging that displays cardiac motion.

Respiratory motion compensation is equally critical for high-quality cardiac imaging. Several strategies are employed, including breath-holding, respiratory gating, and navigator echoes. Breath-hold imaging requires patients to hold their breath for 10-20 seconds during image acquisition, eliminating respiratory motion but limiting the amount of data that can be acquired in a single breath-hold (van der Velde et al., 2021). This approach is suitable for most patients but may be challenging for those with dyspnoea or limited breath-hold capacity. Respiratory gating uses bellows or other sensors to monitor respiratory motion and acquires data only during a specific phase of the respiratory cycle, typically end-expiration. More advanced techniques such as self-gating extract motion information directly from the imaging data without external sensors.

2.3.2 Late Gadolinium Enhancement Cardiac Resonance Imaging in Medical Analysis

Among various CMRI techniques, LGE imaging has become the reference standard for myocardial scar visualization and quantification. First, the patient receives an injection of a contrast agent called gadolinium through an intravenous line. Gadolinium was a rare earth metal that has special magnetic properties (Wojnicki et al., 2024). After the gadolinium was injected, it quickly spreads through the bloodstream and into all the tissues of the body, including the heart. In normal, healthy heart muscle, the gadolinium enters the tissue but then washes out fairly quickly, usually within a few minutes. However, in areas of scar tissue, something different happens. Scar tissue has a different structure than normal heart muscle (Blomqvist et al., 2022). It has more space between cells and different properties that cause the gadolinium to stay in the tissue much longer. If doctors wait about 10 to 15 minutes after injecting the gadolinium and then take special CMRI pictures, the scar tissue appears very bright white because it still contains a lot of gadoliniums, while the normal heart muscle appears dark because the gadolinium has washed out. This creates a very strong contrast that makes scars easy to see as shown in Fig 2.5 compared to CMRI without agent.

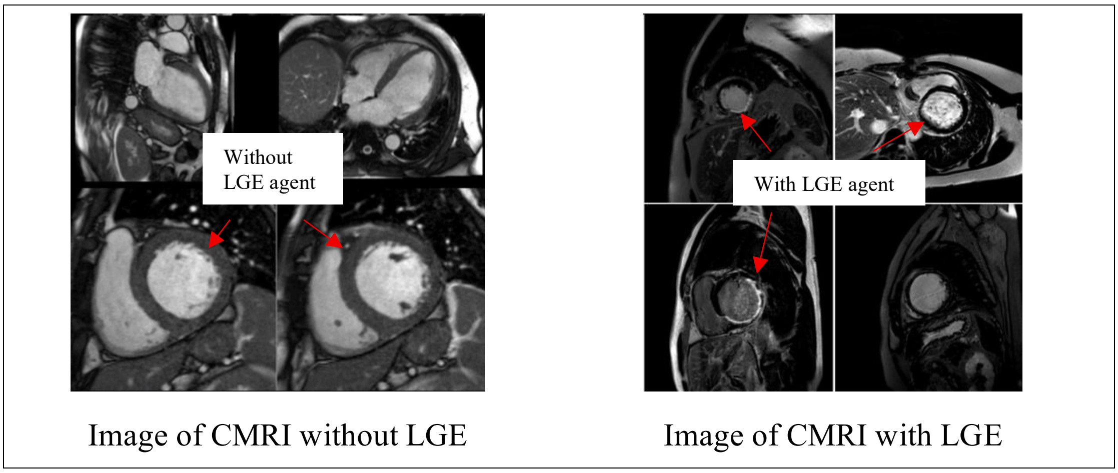

Figure 2.5 Example of the Difference Between CMRI and LGE-CMRI Image Showing Enhanced Scar Visibility (Ingkanisorn Bandettini et al., 2020)

The images from late gadolinium enhancement MRI are remarkably detailed as illustrated in Figure 2.6. It can show scars that are just a few millimetres in size, which was much smaller than what other imaging methods can detect. The images show not only where the scars are located but also their exact size and shape. Despite all these advantages, late gadolinium enhancement imaging has several important limitations and challenges. One major issue was image quality variability. The quality of LGE images can vary significantly from patient to patient and even from scan to scan in the same patient (Jenista et al., 2023). Many factors affect image quality and movement during the scan will causes blurring.

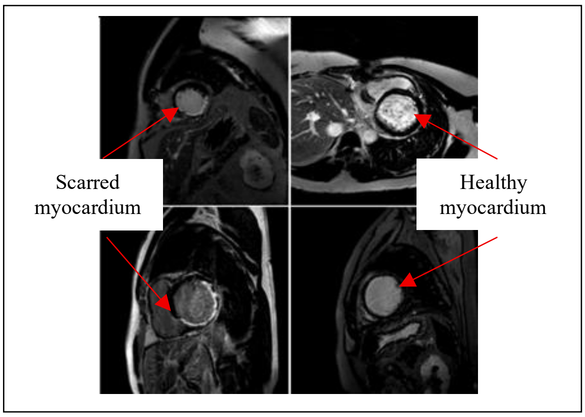

Figure 2.6 LGE-CMRI Image Demonstrating Contrast Between Scar Tissue and Healthy Myocardium

Another significant challenge, was the process of analysing LGE-CMRI images was also very time-consuming and requires significant expertise. After the images are acquired, someone needs to go through them carefully to identify where the scars are. Manual segmentation of LGE-CMRI images is conventionally performed by experienced radiologists or cardiologists, who delineate the boundaries of myocardial scar tissue on each image slice. Although this approach serves as the clinical reference standard, it is labour-intensive, time-consuming, and subject to inter- and intra-observer variability. These limitations reduce its efficiency and reproducibility, particularly when processing large datasets, thereby motivating the development of automated semantic segmentation methods for accurate and consistent myocardial scar delineation. (Sheikhjafari et al., 2023). A typical CMRI study includes many image slices covering the entire heart, often 10 to 15 slices or more. Going through all these slices and carefully marking the scars can take 30 minutes to an hour or even longer, depending on how complex the scarring was (Moafi et al., 2026; Vesal et al., 2020). This was a significant burden in busy clinical practices where doctors need to read many scans each day. Manual segmentation also suffers from variability. Even the same doctor might be slightly inconsistent when analysing the same images on different occasions. This inter-observer and intra-observer variability makes it difficult to compare results between different center or different time points.

2.3.3 Advantages of CMRI Over Other Imaging Modalities

CMRI offers several distinct advantages over other cardiac imaging modalities, making it the reference standard for myocardial tissue characterization and scar detection. First and foremost, CMRI provides superior soft tissue contrast compared to other modalities, enabling excellent differentiation between myocardium, blood pool, epicardial fat, and scar tissue as shown in Figure 2.7 (Chen et al., 2023). This inherent tissue contrast was particularly valuable for detecting subtle abnormalities and characterizing tissue composition. The high spatial resolution of CMRI, typically 1-2 mm in-plane resolution, allows detailed visualization of cardiac anatomy and precise delineation of small structures and lesions. Three-dimensional coverage of the entire heart enables comprehensive assessment without geometric assumptions, unlike echocardiography which relies on geometric models.

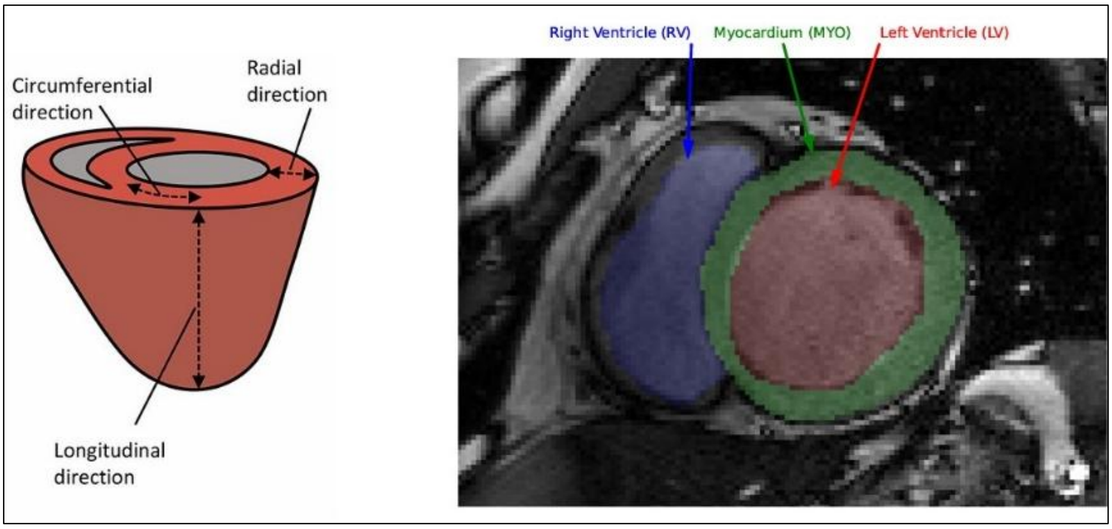

Figure 2.7 Anatomical Direction of the Myocardial (Radial, Circumferential, Longitudinal (Dhaene et al., 2023)

A major advantage of CMRI was the absence of ionizing radiation, making it safe for repeated examinations and suitable for younger patients and research studies requiring serial imaging. This was particularly important given that many cardiac patients require multiple imaging studies over their lifetime for disease monitoring and treatment evaluation. The ability to perform comprehensive functional and anatomical assessment in a single examination was another key strength of CMRI. A typical CMRI study includes cine imaging for ventricular function and wall motion assessment, LGE imaging for scar detection, perfusion imaging for ischemia evaluation, and various tissue characterization sequences, providing a complete picture of cardiac structure and function without requiring multiple separate tests (Wu et al., 2021).

Although CMRI provides superior soft tissue contrast, high spatial resolution, and comprehensive cardiac assessment compared to traditional imaging modalities, several challenges continue to limit its effectiveness for automated myocardial scar analysis. The quality of LGE-CMRI images remains susceptible to motion artifacts, intensity inhomogeneity, low contrast between healthy and infarcted tissues, and variability in image acquisition protocols (Luo et al., 2020). Furthermore, manual scar delineation remains time-consuming and highly dependent on observer expertise, resulting in potential inconsistencies across clinical assessments. While the superior tissue characterization capability of LGE-CMRI makes it the preferred modality for myocardial scar evaluation, these image quality and analysis challenges indicate that the diagnostic potential of LGE-CMRI is not fully exploited using conventional approaches alone (Chen et al., 2023). Therefore, additional image enhancement and automated segmentation techniques are required to improve scar visibility, reduce observer dependency, and facilitate more reliable myocardial scar detection.

2.4 Medical Image Enhancement Techniques

Medical image enhancement plays a crucial role in improving the visual quality and diagnostic utility of medical images, including CMRI (Abduvaitov et al., 2025; Qi et al., 2021). The goal of image enhancement is to improve the contrast between different tissue types and reduce blurriness (Luo et al., 2020; Srinivas et al., 2020). In the context of myocardial scar detection from LGE-MRI, image enhancement can significantly improve the conspicuity of scar tissue, enhance the delineation of scar boundaries, and ultimately improve the accuracy of automated segmentation algorithms (Liu et al., 2021). This section provides a comprehensive review of medical image enhancement techniques, progressing from traditional methods to state-of-the-art deep learning-based approaches, with specific emphasis on techniques applicable to CMRI.

2.4.1 Contrast Enhancement for CMRI

Contrast enhancement specifically tailored for CMRI and myocardial scar detection requires consideration of the unique characteristics and clinical requirements of these images. The primary goal was to maximize the contrast between scar tissue and normal myocardium while preserving the contrast between myocardium and blood pool, minimizing noise amplification, and avoiding the introduction of artifacts that could lead to false positive or false negative scar detection. Several specialized techniques have been developed or adapted for CMRI contrast enhancement.

Histogram equalization (HE) is a global enhancement method that redistributes pixel intensities to achieve a uniform histogram, thereby increasing the overall contrast of the image (Srinivas et al., 2020). The method computes the cumulative distribution function of the image histogram and uses it as a transformation function to map original intensities to new values that span the full available intensity range (Zhou et al., 2023). While HE can dramatically improve contrast in low-contrast images, it has several limitations for medical imaging applications. The global nature of the transformation means that it treats all regions of the image equally, potentially over-enhancing some regions while under-enhancing others. It can amplify noise in homogeneous regions and may produce unnatural-looking results. For CMRI, where the region of interest (myocardium and scar) occupies a relatively small portion of the image, global HE may not optimally enhance the relevant structures. Adaptive histogram equalization addresses some of these limitations by performing HE locally within small neighbourhoods around each pixel. The most widely used variant, CLAHE, limits the contrast enhancement to prevent over-amplification of noise in homogeneous regions (Abduvaitov et al., 2025).

Contrast limited adaptive histogram equalization (CLAHE) divides the image into small non-overlapping regions called tiles and performs HE independently in each tile. To avoid boundary artifacts, bilinear interpolation was used to combine the results from adjacent tiles. The key parameter was the clip limit, which restricts the maximum height of the histogram before equalization, thereby limiting the contrast enhancement and noise amplification. CLAHE has been widely used as a preprocessing step for medical image analysis, including CMRI, due to its ability to enhance local contrast while controlling noise amplification. However, CLAHE can sometimes produce artifacts at tile boundaries and may not preserve the relative intensity relationships between different tissue types, which can be important for subsequent analysis (Avard et al., 2022).

2.4.2 Image Sharpening Techniques

Image sharpening techniques aim to enhance edges and fine details, improving the perceived sharpness and clarity of images. For myocardial scar detection, sharpening can improve the delineation of scar boundaries, enhance the visibility of small scars, and facilitate more accurate segmentation (Song et al., 2022). Traditional sharpening methods include unsharp masking, high-pass filtering, and Laplacian-based enhancement.

Unsharp masking is a classical technique for edge enhancement and sharpening. It works by subtracting a blurred version of the image from the original, creating a high-pass filtered image that emphasizes edges and fine details, and then adding this back to the original image with a controllable weight (Deng et al., 2021). The technique can improve the perceived sharpness of images and enhance the visibility of boundaries, which was beneficial for myocardial scar delineation. However, Bogdan et. al. stated that unsharp masking can also amplify noise and may create halo artifacts around strong edges (Bogdan et al., 2024). Morphological operations based on mathematical morphology provide another class of enhancement techniques. Operations such as opening, closing, top-hat transform, and bottom-hat transform can be used to enhance specific structures, remove small objects, or fill gaps. The top-hat transform, which computes the difference between the original image and its morphological opening, has been specifically applied to myocardial scar enhancement in LGE-MRI (Luo et al., 2020).

For CMRI, sharpening must be applied judiciously to avoid introducing false details or artifacts that could be misinterpreted as pathology. Edge-aware sharpening methods that selectively enhance edges while preserving smooth regions are preferable. Multi-scale sharpening approaches that apply different levels of sharpening at different spatial scales can provide more natural-looking results. The combination of sharpening with noise reduction in a unified framework, such as through deep learning, can achieve better results than applying these operations sequentially. Some recent studies have investigated learned sharpening specifically for LGE-MRI, training networks to enhance scar boundaries while preserving overall image characteristics (Lepcha et al., 2022).

2.5 Deep Learning Fundamentals for Medical Imaging

Deep learning has emerged as a transformative technology in medical imaging, enabling automated analysis, pattern recognition, and decision support with unprecedented accuracy. Understanding the fundamental principles, architectures, and training strategies of deep learning is essential for appreciating its applications to myocardial scar detection and for developing improved methodologies. This section provides a comprehensive overview of deep learning fundamentals specifically in the context of medical imaging, covering convolutional neural networks, training processes, transfer learning, data augmentation, and domain-specific challenges (Liu et al., 2021).

2.5.1 Convolutional Neural Networks Architecture

Convolutional neural networks represent the cornerstone of deep learning for image analysis. CNNs are specifically designed to process grid-structured data such as images, exploiting the spatial structure and local correlations inherent in visual data (Wu et al., 2021). The key innovation of CNNs was the use of convolutional layers that apply learned filters to local regions of the input, enabling the network to detect local patterns such as edges, textures, and shapes. Unlike fully connected networks where each neuron connects to all neurons in the previous layer, convolutional layers use sparse connectivity and parameter sharing, dramatically reducing the number of parameters and enabling the processing of high-resolution images.

CNN-based architectures have become a fundamental approach in medical image analysis due to their ability to automatically extract hierarchical features from image data. Chen et al. (Chen et al., 2020) reviewed deep learning methods for cardiac image segmentation and reported that CNN-based models have achieved significant improvements in automated cardiac structure delineation by learning complex spatial representations. Furthermore, Wu et al. (Wu et al., 2021) highlighted the effectiveness of CNN architectures for fibrosis and scar segmentation from CMRI, where deep learning models were able to identify discriminative features associated with myocardial scar regions. These findings demonstrate the suitability of CNN architectures for LGE-CMRI-based myocardial scar segmentation.

A convolutional layer consists of multiple filters also called kernels, each of which was a small matrix of learnable weights, typically 3×3 or 5×5 in size. Each filter was convolved with the input image or feature map, producing an output feature map that highlights regions where the pattern represented by the filter was present (Chen et al., 2020). The convolution operation involves sliding the filter across the input, computing the element-wise product between the filter weights and the input values at each position, and summing the results to produce a single output value. This process was repeated for all spatial positions and all filters, producing multiple output feature maps. The use of multiple filters enables the network to detect multiple different patterns simultaneously.

Pooling layers are typically inserted between convolutional layers to progressively reduce the spatial dimensions of feature maps, providing translation invariance and reducing computational requirements (Luo et al., 2020). Max pooling, the most common pooling operation, divides the input into non-overlapping rectangular regions and outputs the maximum value within each region (Lechien et al., 2023). Average pooling computes the average instead of the maximum. Pooling reduces the spatial resolution by a factor determined by the pooling size (typically 2×2) and stride (typically 2), effectively downsampling the feature maps. While pooling provides computational benefits and some degree of invariance to small translations, it also discards spatial information, which can be problematic for tasks requiring precise localization such as segmentation.

Batch normalization has become a standard component of modern CNN architectures. Batch normalization normalizes the activations of each layer across the mini-batch during training, reducing internal covariate shift and enabling the use of higher learning rates. The normalization was performed by subtracting the mini-batch mean and dividing by the mini-batch standard deviation, followed by a learned affine transformation. Batch normalization has been shown to accelerate training, improve generalization, and reduce sensitivity to initialization (Fahmy et al., 2021). However, its behaviour differs between training and inference, and alternative normalization schemes such as layer normalization, instance normalization, and group normalization have been proposed for specific applications.

2.5.2 Training Process and Optimization

Training a deep neural network involves learning the optimal values of millions of parameters that minimize a loss function measuring the discrepancy between network predictions and ground truth labels. This optimization is performed using variants of gradient descent, which iteratively update network parameters in the direction that reduces the loss. The training process begins with initialization of network parameters, where appropriate weight initialization strategies are important to ensure stable learning and effective convergence during training.

The loss function, also called the objective function or cost function, quantifies how well the network's predictions match the ground truth. For classification tasks, cross-entropy loss was the standard choice, measuring the dissimilarity between the predicted probability distribution and the true distribution. For regression tasks, MSE or mean absolute error (MAE) are common choices (Chen et al., 2023; Deepika & Jaisankar, 2024). For segmentation tasks, various loss functions have been proposed, including pixel-wise cross-entropy, Dice loss, focal loss, and combinations thereof, each with different properties regarding class imbalance handling and boundary precision (Abbas et al., 2024). In CMRI segmentation, Qiu et al. (Qiu et al., 2022) developed MyoPS-Net for myocardial pathology segmentation and employed segmentation-specific loss functions to improve the learning of myocardial pathology regions from multi-sequence CMRI images. Their findings demonstrated the importance of suitable training strategies and loss function selection in achieving accurate segmentation of complex cardiac structures.

2.5.3 Challenges in Medical Imaging

Deep learning for medical imaging faces several unique challenges compared to natural image analysis. Limited training data was perhaps the most significant challenge. While natural image datasets like ImageNet contain millions of labelled images, medical imaging datasets typically contain hundreds to thousands of images due to the high cost and expertise required for annotation. Medical image annotation requires trained clinicians or radiologists, and even expert annotations can have inter-observer variability. The limited data makes models prone to overfitting and limits the complexity of models that can be effectively trained. Strategies to address limited data include transfer learning, data augmentation, semi-supervised learning, and few-shot learning (Almajmaie et al., 2022).

Computational requirements for training and deploying deep learning models can be substantial. Training state-of-the-art models may require multiple GPUs and days or weeks of computation time. Inference on high-resolution medical images can also be computationally demanding, which was problematic for real-time clinical applications or deployment on resource-constrained devices. Model compression techniques such as pruning, quantization, and knowledge distillation can reduce model size and computational requirements while maintaining accuracy. Efficient architectures such as MobileNet and EfficientNet are specifically designed to achieve good accuracy with reduced computational cost (Liu et al., 2021).

Although deep learning has achieved remarkable success in medical image analysis, its performance remains highly dependent on the availability of high-quality training data, effective feature extraction, and appropriate network architectures as stated by Hasny et al. (Hasny et al., 2024). CNN-based models have demonstrated strong capability in learning discriminative representations from medical images, while advances in training strategies and optimization techniques have further improved segmentation accuracy (Liu et al., 2021). However, challenges such as limited annotated datasets, class imbalance, variability in image quality, and the complex appearance of pathological regions continue to affect model performance, particularly in myocardial scar segmentation (Almajmaie et al., 2022). These limitations suggest that conventional deep learning approaches alone may not be sufficient to achieve robust and reliable scar delineation (Hong & Zhang, 2023). Therefore, the selection of an effective semantic segmentation architecture capable of capturing both global contextual information and fine structural details is critical for improving segmentation performance in LGE-CMRI images.

2.6 Semantic Segmentation Architectures

Semantic segmentation was the task of assigning a class label to every pixel in an image, effectively partitioning the image into meaningful regions corresponding to different objects or tissue types. In medical imaging, semantic segmentation was fundamental for automated analysis, enabling quantification of anatomical structures, detection of pathologies, and treatment planning (W. Zhang et al., 2023). For myocardial scar detection, semantic segmentation aims to classify each pixel as background, blood pool, normal myocardium, or scar tissue. This section provides a comprehensive review of semantic segmentation architectures, progressing from early fully convolutional networks to advanced architectures, with particular emphasis on the DeepLabV3+ framework that has shown excellent performance for medical image segmentation.

2.6.1 Fully Convolutional Networks

Fully Convolutional Networks, introduced by Long et al. in 2015 (Liu et al., 2021), marked a paradigm shift in semantic segmentation by demonstrating that networks composed entirely of convolutional layers, without fully connected layers, could perform dense pixel-wise prediction. Prior to FCN, semantic segmentation was typically approached through patch-based classification, where a classifier was applied to image patches cantered at each pixel to determine the pixel's class. This approach was computationally inefficient due to redundant computation for overlapping patches and could not effectively leverage global context.

FCN architecture consists of two main components: a downsampling path (encoder) that progressively reduces spatial resolution while increasing the number of feature channels, and an upsampling path (decoder) that progressively increases spatial resolution to produce a full-resolution segmentation map (Rayed et al., 2024). The encoder was typically a standard CNN architecture such as VGG or ResNet, pre-trained on ImageNet, with the fully connected layers removed. The encoder extracts hierarchical feature representations, with early layers capturing low-level features and deeper layers capturing high-level semantic information. However, the repeated application of pooling layers in the encoder reduces the spatial resolution by a factor of 32 or more, losing fine spatial details necessary for precise segmentation.

The decoder uses transposed convolutions also called deconvolutions or upsampling convolutions to progressively increase the spatial resolution of feature maps back to the input image resolution. Transposed convolution was a learnable upsampling operation that applies a regular convolution to an upsampled version of the input. However, naive upsampling from very low-resolution feature maps results in coarse segmentation with poor boundary localization. To address this, FCN introduced skip connections that combine features from the encoder with features in the decoder at corresponding spatial resolutions. Specifically, FCN-8s combines predictions from the final layer with predictions from two intermediate layers (pool4 and pool3), enabling the network to leverage both high-level semantic information and low-level spatial details.

2.6.2 U-Net and Variants

U-Net, introduced by Ronneberger et al. in 2015 (Chen et al., 2023) specifically for biomedical image segmentation, has become one of the most influential and widely used architectures in medical imaging. The U-Net architecture consists of a symmetric encoder-decoder structure with extensive skip connections, forming a U-shaped architecture that gives the network its name. The encoder follows the typical CNN architecture with repeated application of convolutions and max pooling, progressively reducing spatial resolution while increasing feature channels. The decoder uses upsampling operations followed by convolutions to progressively increase spatial resolution.

The key innovation of U-Net was the use of concatenative skip connections that directly connect corresponding layers in the encoder and decoder. Unlike FCN which used additive skip connections, U-Net concatenates feature maps from the encoder with feature maps in the decoder at the same spatial resolution (Rayed et al., 2024). This allows the decoder to access both high-resolution spatial information from the encoder and high-level semantic information from the bottleneck. The concatenation provides the decoder with rich multi-scale features that enable precise localization while maintaining semantic understanding. The symmetric architecture with skip connections at multiple resolutions enables effective information flow and gradient propagation during training.

U-Net was designed to work well with limited training data, which was common in medical imaging. The architecture uses data augmentation extensively during training, applying random transformations to the training images to artificially increase the dataset size. U-Net also uses a weighted loss function that gives more importance to pixels near boundaries between different classes. This helps the network learn to accurately segment boundaries even when they are thin or ambiguous. Since the original U-Net was introduced, many variants and improvements have been proposed. Residual U-Net incorporates residual connections, similar to ResNet, which help train deeper networks. For myocardial scar segmentation, U-Net and its variants have been widely used and have shown excellent results. The architecture's ability to capture both local details and global context makes it well-suited for detecting scars, which can vary in size and location. The skip connections help preserve the precise boundaries of scars, which was important for accurate quantification. Several studies have developed specialized U-Net variants specifically for cardiac segmentation, incorporating domain knowledge about cardiac anatomy and scar characteristics (Papetti et al., 2023).

2.6.3 DeepLab Family

The DeepLab family of semantic segmentation architectures, developed by Google Research, represents another major line of development in semantic segmentation, with particular emphasis on capturing multi-scale context and producing high-resolution segmentation maps (Gavirni et al., 2023). The DeepLab series includes DeepLabV1, DeepLabV2, DeepLabV3, and DeepLabV3+, each introducing important innovations that have influenced the field (Liu et al., 2021). Unlike U-Net which uses an encoder-decoder structure with skip connections, DeepLab architectures are based on dilated (atrous) convolutions and spatial pyramid pooling to capture multi-scale context while maintaining resolution.

DeepLabV1, introduced in 2015, made two key contributions: the use of atrous (dilated) convolutions to increase the receptive field without reducing spatial resolution, and the use of fully connected Conditional Random Fields (CRF) as a post-processing step to refine segmentation boundaries. Atrous convolution was a modification of standard convolution where the filter was expanded by inserting zeros (holes) between filter elements, effectively increasing the receptive field without increasing the number of parameters or computations. By using atrous convolutions in the later layers of the network instead of pooling, DeepLabV1 maintained higher spatial resolution throughout the network, producing segmentation maps at 1/8 of the input resolution instead of 1/32, which improved boundary localization (Rayed et al., 2024).

DeepLabV3+, introduced in 2018, represents the current state-of-the-art in the DeepLab family and combines the strengths of DeepLab's atrous convolution and ASPP with an encoder-decoder structure inspired by U-Net. This hybrid architecture addresses a key limitation of DeepLabV3: while ASPP captures rich multi-scale context, the lack of a decoder structure limits the recovery of fine spatial details, resulting in relatively coarse segmentation boundaries. DeepLabV3+ introduces a simple yet effective decoder that refines the segmentation boundaries while maintaining the benefits of ASPP for multi-scale context capture.

The DeepLabV3+ architecture consists of three main components: an encoder, an ASPP module, and a decoder. The encoder was typically a deep CNN such as ResNet, Xception, or MobileNet, modified to use atrous convolutions in the later stages to maintain higher spatial resolution (Damit et al., 2024). The encoder progressively extracts hierarchical features, with the final feature maps having a spatial resolution of 1/16 or 1/8 of the input image, depending on the output stride. These encoder features are processed by the ASPP module to capture multi-scale context. The ASPP output was then fed to the decoder for spatial resolution recovery and boundary refinement.

The decoder in DeepLabV3+ was designed to be simple yet effective. It first upsamples the ASPP output by a factor of 4 using bilinear interpolation. The upsampled features are then concatenated with corresponding low-level features from the encoder (typically from the layer that has 1/4 of the input resolution). Before concatenation, the low-level features are processed by a 1×1 convolution to reduce the number of channels, preventing the low-level features from dominating the concatenated representation. After concatenation, a few 3×3 convolutions are applied to refine the features. Finally, the features are upsampled by another factor of 4 to produce the full-resolution segmentation map.

The combination of ASPP and decoder in DeepLabV3+ provides complementary benefits. ASPP captures rich multi-scale semantic context through parallel atrous convolutions with different dilation rates, enabling robust classification of pixels based on their semantic meaning. The decoder recovers spatial details and refines boundaries by incorporating low-level features that preserve fine spatial information. This combination enables DeepLabV3+ to achieve both accurate semantic classification and precise boundary localization, which are both essential for high-quality segmentation. Experimental results have demonstrated that DeepLabV3+ achieves state-of-the-art performance on various segmentation benchmarks while maintaining reasonable computational efficiency.

Although FCN and U-Net have significantly advanced medical image segmentation, both architectures exhibit limitations when applied to complex myocardial scar segmentation tasks. FCN suffers from the loss of fine spatial information due to repeated downsampling (Rayed et al., 2024), while U-Net relies heavily on skip connections to recover spatial details and may have difficulty capturing sufficient multi-scale contextual information for highly heterogeneous scar regions. In contrast, DeepLabV3+ combines atrous convolutions, ASPP and an encoder-decoder structure, enabling simultaneous extraction of rich multi-scale contextual features and precise boundary information (El-Taraboulsi et al., 2023). These characteristics are particularly important for LGE-CMRI images, where myocardial scars often appear as small, irregular, and highly variable regions with unclear boundaries. Furthermore, the ability of DeepLabV3+ to preserve spatial resolution while capturing broader contextual information provides a distinct advantage over conventional segmentation architectures. Therefore, DeepLabV3+ represents a promising architecture for myocardial scar segmentation and serves as the primary segmentation framework investigated in this study.

2.7 Backbone Networks for Feature Extraction

The backbone network, also called the encoder or feature extractor, was a critical component of semantic segmentation architectures. The backbone was responsible for extracting hierarchical feature representations from input images, with early layers capturing low-level features such as edges and textures, and deeper layers capturing high-level semantic features such as object parts and object categories. The choice of backbone network significantly impacts the segmentation performance, computational efficiency, and memory requirements of the overall system. This section provides a detailed examination of three prominent backbone networks: ResNet-50, MobileNetV2, and Xception, analyzing their architectures, design principles, performance characteristics, and suitability for myocardial scar segmentation.

2.7.1 ResNet-50 Architecture and Design

Residual Networks (ResNets), introduced by He et al. in 2016 (He et al., 2016), revolutionized deep learning by enabling the training of very deep networks with hundreds or even thousands of layers. Prior to ResNet, training very deep networks was challenging due to the vanishing gradient problem, where gradients become exponentially small as they are backpropagated through many layers, preventing effective learning in early layers. ResNet address this problem through the introduction of residual connections that allow gradients to flow directly through the network without attenuation.

The fundamental building block of ResNet was the residual block, which implements the residual learning framework. Instead of learning a direct mapping H(x) from input x to output, a residual block learns the residual function F(x) = H(x) - x, with the final output being F(x) + x. The residual connection (the +x term) provides a direct path for gradients to flow backward and for information to flow forward, bypassing the convolutional layers. This simple modification has profound implications: it enables training of much deeper networks, accelerates convergence, and often improves generalization. The intuition was that it was easier to learn a residual (the difference from identity) than to learn the complete transformation, especially when the optimal transformation was close to identity.

ResNet-50 was a specific ResNet variant with 50 layers, providing a good balance between depth (and thus representational capacity) and computational efficiency. The architecture consists of an initial convolutional layer with 7×7 filters and stride 2, followed by max pooling, then four stages of residual blocks with progressively increasing numbers of channels (64, 128, 256, 512) and decreasing spatial resolutions. Each stage contains multiple residual blocks: stage 1 has 3 blocks, stage 2 has 4 blocks, stage 3 has 6 blocks, and stage 4 has 3 blocks, totalling 16 residual blocks. Each residual block in ResNet-50 uses a bottleneck design with three convolutional layers: a 1×1 convolution that reduces channels, a 3×3 convolution that processes features, and a 1×1 convolution that expands channels back.

2.7.2 MobileNetV2 Architecture and Efficiency

MobileNetV2, introduced by Sandler et al. in 2018 (S. Wang et al., 2023), was specifically designed for efficient inference on mobile and embedded devices with limited computational resources. While ResNet-50 prioritizes accuracy and representational capacity, MobileNetV2 prioritizes computational efficiency and small model size while maintaining competitive accuracy. This makes MobileNetV2 an attractive backbone for clinical deployment scenarios where real-time or near-real-time performance was required, or where the segmentation system must run on devices with limited computational capabilities such as mobile devices or edge computing platforms.

The key innovation in MobileNetV2 was the inverted residual block with linear bottleneck. This design was fundamentally different from the bottleneck blocks in ResNet (Sharma et al., 2021). While ResNet bottleneck blocks use a wide-narrow-wide structure (reduce channels, process, expand channels), MobileNetV2 inverted residual blocks use a narrow-wide-narrow structure which expand channels, process and reduce channels. The rationale for this design was based on the manifold hypothesis: the important information in deep networks lies in a low-dimensional manifold, and nonlinear activations can destroy information in low-dimensional spaces. Therefore, MobileNetV2 uses linear activation (no ReLU) in the narrow bottleneck layers to preserve information.

Each inverted residual block in MobileNetV2 consists of three operations: expansion, depthwise convolution, and projection. The expansion step uses a 1×1 convolution to expand the number of channels by a factor, creating a higher-dimensional representation. The depthwise convolution step applies a 3×3 depthwise separable convolution to the expanded features. Depthwise separable convolution was a key efficiency technique that factorizes a standard convolution into a depthwise convolution (applying a single filter per input channel) followed by a pointwise convolution (1×1 convolution to combine channels). This factorization dramatically reduces computational cost: a standard 3×3 convolution on C channels requires 3×3×C×C operations, while depthwise separable convolution requires only 3×3×C + 1×1×C×C operations, a reduction of approximately 8-9× for typical channel numbers.

The efficiency of MobileNetV2 was quantified by several metrics. The number of parameters in MobileNetV2 was approximately 3.5 million, compared to 25.6 million in ResNet-50, a reduction of over 7×. The number of multiply-add operations for a 224×224 input image was approximately 300 million for MobileNetV2 compared to 4,100 million for ResNet-50, a reduction of over 13×. This dramatic reduction in computational cost enables MobileNetV2 to run efficiently on mobile devices and achieve real-time performance. Despite the reduced computational cost, MobileNetV2 achieves competitive accuracy on ImageNet classification, demonstrating the effectiveness of its efficient design.

2.7.3 Xception Architecture and Depthwise Separable Convolutions

Xception, introduced by Chollet in 2017 (Chollet, 2017), represents an extreme version of the Inception architecture, hence the name "Extreme Inception." The key idea behind Xception was to completely replace standard convolutions with depthwise separable convolutions, taking the concept of separating spatial and channel-wise operations to its logical extreme. Xception demonstrates that depthwise separable convolutions, when used throughout a deep network with appropriate architectural design, can achieve state-of-the-art accuracy while being more parameter-efficient than standard convolutions.

Xception architecture consists of 36 convolutional layers organized into 14 modules, with residual connections around most modules. The architecture was divided into three flows: entry flow, middle flow, and exit flow. The entry flow consists of several convolutional and depthwise separable convolutional layers with stride-2 operations to reduce spatial resolution and increase channels. The middle flow consists of 8 repeated modules, each containing 3 depthwise separable convolutional layers with residual connections. The exit flow consists of additional depthwise separable convolutional layers leading to the final feature representation. All depthwise separable convolutions use 3×3 depthwise filters.

A key difference between Xception and MobileNet was the order of operations in depthwise separable convolution and the use of nonlinearities. In MobileNet, the pointwise convolution (channel mixing) comes after the depthwise convolution (spatial processing), with ReLU after each operation. In Xception, the order was reversed in some modules, and the presence of nonlinearities between depthwise and pointwise operations was carefully designed. Xception also uses residual connections more extensively than MobileNet, with residual connections around most modules. These design differences, while subtle, contribute to Xception's superior accuracy compared to MobileNet.

The use of depthwise separable convolutions throughout Xception provides computational efficiency compared to standard convolutions, though not as extreme as MobileNetV2. Xception has approximately 23 million parameters, slightly fewer than ResNet-50's 25.6 million, but the depthwise separable convolutions require fewer operations. For a 299×299 input image, Xception requires approximately 8,400 million multiply-add operations compared to ResNet-50's 4,100 million for 224×224 input (note the different input sizes). When normalized for input size, Xception was more efficient than ResNet-50 while achieving higher accuracy on ImageNet classification.

The flexibility to choose different backbones was a significant advantage of the DeepLabV3+ architecture. By maintaining a consistent overall architecture (encoder-ASPP-decoder) while allowing different backbone networks, DeepLabV3+ enables adaptation to different deployment scenarios and requirements. This flexibility has contributed to the widespread adoption of DeepLabV3+ for medical image segmentation. Future work may explore neural architecture search to automatically discover optimal backbone architectures for specific medical imaging tasks, or develop adaptive systems that dynamically select backbones based on available computational resources and required accuracy.

2.8 Performance Evaluation Metrics

Evaluating the performance of myocardial scar segmentation algorithms was crucial for comparing different methods, tracking progress, and determining whether algorithms are ready for clinical use. Various metrics have been developed to measure different aspects of segmentation performance. This section will discuss the most commonly used metrics for evaluating scar segmentation, explaining what they measure and their strengths and limitations.

2.8.1 Image Enhancement Performance Evaluation

Image enhancement performance evaluation was carried out to quantitatively assess the effectiveness of the proposed enhancement techniques in improving the visual quality of LGE-CMRI images while preserving diagnostically important anatomical and pathological information. In medical image analysis, particularly for cardiac imaging, enhancement plays a crucial role in addressing challenges such as low contrast, intensity inhomogeneity, and noise, which can significantly affect subsequent segmentation performance (Abduvaitov et al., 2025). Since image enhancement does not involve pixel-wise ground truth labels, objective image quality assessment metrics have been widely adopted in previous studies to evaluate enhancement outcomes. In this study, PSNR, MSE, SSIM, CRMS, and Entropy were employed to provide a comprehensive evaluation of enhancement performance and preservation (Hasny et al., 2024).

PSNR has been extensively used in prior medical image enhancement studies to measure the fidelity of enhanced images relative to their original counterparts (Rehman et al., 2024). Previous research on CMRI enhancement reported that higher PSNR values indicate effective noise suppression while maintaining essential tissue information, which is critical for reliable clinical interpretation. In the context of LGE-CMRI, preserving signal integrity is particularly important, as excessive distortion may obscure myocardial boundaries or scar regions. In this study, PSNR was used to evaluate how well the enhancement techniques improved image clarity without introducing significant degradation. Higher PSNR values were interpreted as evidence that the enhancement process successfully retained the original image characteristics while improving overall visual quality.

MSE has commonly been applied in earlier image processing studies to quantify the average pixel-wise error introduced by enhancement algorithms (Chen et al., 2023; Deepika & Jaisankar, 2024). Several previous works highlighted that lower MSE values correspond to minimal alteration of the original image content, which is desirable in medical imaging applications. For LGE-CMRI enhancement, maintaining low MSE values ensured that the enhancement process did not distort clinically meaningful features such as myocardial thickness, scar extent, or ventricular boundaries. Although MSE alone does not reflect perceptual quality, it remains an important complementary metric for quantifying enhancement-induced distortion.

SSIM has been widely recognised in previous medical imaging studies as a perceptually meaningful metric that correlates well with human visual assessment. Prior research on MRI enhancement demonstrated that SSIM is particularly effective in evaluating the preservation of structural information, which is essential for downstream tasks such as segmentation and classification (Rehman et al., 2024). In LGE-CMRI images, subtle structural variations between healthy myocardium and infarcted tissue are critical for accurate scar detection. Therefore, SSIM was employed in this study to assess whether the enhancement techniques preserved anatomical structure while improving contrast and visibility. High SSIM values indicated that structural integrity was maintained, making the enhanced images suitable for deep learning-based segmentation (Qi et al., 2021).

CRMS has been utilised in earlier studies to evaluate global contrast improvement in medical images, particularly in scenarios where low contrast limits diagnostic accuracy. Previous cardiac imaging research reported that increased CRMS values are associated with enhanced tissue separability, especially between myocardium, scar tissue, and blood pool regions. In LGE-CMRI, scar tissue often appears with intensity levels close to surrounding myocardial tissue, making contrast enhancement essential. In this study, CRMS was used to quantify the effectiveness of the enhancement techniques in amplifying contrast differences, thereby improving the visibility of infarcted regions for subsequent segmentation.

Entropy has frequently been applied in prior image enhancement research as a measure of information content and texture complexity. Earlier studies suggested that an increase in entropy generally reflects improved detail visibility and richer image information, which is beneficial for feature extraction in deep learning models (Song et al., 2022). In the context of LGE-CMRI enhancement, higher entropy values indicated that subtle scar-related features were better revealed (Sharma & Kamra, 2023). However, previous literature also cautioned that excessive entropy could be associated with noise amplification. Therefore, in this study, entropy was analysed together with PSNR and SSIM to ensure that increased information content corresponded to meaningful structural detail rather than unwanted noise (Zhou et al., 2023).

Overall, the use of PSNR, MSE, SSIM, CRMS, and Entropy provided a comprehensive and balanced evaluation framework, consistent with methodologies adopted in previous medical image enhancement studies. By integrating signal-based, perceptual, contrast-based, and information-based metrics, this evaluation ensured that the proposed enhancement techniques improved LGE-CMRI image quality in a controlled and clinically meaningful manner. The results of this evaluation further justified the use of the enhanced images as reliable inputs for the subsequent multi-stage deep learning-based myocardial scar segmentation framework.

2.8.2 Image Segmentation Performance Evaluation

The Dice coefficient, also called the Dice similarity coefficient or Dice score, was probably the most widely used metric for evaluating medical image segmentation (Mosquera-Rojas et al., 2023). The Dice coefficient measures the overlap between the predicted segmentation and the ground truth segmentation (Luo et al., 2020). It was calculated as two times the intersection of the predicted and ground truth regions divided by the sum of their sizes. Mathematically, if P was the predicted segmentation and G was the ground truth, the Dice coefficient was $2|P \cap G| / (|P|+|G|)$, where $|\cdot|$ denotes the number of pixels in a region and $\cap$ denotes intersection. The Dice coefficient ranges from 0 to 1, where 0 means no overlap at all and 1 means perfect overlap (Zhang et al., 2024). A Dice coefficient above 0.7 is generally considered an acceptable indicator of good segmentation performance in medical image segmentation, while higher Dice values indicate stronger agreement between the predicted segmentation and the ground truth annotations (Liu et al., 2023). The Dice coefficient was popular because it was easy to understand and interpret, it handles class imbalance reasonably well, and it directly measures what we care about, which was how well the predicted segmentation matches the ground truth (Papetti et al., 2023).

The Jaccard index, also called Intersection over Union or IoU, was another commonly used overlap metric. It was calculated as the intersection of the predicted and ground truth regions divided by their union (S. Wang et al., 2023). Mathematically, the Jaccard index was $|P \cap G| / |P \cup G|$, where $\cup$ denotes union. The Jaccard index also ranges from 0 to 1, with 1 being perfect overlap. The Jaccard index was related to the Dice coefficient by the formula Dice = 2×Jaccard / (1+Jaccard). The two metrics are highly correlated and usually lead to similar conclusions. The Jaccard index was slightly stricter than the Dice coefficient, meaning it gives lower scores for the same segmentation. Some researchers prefer Jaccard because it has a clearer geometric interpretation as the ratio of intersection to union.

Sensitivity, also called recall or true positive rate, measures the proportion of actual scar pixels that are correctly identified by the algorithm. It was calculated as the number of true positive pixels divided by the total number of actual scar pixels (Wu et al., 2021). Mathematically, sensitivity = TP / (TP+FN), where TP was true positives and FN was false negatives. Sensitivity ranges from 0 to 1, with 1 meaning all actual scar pixels were detected. High sensitivity was important because missing scars can have serious clinical consequences. However, sensitivity alone was not sufficient because an algorithm could achieve perfect sensitivity by simply labelling all pixels as scar, which would obviously not be useful.

Specificity, also called true negative rate, measures the proportion of actual non-scar pixels that are correctly identified as non-scar. It was calculated as TN / (TN+FP), where TN was true negatives and FP was false positives. Specificity also ranges from 0 to 1, with 1 meaning all non-scar pixels were correctly identified. High specificity was important because false positives can lead to overestimation of scar burden and potentially inappropriate treatment decisions. Like sensitivity, specificity alone was not sufficient because an algorithm could achieve perfect specificity by labelling all pixels as non-scar.

Precision, also called positive predictive value, measures the proportion of pixels labelled as scar by the algorithm that are actually scar. It was calculated as TP / (TP+FP). Precision ranges from 0 to 1, with 1 meaning all predicted scar pixels are correct. Precision was important because it tells us how reliable the algorithm's positive predictions are. Low precision means many false positives, which can be problematic clinically.

The F1 score was the harmonic mean of precision and sensitivity. It was calculated as 2×(precision×sensitivity) / (precision+sensitivity). The F1 score provides a single metric that balances precision and sensitivity. It was useful when you want to consider both false positives and false negatives. The F1 score was actually equivalent to the Dice coefficient when applied to binary segmentation, which was why Dice was sometimes called the F1 score in the segmentation literature.

For myocardial scar segmentation, researchers typically report multiple metrics to provide a comprehensive evaluation. A common set includes Dice coefficient for overall overlap, sensitivity and specificity for understanding the balance between false negatives and false positives. Some studies also report scar volume or scar percentage of myocardium, comparing the algorithm's measurements to manual measurements.

2.9 Datasets and Benchmarks

The availability of high-quality datasets was crucial for developing and evaluating deep learning algorithms for myocardial scar segmentation. Datasets provide the training data that algorithms learn from and the test data used to evaluate performance. Benchmark datasets, which are publicly available and widely used by multiple research groups, enable fair comparison between different methods and help track progress in the field. This section discusses the datasets that have been used for myocardial scar segmentation research and the challenges related to data availability.

One of the challenges in medical imaging research was that most datasets are private and not publicly available. Hospitals and research institutions collect CMRI data as part of clinical care and research studies, but this data typically cannot be shared publicly due to privacy regulations and institutional policies. Patient data contains sensitive health information that must be protected. Even when images are de-identified by removing patient names and other obvious identifiers, there are concerns about re-identification. This means that most research on myocardial scar segmentation uses private datasets that are only available to the researchers who collected them. This makes it difficult to compare results across different studies because they use different data.

Despite these challenges, some public datasets for CMRI segmentation have been made available. The MICCAI, which are annual competitions in medical image analysis, have released several CMRI datasets (Li et al., 2024; Liu et al., 2021). The ACDC challenge (Automated Cardiac Diagnosis Challenge) provided a dataset of cardiac cine MRI images with annotations of cardiac chambers (L. Wang et al., 2023). While this dataset does not include late gadolinium enhancement images or scar annotations, it has been useful for developing methods for cardiac structure segmentation, which was often a first step in scar segmentation pipelines (Jafari et al., 2022; Xiong et al., 2021). The M&Ms challenge (Multi-Centre, Multi-Vendor & Multi-Disease Cardiac Image Segmentation Challenge) provided a more diverse dataset with images from multiple hospitals and multiple MRI vendors, helping to evaluate generalization across different imaging conditions.

For late gadolinium enhancement imaging and scar segmentation specifically, public datasets are more limited. The EMIDEC challenge (Automatic Evaluation of Myocardial Infarction from Delayed-Enhancement Cardiac MRI) provided a dataset of LGE images with scar annotations(Shaaf et al., 2023). This challenge focused specifically on myocardial infarction detection and quantification, making it directly relevant to the topic of this review (Shaaf et al., 2023). However, the dataset was relatively small, with only a few dozen cases, which limits its use for training large deep learning models. Nevertheless, it has been valuable for benchmarking different methods and has been used in several research studies.

Some research groups have created their own datasets by collecting and annotating CMRI images from their institutions. These datasets vary widely in size, from a few dozen cases to several hundred cases. Larger datasets generally allow training of more sophisticated models and provide more reliable evaluation. However, creating large annotated datasets was very time-consuming and expensive. Each case requires expert manual segmentation, which can take 30 minutes to an hour or more. For a dataset of 100 cases, this represents 50 to 100 hours of expert time, not counting the time for quality control and corrections (G. Wang et al., 2023).

2.10 Summary of Literature Review

This comprehensive literature review has examined the current state of research in magnetic resonance image enhancement and segmentation for myocardial scar detection using deep learning, covering fundamental concepts, methodological approaches, recent advances, and current challenges. The review has synthesized knowledge across multiple interconnected domains to provide a thorough foundation for developing improved methodologies for automated myocardial scar detection.

2.10.1 Key Findings and Insights

Cardiac magnetic resonance imaging, particularly late gadolinium enhancement imaging, has emerged as the gold standard for myocardial scar detection and quantification due to its superior soft tissue contrast, high spatial resolution, and ability to directly visualize scar tissue (Schulz-Menger et al., 2020). However, LGE-MRI interpretation and quantification remain challenging due to image quality issues, inter-observer variability, and the time-consuming nature of manual analysis (Mukaida et al., 2023). These limitations motivate the development of automated analysis methods using deep learning (Avard et al., 2022; El-Taraboulsi et al., 2023; Lepcha et al., 2022; Sahu & Ray, 2022).

Image enhancement techniques, play a crucial role in improving the quality of CMRI and facilitating accurate segmentation. Traditional methods such as CLAHE, bias field correction, and noise reduction provide consistent improvements but are limited by their generic nature and inability to adapt to specific image characteristics (Sharma & Kamra, 2023). Deep learning-based enhancement methods, including GANs for virtual native enhancement and deep learning reconstruction, have shown promise for more sophisticated, task-specific enhancement (Jiang et al., 2024; Sharma et al., 2021). The integration of enhancement and segmentation, whether through sequential pipelines or end-to-end learning, significantly impacts overall system performance (Z. Chen et al., 2022; Sahu & Ray, 2022; Sinha et al., 2020; Wu et al., 2021).

Deep learning fundamentals, particularly convolutional neural networks, provide the foundation for automated medical image analysis. The key innovations enabling effective deep learning for medical imaging include residual connections for training very deep networks, batch normalization for training stability, transfer learning for leveraging pre-trained models, and data augmentation for improving generalization with limited training data. However, medical imaging presents unique challenges including limited training data, severe class imbalance, domain shift across scanners and institutions, and the need for interpretability and clinical validation.

Semantic segmentation architectures have evolved from early fully convolutional networks to sophisticated architectures like U-Net and DeepLabV3+ that combine multi-scale feature extraction, precise boundary localization, and computational efficiency (D. Chen et al., 2022; Liu et al., 2021). U-Net, with its symmetric encoder-decoder structure and concatenative skip connections, has become the dominant architecture for medical image segmentation due to its effectiveness with limited training data. DeepLabV3+, combining ASPP for multi-scale context capture with an encoder-decoder structure for boundary refinement, represents the state-of-the-art for semantic segmentation and has shown excellent performance for medical imaging applications.

The choice of backbone network for feature extraction significantly impacts the trade-off between segmentation accuracy and computational efficiency. ResNet-50 provides strong feature extraction capability with good balance between depth and efficiency, making it suitable for research applications and clinical deployment with adequate computational resources. MobileNetV2 offers dramatic computational efficiency improvements through depthwise separable convolutions and inverted residual blocks, enabling real-time performance for point-of-care and mobile applications. Xception achieves state-of-the-art accuracy through extensive use of depthwise separable convolutions and deep architecture, suitable for applications where accuracy was paramount. The flexibility to choose different backbones enables adaptation to different deployment scenarios and requirements.

Multi-stage segmentation approaches that decompose the complex segmentation task into simpler sub-tasks have shown promise for myocardial scar detection (Damit et al., 2024). Compared with single-stage segmentation, which attempts to segment all anatomical structures simultaneously, multi-stage segmentation performs the task sequentially by first localizing the region of interest before conducting detailed segmentation as stated by Jacobson et al. (Jacobson et al., 2026) from his proposed methods and comparison. Coarse-to-fine strategies that first localize the region of interest then perform detailed segmentation can improve computational efficiency and accuracy. Cascaded architectures that use separate networks for myocardium segmentation and scar detection enable incorporation of anatomical constraints and reduce false positives. However, multi-stage approaches face challenges related to error propagation and increased system complexity.

Myocardial scar segmentation using deep learning has been extensively studied, with various architectures and approaches proposed. The specific challenges of myocardial scar segmentation-severe class imbalance, small object detection, variable scar appearance, and image quality issues-have motivated specialized approaches including weighted loss functions, attention mechanisms, multi-scale processing, and multi-modal fusion. U-Net variants, particularly those incorporating attention mechanisms and 3D processing, have shown strong performance. Recent work on virtual native enhancement and deep learning reconstruction demonstrates the potential for eliminating contrast agents or improving image quality at the acquisition stage.

Evaluation of myocardial scar segmentation methods requires comprehensive metrics covering spatial overlap (Dice coefficient, IoU), boundary localization and clinical relevance. The severe class imbalance in myocardial scar segmentation makes standard metrics like accuracy misleading, necessitating focus on minority class metrics. Inter-observer variability in manual segmentation complicates evaluation, as ground truth was not perfectly reliable. Clinical validation through prospective studies assessing impact on patient outcomes remains limited but was essential for clinical adoption.

Available datasets for myocardial scar segmentation remain limited, with public datasets typically including only 50-150 patients. The EMIDEC challenge dataset has become a widely used benchmark, but larger and more diverse datasets are needed for training robust models (Z. Chen et al., 2022). Annotation challenges, including the time-consuming nature of manual segmentation and inter-observer variability, limit dataset growth. Data augmentation strategies are essential for maximizing the utility of limited data, but must be carefully designed to preserve anatomical plausibility and clinical relevance.

Current challenges and research gaps include computational efficiency for real-time processing, generalizability across scanners and protocols, clinical validation and regulatory approval, explainability and clinical trust, handling of edge cases and rare pathologies, and standardization and reproducibility. Addressing these challenges requires not just technical innovations but also multi-disciplinary collaboration involving computer scientists, clinicians, regulatory experts, and patients. The path from research prototype to clinically deployed system was long and requires addressing numerous practical, regulatory, and clinical considerations

2.10.2 Identified Research Gaps

Despite significant progress, several important research gaps remain that motivate the proposed research. First, while image enhancement and segmentation have been studied extensively as separate problems, the optimal integration of these components for myocardial scar detection remains unclear. Most studies use either simple preprocessing with traditional enhancement methods or train segmentation networks on unenhanced images as stated by Zamir et al. (Zamir et al., 2021). The potential benefits of hybrid enhancement approaches that combine multiple enhancement techniques, and the optimal strategy for integrating enhancement with segmentation have not been thoroughly investigated for myocardial scar detection

Second, while DeepLabV3+ has shown excellent performance for various segmentation tasks and has been applied to some medical imaging applications, its application to myocardial scar segmentation has been limited. Most studies of myocardial scar segmentation use U-Net or its variants, with relatively few exploring DeepLabV3+ despite its theoretical advantages for this task. The multi-scale context capture through ASPP and the encoder-decoder structure with skip connections make DeepLabV3+ particularly well-suited for myocardial scar segmentation, where scars appear at multiple scales and precise boundary localization was critical. A comprehensive evaluation of DeepLabV3+ for myocardial scar segmentation was needed.

Third, the comparative analysis of different backbone networks (ResNet-50, MobileNetV2, Xception) for myocardial scar segmentation has not been thoroughly investigated. While these backbones have been compared for natural image segmentation and some medical imaging tasks, their specific performance characteristics for myocardial scar segmentation-considering the unique challenges of severe class imbalance, small object detection, and variable scar appearance-remain unclear. Understanding the accuracy-efficiency trade-offs of different backbones was essential for selecting appropriate architectures for different deployment scenarios.

Fourth, multi-stage segmentation approaches for myocardial scar detection have been explored in some studies, but the optimal stage decomposition, the choice of architectures for each stage, and strategies for training and integrating multiple stages have not been systematically investigated (Zhao et al., 2025). The potential benefits of multi-stage approaches-including improved accuracy through hierarchical processing, reduced false positives through anatomical constraints, and improved computational efficiency through region-of-interest processing-motivate further research in this direction.

Based on the identified research gaps, this research proposes a comprehensive Hybrid Image Enhancement–Image Segmentation framework that integrates hybrid image enhancement techniques with a multi-stage DeepLabV3+ segmentation architecture for automated myocardial scar detection. Unlike conventional approaches that independently perform image enhancement or segmentation, the proposed framework establishes a unified pipeline where enhanced image characteristics are utilized to improve feature representation during segmentation. Furthermore, the multi-stage strategy progressively identifies cardiac anatomical structures before myocardial scar delineation, enabling more accurate segmentation of complex and irregular scar regions. This integrated framework represents the main methodological contribution of this research by combining image processing and deep learning approaches to improve the reliability of myocardial scar analysis in LGE-CMRI images.

Table 2.1
The Overview of Literature Review on Image Segmentation Using Deep Learning for Myocardial Infarction

No	Author	Year	Dataset	Deep Learning	Performance	Image
1	Curiale et al. (Curiale et al., 2017)	2017	Sunnybrook Cardiac Dataset (SCD)	UNet	Dice= 0.8799	CMRI
2	S. Deepika et al. (Deepika & Jaisankar, 2024)	2024	Physikalisch-Technische Bundesanstalt Public: Cleveland HD	Enhanced CNN ECV-3D	Accuracy 92%	ECG MRI CT-scan
3	W. Ding et al. (Ding et al., 2023)	2023	Private: MS-CMR, Public: MYOPS2020	U-MyoPS	Dice= 62.32%	LGE-MRI
4	Z. Shaaf et al. (Shaaf et al., 2023)	2023	EMIDEC	CNN	Accuracy =0.86 IOU =0.83 DSC =0.81	LGE-CMRI
5	Fahmy et al. (Fahmy et al., 2021)	2021	Tufts Medical Center Beth Israel Deaconess Medical Center	2D U-Net	Accuracy = 91.57%.	LGE-MRI
6	Xiong, J. et al. (Xiong et al., 2021)	2021	ACDC 2017 Sunnybrook 2009	Deep RL +First P-Net (CNN) +Next-P-Net (point-centric concatenated matrix) + Deep Q Network	Precision= 0.9048 Recall= 0.9360	MRI
7	K. Wang et al. (Wang et al., 2022)	2022	MyoPS 2020	AWSNet Cascaded Anatomical Segmentation Network	Dice =0.658±0.253	LGE-CMRI

CHAPTER 3
RESEARCH METHODOLOGY

3.1 Introduction

This chapter presents the methodological framework developed to achieve accurate myocardial scar detection from LGE-CMRI images using deep learning. The proposed method integrates multiple processes, starting from data collection and pre-processing to image enhancement, segmentation, and performance evaluation. Each component of the workflow was designed to ensure data quality, model reliability, and diagnostic precision.

The primary motivation behind this framework is the clinical challenge in detecting myocardial scars accurately due to the low contrast between scar and healthy myocardium complex textures and the present of blurriness in LGE-CMRI images. Traditional segmentation techniques are often limited by intensity inhomogeneity and the variations in cardiac anatomy across patients (Fahmy et al., 2021). Consequently, manual delineation of myocardial regions remains time-consuming and prone to observer variability (Sheikhjafari et al., 2023). To overcome these limitations, this study employs a combination of image enhancement and a multi-stage deep learning segmentation model to automate and improve myocardial scar detection.

The proposed methodology follows a systematic sequence, beginning with ethically approved data acquisition from Radiology Department, AMDI USM. The LGE-CMRI data undergo a comprehensive image pre-processing phase involving resizing, augmentation, and labelling. Subsequently, two processes are proposed concurrently which are image enhancement and image segmentation. Image enhancement improves the visibility of myocardial structures using contrast enhancement and image sharpening techniques. In this process, a hybrid image enhancement was proposed by combining the best method from each of contrast enhancement and image sharpening techniques. Meanwhile in image segmentation process, a new multi-stage deep learning framework was proposed that isolates and classifies myocardial scar tissue with high precision.

The final process involved with a detailed performance evaluation to assess image enhancement and image segmentation accuracy and model generalization.

Quantitative performance metrics such as Dice Similarity Coefficient (DSC), Precision, and Recall are used to validate the efficiency of the proposed framework.

3.2 Methodology Overview

This research aims to develop an automated deep learning-based framework for myocardial scar detection using LGE-CMRI images. The overall workflow of the proposed framework, illustrated in Figure 3.1, consists of five main phases: data collection and ethical approval, image pre-processing, image enhancement, image segmentation, and performance evaluation. The pipeline follows a left-to-right structure where the pre-processed data are branched into two major components; image enhancement and image segmentation which are later integrated into a hybrid analysis for improved myocardial scar detection accuracy.

The first phase begins with data collection and ethical approval, where LGE-CMRI datasets were obtained from an ethically approved medical database. All LGE-CMRI images were anonymized to ensure patient confidentiality and standardized to a uniform image size and format. Each image was accompanied by expert-provided ground truth annotations that delineate the LV, cavity, and myocardial scar regions, serving as references for segmentation training and evaluation.

Following data acquisition, image pre-processing was performed to prepare the data for deep learning analysis. This includes image resizing, image augmentation and image labelling using MATLAB's Image Labeller to ensure consistent annotation across the dataset. Image augmentation techniques are applied to expand the dataset and improve model robustness against overfitting. The augmentation strategies include rotations at 90°, 180°, and 270°, horizontal flipping, and sequential flipping followed by rotation. Through this process, the total number of training images was significantly increased, providing a more diverse input for model learning.

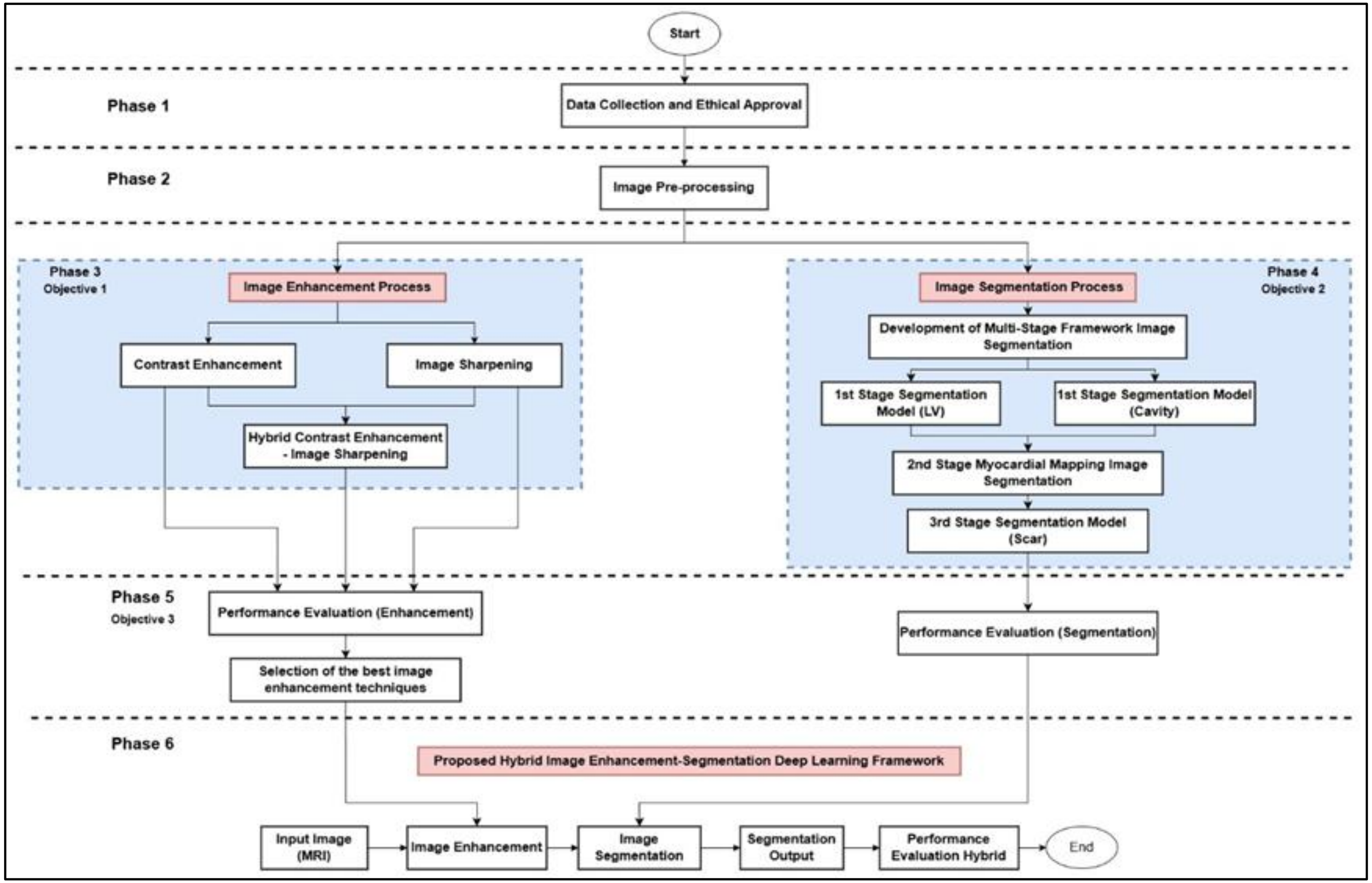

Figure 3.1 Research Overview Flowchart

After pre-processing, the workflow diverges into two key branches processes: image enhancement and image segmentation. The image enhancement process applies several contrast enhancements and image sharpening was applied to improve the visual quality of LGE-CMRI images. Enhanced images are expected to help the deep-learning based segmentation model to learn more distinct myocardial boundaries, particularly in low-contrast regions and blurry LGE-CMRI images. The proposed hybrid image enhancement approach combines both contrast enhancement and image sharpening to generate clearer representations of myocardial textures, ensuring that the deep learning model receives the most informative inputs for scar detection (Srinivas et al., 2020).

The second process was image segmentation, employs a multi-stage deep learning framework to accurately delineate myocardial regions. The overall framework is adapted from A. Damit (2024) , with modifications including the incorporation of the proposed Hybrid CE-IS module and a multi-stage segmentation strategy (Damit et al., 2024). The first stage involves two separate deep learning models for segmenting the LV and cavity independently, allowing each model to specialize in learning distinct structural features. In the second stage, the myocardial mask was generated by subtracting the cavity segmentation from the LV segmentation, thus forming an accurate myocardial region of interest (ROI). The third stage focuses on myocardial scar segmentation using a separate model trained specifically on enhanced myocardial ROIs. This multi-stage design ensures that each model focuses on a specific anatomical structure, improving segmentation precision compared to single-stage models that attempt to learn all structures simultaneously.

Finally, the performance evaluation stage measures the accuracy and reliability of the proposed framework using various quantitative metrics such DSC, IoU and accuracy. Comparative analysis was conducted between single-stage and multi-stage segmentation approaches, as well as among different backbone networks including ResNet-18, ResNet-50, and MobileNetV2. The evaluation results validate the effectiveness of the hybrid image enhancement and multi-stage segmentation framework in achieving more reliable myocardial scar detection.

3.3 Data Collection and Ethical Approval

The dataset employed in this study was obtained from the Advance Medical and Dental Institute (AMDI), Universiti Sains Malaysia (USM), consisting of LGE-CMRI images collected between 2020 and 2023. Imaging was performed at AMDI on Philips Achieva 3.0T CMRI scanner as shown in Figure 3.2. The dataset included anonymized patient scans encompassing both scar-absent (normal) and scar-present images to ensure variability in myocardial tissue appearance. All subjects involved were adults aged 18 years and above, representing a diverse range of cardiac abnormalities.

Figure 3.2 Example of CMRI Scanner (Clinical Imaging)

The dataset was curated under clinical supervision to guarantee diagnostic validity and ensure that all images adhered to standardized acquisition protocols. The original image was in DICOM format. The images were then converted and stored in BMP format with a fixed resolution of 320 × 320 pixels to maintain consistency and compatibility with the deep learning framework used in this research. Table 3.1 shows the distribution dataset of the obtained LGE-CMRI image across normal and scarred image.

Table 3.1
Distribution of Dataset for Both Normal and Scar Present LGE-CMRI Image

Type of Dataset	No. of Dataset
Normal	159
Scar-present	304
Total	463

LGE-CMRI was acquired after gadolinium administration using an inversion-recovery preparation with a gradient-echo readout, with the inversion time adjusted to null the signal from normal myocardium so that fibrotic or infarcted tissue appears conspicuously hyper enhanced as illustrated in Figure 3.3. Motion was minimized with brief breath-holds, and phase-sensitive inversion recovery (PSIR) reconstruction was used where available to stabilize contrast across varying tissue T1 values and reduce sensitivity to imperfect nulling (Wong et al., 2013). Coverage consisted of a contiguous short-axis stack from the mitral-valve plane to the apex, complemented by long-axis views when needed to clarify scar extent and transmurally. Figure 3.4 shows the difference between normal and scar-present image in LGE-CMRI. This acquisition strategy provides high conspicuity of myocardial scar and clear blood and myocardium contrast, yielding images well suited for downstream expert annotation and robust deep-learning–based segmentation.

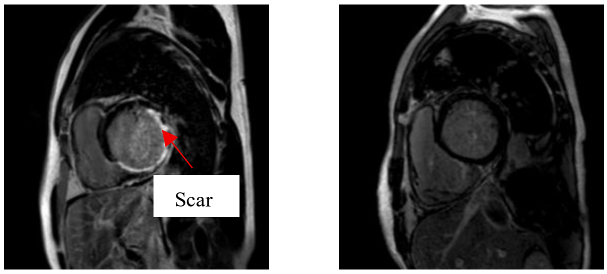

(a) Scar-present image (b) Scar-absent image

Figure 3.3 Example of Normal and Scar Image in LGE-CMRI

Prior to data collection, ethical clearance was obtained from the AMDI Research and Ethics Committee, ensuring that all research procedures complied with institutional, national, and international ethical standards for human data usage. Patient information was fully anonymized by removing all identifiable details such as name, ID, and demographic data to protect confidentiality. Informed consent was obtained from all participants prior to image acquisition, and the data were used strictly for academic and research purposes. These ethical measures were essential to maintain compliance with the Declaration of Helsinki and Malaysia’s Personal Data Protection Act (PDPA) (JEPeM Code: USM/JEPeM/21090623).

The collected LGE-CMRI images provided a diverse representation of myocardial structures and scar patterns, serving as a robust foundation for deep learning–based analysis as shown in Figure 3.4 of image with cardiac anatomical variation and Figure 3.5 of LGE-CMRI of image inhomogeneity. Each image was manually reviewed and verified by clinical experts to ensure high-quality annotations and accurate labelling of myocardial scar regions. This expert validation process helped minimize potential mislabelling errors and enhanced the reliability of ground truth data used for model training and evaluation (Wu et al., 2021). The resulting dataset formed the cornerstone of this study, supporting both the image enhancement and segmentation stages with clinically relevant and high-quality inputs.

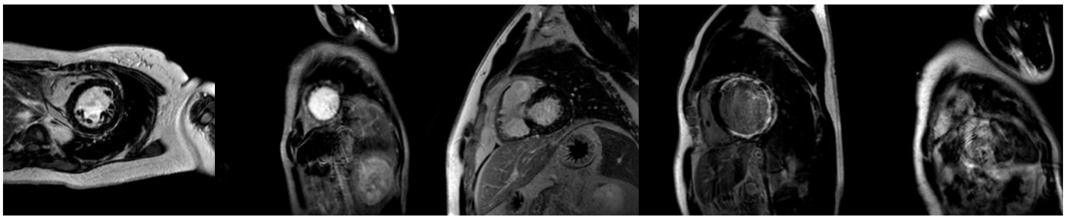

Figure 3.4 Example of LGE-CMRI Images with Variation in Cardiac Anatomy, Including Differences in Ventricular Size, Myocardial Thickness, and Heart Shape Across Patients

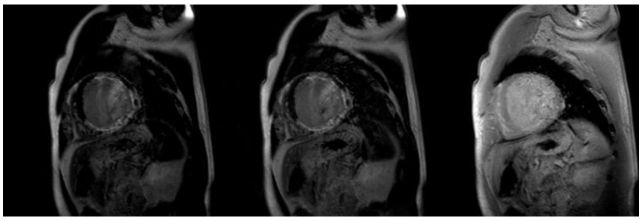

Figure 3.5 Example of LGE-CMRI Images with Intensity Inhomogeneity

3.4 Image Preprocessing

Image preprocessing is an essential procedure in preparing medical imaging datasets for deep learning applications, particularly in segmentation tasks that demand high-quality and consistent input data. Since the number of available myocardial LGE-CMRI images in this study was relatively limited, data augmentation was introduced to increase sample diversity and improve the robustness of the segmentation model. Augmentation enhances the model's generalization ability by synthetically generating new variations of existing data through controlled geometric transformations. This approach allows the model to recognize and learn from features that may appear in different intensity, size, orientations or positions.

Initially, image labelling was conducted to establish accurate ground truth annotations for supervised deep learning segmentation. The Image Labeller tool in MATLAB was utilized to manually label regions of interest (ROIs) as shown in Figure 3.6, specifically focusing on myocardial scars, LV, myocardium, and cavity regions. This tool enables precise pixel-wise annotation and ensures that each LGE-CMRI image is associated with a corresponding ground truth mask. The annotation process was performed under expert supervision to maintain clinical accuracy and consistency. Figure 3.7 illustrates an example of an original LGE-CMRI image together with its corresponding manually labelled mask. These labelled masks served as the reference data during model training and performance evaluation.

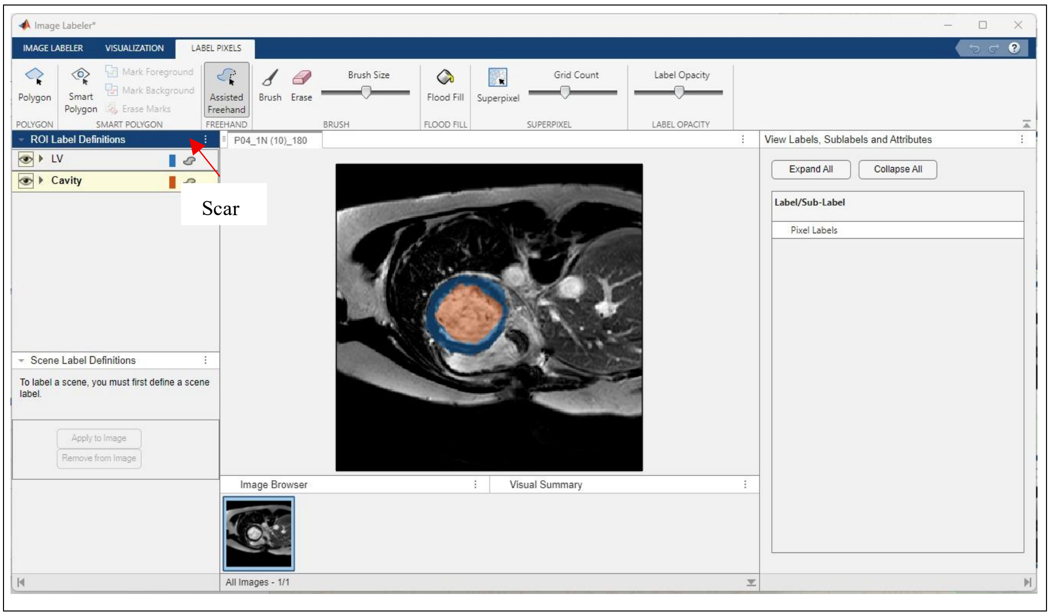

Figure 3.6 Manual Image Labelling of ROI Using MATLAB Image Labeller

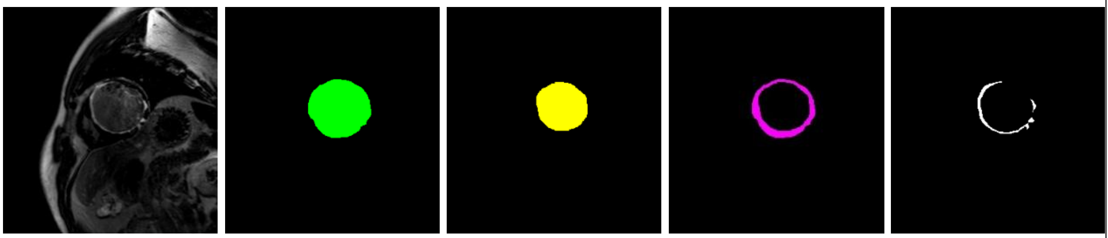

(a) Original image | (b) LV labelled image | (c) Cavity labelled image | (d) Myocardium labelled image | (e) Scar labelled image

Figure 3.7 Example of a LGE-CMRI Image and Its Cavity, Myocardium and Scar Labelled Images

Following the labelling process, data augmentation was applied to increase dataset diversity and improve the robustness of the segmentation model. Augmentation enhances model generalization by synthetically generating additional training samples through controlled geometric transformations while maintaining the correspondence between the original images and their ground truth mask. In this study, three augmentation strategies were used: (1) rotation at 90°, 180°, and 270°, (2) horizontal flipping, and (3) sequential flipping followed by rotation at 90°, 180°, and 270°. These methods were selected because they effectively simulate possible variations in patient positioning or image acquisition angles while preserving the anatomical integrity of the myocardial structures.

Through the augmentation process, the dataset was expanded from 463 original images to a total of 3,704 images. As shown in Table 3.2 show the distribution of dataset before and after augmentation process. This expansion provided a more comprehensive representation of the myocardium and scar patterns, ensuring that the model could learn from a wider range of spatial distributions. The augmented dataset consequently strengthened the model's ability to detect myocardial scars under varying conditions of orientation and geometry.

Table 3.2
The Distribution of Dataset Before and After Augmentation Process

Type of Dataset	**Original Image**	**Rotational**			**Horizontal Flipping**	**Horizontal Flipping Followed by Rotational**			**Total**
		90	**180**	**270**		**90**	**180**	**270**	
Normal	159	159	159	159	159	159	159	159	1272
Scar-present	304	304	304	304	304	304	304	304	2432
Total	463	463	463	463	463	463	463	463	3704

Following the completion of augmentation process, the dataset of 3,704 LGE-CMRI images was distributed into training and testing sets to support supervised deep learning and objective performance evaluation. The distribution was performed after image augmentation, ensuring that augmented images were properly included while maintaining the pairing between each image and its corresponding ground truth mask. A 70%–30% allocation was adopted, resulting in 2,593 images for training and 1,111 images for testing. The training set was used for model learning, allowing the network to learn to identify and distinguish the left ventricle (LV), myocardium, cavity, and myocardial scar regions. During this phase, the model's parameters were optimized by minimizing the loss function through repeated comparison between predicted outputs and manually labelled masks. Incorporating augmented images in the training set increased data variability, enhancing the model's ability to generalize across differences in image intensity, orientation, and anatomical structure.

The testing dataset, consisting of 1,111 images, was used to evaluate the performance of the trained model. By keeping these images separate from the training data, an unbiased assessment of the model's generalization capability was ensured. Segmentation performance was quantified using metrics such as DSC and IoU, which reflect how accurately the predicted masks correspond to the ground truth annotations. The 70%–30% distribution thus provides a balanced approach, allowing the model to learn effectively from a substantial training set while preserving an independent subset for reliable and clinically meaningful performance evaluation.

Through this comprehensive image preprocessing workflow, the dataset became more balanced and statistically diverse, providing the deep learning model with sufficient variability for effective feature learning. The integration of augmentation and expert-guided labelling ensured that the model was exposed to realistic myocardial variations, ultimately improving segmentation accuracy and generalization across unseen CMRI data.

3.5 Proposed Image Enhancement of LGE-CMRI Images

Image enhancement plays a vital role in the preprocessing stage of medical image analysis, particularly for LGE-CMRI-based studies where low contrast and blurriness are common (Qiu et al., 2022; Srinivas et al., 2020). In LGE-CMRI, these challenges often obscure the myocardial boundaries, making it difficult to differentiate between normal and scarred tissue. Enhancement techniques aim to improve the visibility of relevant structures by adjusting pixel intensity distributions, increasing contrast, and emphasizing important anatomical details. The primary objective of image enhancement in this study was to optimize visual quality for subsequent segmentation using a deep learning framework, thereby ensuring that the model can learn meaningful features from high-quality input data.

Several enhancement techniques have been proposed in previous research to address the limitations of LGE-CMRI quality. Conventional approaches such as Histogram Equalization (HE), Contrast-Limited Adaptive Histogram Equalization (CLAHE), Type-II Fuzzy enhancement, and Morphological Residual Processing (MRP) have been widely applied to improve global and local contrast in medical images. These four techniques were selected because they are effective and widely recognized for general image enhancement and are particularly suitable for LGE-CMRI data characterized by low contrast and subtle myocardial scar blurry boundaries, where improved visibility of myocardial structures and scar regions is critical for accurate segmentation (Rehman et al., 2024). Although numerous contrast enhancement methods are available in the literature, only these four techniques were chosen in this study because they represent complementary strategies with proven effectiveness in medical imaging applications. Specifically, HE provides global contrast redistribution, CLAHE offers localized contrast improvement with noise control, Type-II Fuzzy enhancement handles uncertainty and subtle intensity variations, and MRP enhances multi-scale details while preserving structural consistency.

To overcome these limitations of low contrast and blurry LGE-CMRI images, this study integrates both contrast enhancement and sharpening into a hybrid image processing approach, aiming to balance contrast improvement and edge preservation. The hybrid method leverages the global contrast optimization capability of enhancement algorithms and the edge refinement ability of sharpening filters, resulting in a more visually consistent and diagnostically informative image. This enhanced image quality serves as a stronger foundation for deep learning-based segmentation, particularly in detecting myocardial scars where precision and clarity are critical.

3.5.1 Contrast Enhancement Technique

Contrast enhancement was one of the fundamental preprocessing operations in medical imaging, primarily aimed at improving the perceptual quality and diagnostic interpretability of grayscale LGE-CMRI images. In LGE-CMRI, the myocardium often exhibits low-intensity variations between healthy and infarcted regions due to limitations in acquisition settings, magnetic field inhomogeneities, and patient motion artifacts. Such issues reduce the visibility of tissue contrast, leading to potential misclassification during automated segmentation. Hence, contrast enhancement becomes essential for redistributing pixel intensity values and improving the visibility of relevant structures before applying advanced segmentation frameworks.

Histogram Equalization

A classical and widely used technique for global contrast improvement is Histogram Equalization (HE). HE works by uniformly redistributing the intensity values across the entire histogram, thereby expanding the dynamic range of pixel brightness (Jiang et al., 2024). This method enhances global contrast and reveals hidden structural details in underexposed regions. However, HE has the tendency to amplify noise and over-enhance bright regions, especially in medical images where the tissue intensity differences are subtle. For instance, when applied to myocardial LGE-CMRI, HE may exaggerate background intensities or suppress fine textural information, leading to visual distortion. Despite these limitations, HE serves as a valuable baseline due to its simplicity and effectiveness in increasing overall image contrast.

In this study, HE was applied to the pre-processed grayscale LGE-CMRI images using the default parameter settings, where no additional adjustment was performed, to enhance overall brightness distribution and reveal low-contrast regions. The simplicity of this method allows for straightforward implementation without parameter tuning, making it suitable as an initial reference for contrast enhancement. The application of HE provides a uniform intensity transformation across the image, ensuring that all regions are enhanced consistently (Srinivas et al., 2020). Although global enhancement may not account for local intensity variations, the method serves as a useful benchmark for evaluating the effectiveness of more adaptive contrast enhancement techniques. The enhanced images obtained using HE were retained for comparative analysis during the enhancement selection process.

Contrast Limited Adaptive Histogram Equalization

To address the over-enhancement problem of traditional HE, an adaptive version known as CLAHE has been widely adopted (Rehman et al., 2024). Unlike HE, which treats the image globally, CLAHE divides the image into smaller contextual regions called tiles and applies localized histogram equalization on each. A clipping limit was then introduced to prevent the excessive amplification of noise within homogeneous regions. This localized adjustment enables CLAHE to enhance local contrast without distorting the global brightness distribution, making it particularly suitable for medical applications (Sharma & Kamra, 2023).

In this study, CLAHE was applied to the pre-processed grayscale LGE-CMRI images with a ClipLimit of 0.002, which ensured controlled local contrast enhancement while preventing noise amplification. By focusing on local intensity variations, CLAHE improved the visibility of myocardial structures and subtle scar regions, which are often difficult to distinguish in LGE-CMRI due to low contrast and gradual intensity transitions. This method produced images with a more stable intensity balance within the myocardium, maintaining smooth transitions between adjacent tissues. Compared to traditional HE, CLAHE provided clearer and more diagnostically informative images, making it highly suitable as a preprocessing step for deep learning-based segmentation.

Moreover, CLAHE's adaptive approach allowed it to enhance low-contrast areas without over-brightening high-intensity regions, preserving overall image integrity. This balance between enhancement and preservation of natural tissue appearance is critical for accurate segmentation of myocardial scars, as the subsequent deep learning model relies on both intensity cues and structural details to generate precise masks. The images enhanced using CLAHE were therefore retained as part of the hybrid enhancement pipeline and served as a benchmark to evaluate other contrast enhancement methods.

Type-II Fuzzy Set-based contrast enhancement

Another method considered in this research was the Type-II Fuzzy Set (T2FS)-based contrast enhancement approach. Unlike traditional methods that rely solely on histogram statistics, T2FS employs fuzzy logic to manage uncertainties in pixel intensity classification (Abduvaitov et al., 2025; Al-Ameen, 2021). Type-II fuzzy set–based contrast enhancement has been widely investigated as an advanced alternative to conventional image enhancement techniques, particularly for images with ambiguous or overlapping intensity distributions. In medical images, pixel intensities often do not follow clear boundaries due to noise, partial volume effects, and low contrast between adjacent tissues. Traditional enhancement methods and Type-I fuzzy systems assume precise membership values, which limits their ability to handle such uncertainty.

The key advantage of Type-II fuzzy sets lies in their ability to explicitly model uncertainty within the membership functions. Instead of assigning a single membership value to each pixel, Type-II fuzzy systems define a range of possible membership values, allowing greater flexibility in representing intensity ambiguity. In this research, the uncertainty parameter η was set to 0.2, providing a controlled degree of fuzziness that enhances subtle intensity differences while preventing over-amplification of noise. This adaptive behaviour helps preserve important structural details and improves overall contrast, which is critical for LGE-CMRI images characterized by low contrast and subtle myocardial scar boundaries. By adjusting η, the enhancement process can better highlight myocardial structures and scar regions, making the images more suitable for subsequent deep learning-based segmentation. Li et al. (Li et al., 2024) demonstrated that this additional degree of uncertainty enables the enhancement process to adapt more effectively to local image characteristics, particularly in regions with gradual intensity transitions.

Recent improvements to Type-II fuzzy enhancement algorithms have focused on optimizing membership function design and inference mechanisms to achieve better visual quality and stability. Several studies reported that improved Type-II fuzzy approaches outperform traditional histogram-based and Type-I fuzzy methods in terms of contrast improvement and noise suppression. According to Zhang et al. (Zhang et al., 2024), these methods produce more balanced enhancement results, avoiding over-enhancement while maintaining texture continuity. Such properties make Type-II fuzzy set–based techniques well suited for medical imaging applications, where accurate visualization of subtle tissue differences is essential for subsequent analysis and diagnosis.

Morphological Residual Processing

Morphologically Residuals Processing (MRP) is a contrast enhancement strategy introduced to address the inherent limitations of conventional enhancement techniques when applied to medical images that exhibit low contrast and subtle structural variations. Lepcha et al. (Lepcha et al., 2022) proposed this method based on the observation that important anatomical details are often embedded in residual components that are suppressed or distorted by traditional global enhancement approaches. Instead of directly enhancing the original image, the MRP method focuses on extracting and processing residual information that represents meaningful intensity transitions, such as tissue boundaries and pathological regions. This residual-driven strategy allows the enhancement process to be more selective and structurally aware, which is essential for medical images where diagnostic information relies on fine grayscale differences.

The MRP framework begins by applying a linear low-pass filtering operation to the original image in order to obtain a smoothed version that represents the global intensity distribution. The residual image is then computed as the difference between the original image and the low-pass filtered output. Lepcha et al. (Lepcha et al., 2022) demonstrated that these residuals effectively capture local contrast variations and edge-related information that are often under-represented in low-contrast medical images. Morphological operations are subsequently applied to the residual image using a specially designed structuring kernel, enabling the selective extraction of significant residual components while suppressing insignificant noise. This morphological processing step is crucial, as it allows the enhancement process to adapt to the size, shape, and spatial distribution of anatomical structures present in the image.

Following residual extraction, the enhanced image is reconstructed by integrating the morphologically processed residuals back into the smoothed image, maintaining global brightness consistency while selectively amplifying local contrast. In this study, the MRP parameters were set as follows: $t = 0.005$, the amplitude threshold for detecting significant residuals; $s = 50$, the size threshold controlling the structuring kernel to match anatomical features; $c = 1.5$, the contrast coefficient determining the contribution of residuals during reconstruction; and $\sigma = 1.5$, the standard deviation of the Gaussian filter used for low-pass smoothing. These parameter settings ensured optimal enhancement of myocardial structures and scar regions while minimizing noise amplification and preserving fine anatomical details.

3.5.2 Image Sharpening Technique

Image sharpening was incorporated in this study as an essential preprocessing step to improve the clarity of anatomical structures in LGE-CMRI images. Previous studies have stated that even after contrast enhancement, medical images may still suffer from blurred edges and weak boundary definition due to acquisition limitations and tissue heterogeneity. In CMRI, this issue is further compounded by intensity inhomogeneity, complex myocardial anatomy, and subtle textural differences between healthy and infarcted tissue.

Several studies have reported that sharpening techniques improve the visibility of high-frequency image components, such as tissue boundaries and structural transitions, which are critical for accurate myocardial analysis (E et al., 2025). However, the sharpening process must be carefully controlled, as excessive sharpening may amplify noise or introduce artificial contours, especially in low-signal regions. Therefore, this study explored multiple image sharpening techniques to identify an approach that enhances edge visibility while preserving anatomical realism and texture integrity. Several commonly used sharpening methods were applied and evaluated, including Unsharp Masking, High-Boost Filtering, Laplacian Filtering, and an adaptive sharpening technique. These techniques were selected to represent different sharpening principles, ranging from linear high-frequency amplification to adaptive and context-aware enhancement. Each method was applied under consistent preprocessing conditions to ensure fair assessment. The sharpening techniques explored in this study are described in the following subsections.

Unsharp Masking

Unsharp Masking was implemented in this study as a baseline image sharpening technique due to its simplicity and widespread use in medical image processing. The method enhances edge visibility by amplifying high-frequency image components that correspond to intensity transitions and structural boundaries. This is achieved by first generating a blurred version of the input image, typically using a Gaussian smoothing operation, and then subtracting this blurred image from the original image. The resulting difference image highlights edges and fine details, which are subsequently added back to the original image to produce a sharpened output. In this study, Unsharp Masking was applied after the contrast enhancement stage to further improve the visibility of myocardial contours, ventricular boundaries, and tissue interfaces in LGE-CMRI images. The default parameter values suggested by the original implementation were used, ensuring balanced edge enhancement while avoiding excessive noise amplification. These settings provided sufficient sharpening to highlight myocardial scar boundaries and subtle tissue structures without introducing artifacts that could interfere with subsequent segmentation.

The application of Unsharp Masking was intended to address residual blurring that remains after contrast enhancement, particularly in regions where myocardial scar boundaries are subtle or poorly defined. By emphasizing local intensity transitions, this method improves the perceptual clarity of anatomical structures, which is important for both visual inspection and automated segmentation. The Gaussian blur used to generate the difference image determines the scale of edges that are enhanced, while the weighting of the difference image controls the strength of sharpening. Together, these parameters ensure that the method can selectively enhance fine structural details without altering the overall intensity distribution of the image.

However, LGE-CMRI images often exhibit complex myocardial textures, low-contrast scar regions, and intensity inhomogeneity across the myocardium. Under these conditions, Unsharp Masking may unintentionally introduce halo artifacts around strong edges or suppress fine textural information in low-intensity regions. These limitations were considered during implementation and motivated the evaluation of additional sharpening techniques that provide improved adaptivity and noise control. By carefully tuning and applying the default parameters, this study ensured that Unsharp Masking effectively complemented the contrast enhancement stage, producing clearer and more diagnostically informative images suitable for subsequent deep learning-based myocardial scar segmentation.

High-Boost Filter

High-Boost Filter was implemented as an extension of the Unsharp Masking technique to provide greater flexibility in controlling the degree of image sharpening (Almas & Sharma, 2020). Unlike standard Unsharp Masking, which only adds the high-frequency components back to the original image, High-Boost Filter introduces a gain factor that allows both the original image and the amplified high-frequency details to contribute to the final output. In this study, the method was applied after the contrast enhancement stage to emphasize myocardial boundaries and intensity transitions that may remain subtle in LGE-CMRI images. The gain parameter was set to $k = 0.3$, which moderates the amplification of high-frequency components while preserving the original image structure. This value was chosen to provide sufficient edge enhancement for subtle myocardial scars without over-amplifying noise or creating artificial edges. High-Boost Filter can be expressed mathematically as equation (3.1):

$$g(x,y)=A\cdot f(x,y)- f_{LP}(x,y) \tag{3.1}$$

where g(x,y)is the enhanced image, f(x,y) is the original image $f_{LP}(x,y)$ is the low-pass filtered image, and *A* is the amplification factor as A=1+k, and k is the gain factor controlling the contribution of the original image intensity in the final output. By including k, the method allows the original pixel values to be reinforced alongside the high-frequency details extracted from the residual, improving the clarity of edges and fine structures. In LGE-CMRI, where myocardial scar regions and ventricular boundaries are often low-contrast, this controlled amplification helps enhance critical anatomical features for better visualization and subsequent segmentation.

However, because High-Boost Filter amplifies high-frequency components more aggressively than standard Unsharp Masking, it can increase sensitivity to noise, particularly in low-signal regions such as infarcted myocardium. Excessive boosting may result in over-enhanced edges, artificial contours, or amplified background noise that do not correspond to true anatomical structures. By selecting k = 0.3, this study balanced enhancement strength and structural preservation, producing images that highlight subtle myocardial scars while minimizing artifacts. This makes High-Boost Filter a suitable complementary sharpening technique for LGE-CMRI preprocessing before deep learning-based myocardial scar segmentation.

Laplacian Filter

Laplacian Filtering was applied as a second-order derivative-based sharpening technique designed to highlight rapid changes in image intensity. The method operates by detecting areas where the intensity changes sharply, such as edges and fine structural details, and enhancing these regions to improve visual clarity (Rehman et al., 2024). In this study, Laplacian Filtering was used to emphasize myocardial boundaries and transitions between healthy and infarcted tissue in LGE-CMRI images. The Laplacian operator was implemented using a scaled kernel defined as Equation (3.2):

$$\nabla^2 f=\frac{\partial^2 f}{\partial x^2}+ \frac{\partial^2 f}{\partial y^2} \tag{3.2}$$

where f(x,y) represents the image intensity at spatial location(x, y) (Woods, 2012). In discrete implementation, this second-order derivative was approximated using a convolution kernel. To control the strength of edge enhancement, a scaling parameter was introduced, and the sharpened image was computed as Equation (3.3):

$$g(x,y)=f(x,y)-k\ \nabla^2 f(x,y) \tag{3.3}$$

where g(x,y) is the enhanced image and k=0.3 is the sharpening coefficient. The parameter $k$regulates the contribution of the Laplacian response to the final output. A moderate value of $k = 0.3$was selected in this study to enhance myocardial contours and subtle tissue transitions while preventing excessive amplification of noise.

Despite its effectiveness in edge enhancement, Laplacian Filtering is inherently sensitive to noise and intensity fluctuations. LGE-CMRI images often exhibit intensity inhomogeneity, acquisition artifacts, and noise due to patient motion or scanner variability (Xing et al., 2023). Under such conditions, the Laplacian operator may amplify irrelevant intensity variations, leading to spurious edges and loss of anatomical consistency. These limitations reduce the suitability of Laplacian Filtering as a standalone sharpening approach and highlight the need for more adaptive techniques.

Nimble Filter

The Nimble Filter was implemented as an adaptive and nonlinear sharpening technique designed to enhance structural details while suppressing noise. Unlike traditional linear sharpening methods, the Nimble Filter combines morphological operations with bilateral filtering principles to selectively enhance edges based on local intensity variance and spatial information (E et al., 2025). In this study, the filter was applied to sharpen myocardial boundaries and texture regions while preserving homogeneous areas such as healthy myocardium and blood pools. The sharpening strength was controlled using the parameter $\eta = 0.3$, which regulates the contribution of the enhancement component to the final output. This adaptive weighting ensures that structural details are enhanced moderately without introducing excessive intensity distortion. Mathematically, the sharpened image can be expressed as Equation (3.4):

$$g(x,y)=f(x,y)-\eta \cdot R(x,y) \tag{3.4}$$

where f(x,y) represents the original image, R(x,y)denotes the detail enhancement response generated by the Nimble filtering process, and $\eta$is the refinement coefficient controlling enhancement strength. The parameter $\eta = 0.3$ was selected to provide balanced sharpening, allowing subtle myocardial scar boundaries to be emphasized while preventing over-amplification of noise (Al-Ameen, 2018).

The Nimble Filter enables progressive refinement of image details, reducing the risk of over-sharpening and artificial contour generation. Its bilateral component considers both spatial proximity and intensity similarity, which helps maintain edge integrity while minimizing noise amplification. Zohair et al. (Al-Ameen, 2018) demonstrated that this approach produces more natural and stable sharpening results in complex medical images compared to conventional methods. These characteristics make the Nimble Filter particularly suitable for LGE-CMRI preprocessing, where accurate representation of myocardial anatomy and scar boundaries is critical for reliable segmentation performance.

3.5.3 Hybrid Contrast Enhancement–Image Sharpening

In this study, hybrid contrast enhancement–image sharpening (Hybrid CE-IS) framework was proposed by combining the best-performing contrast enhancement method with the most effective image sharpening technique, as identified through preliminary experiments (Srinivas et al., 2020). The contrast enhancement stage was applied first to improve the overall intensity distribution of the LGE-CMRI images. This process aimed to increase the visibility of myocardial tissue and scar regions by enhancing subtle grayscale differences while maintaining a consistent appearance across the image. By reducing low-contrast regions and intensity imbalance, the enhanced images provide a clearer representation of myocardial structures.

After contrast enhancement, an image sharpening stage was applied to further refine the visual quality of the images. This stage focused on improving the clarity of myocardial boundaries and fine structural details without excessively increasing noise. The sharpening process selectively emphasized important edges and texture patterns related to the myocardium while preserving smooth regions. Applying sharpening after contrast enhancement allowed the process to focus on meaningful anatomical features rather than amplifying unwanted noise or artifacts.

The combination of enhancement and sharpening was carried out in a sequential manner to ensure stable and balanced image improvement. The contrast enhancement stage prepared the image by improving global visibility, while the sharpening stage refined local details based on the enhanced intensity information. This interaction between the two stages helped to avoid common problems such as over-enhancement, artificial edges, or loss of anatomical realism.

As a result, the hybrid framework was expected to produce images that were clearer and more consistent for further analysis (Chen et al., 2020). The effectiveness of the hybrid approach was observed through both visual inspection and numerical evaluation. The overall workflow of the hybrid contrast enhancement and image sharpening process is illustrated in Figure 3.8 which shows the sequential processing from the original LGE-CMRI image to the final hybrid-enhanced output.

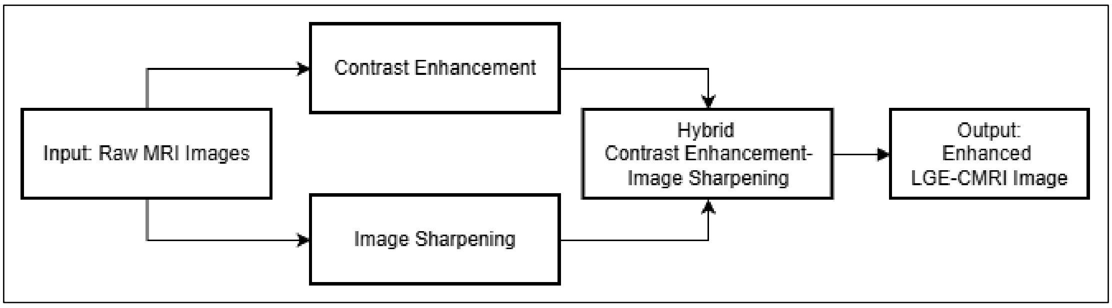

Figure 3.8 Block Diagram on Proposed Hybrid CE – IS

3.6 Proposed Image Segmentation Using Multi-Stage DeepLabV3+ Framework

Image segmentation serves as a fundamental process in medical image analysis, particularly in LGE-CMRI, where it facilitates the extraction of anatomically relevant and clinically significant structures. In the present study, segmentation was conducted to precisely isolate the myocardial scar region from LGE-CMRI images. Accurate segmentation of this region was vital for the quantitative assessment of myocardial infarction, as it enables the estimation of infarct size, the localisation of viable and non-viable myocardial tissue, and the derivation of clinically interpretable parameters that assist cardiologists in diagnosis and therapeutic planning (Luo et al., 2020).

Despite its importance, myocardial scar segmentation remains a technically challenging task due to several factors, including low contrast between fibrotic and healthy myocardium, intensity inhomogeneity, partial volume effects, and inter-patient variations in cardiac anatomy and pathology. To overcome these limitations, a deep learning-based segmentation approach was proposed using the DeepLabV3+ framework, which provides an effective balance between spatial precision and contextual understanding through its encoder–decoder design. This model is capable of capturing both fine-grained boundary details and multi-scale contextual information, making it well suited for the segmentation of complex cardiac structures and pathological regions. A multi-stage segmentation framework is adopted to further enhance segmentation accuracy. Fig 3.9 shows the proposed image segmentation flowchart using Multi-stage DeepLabV3+ framework.

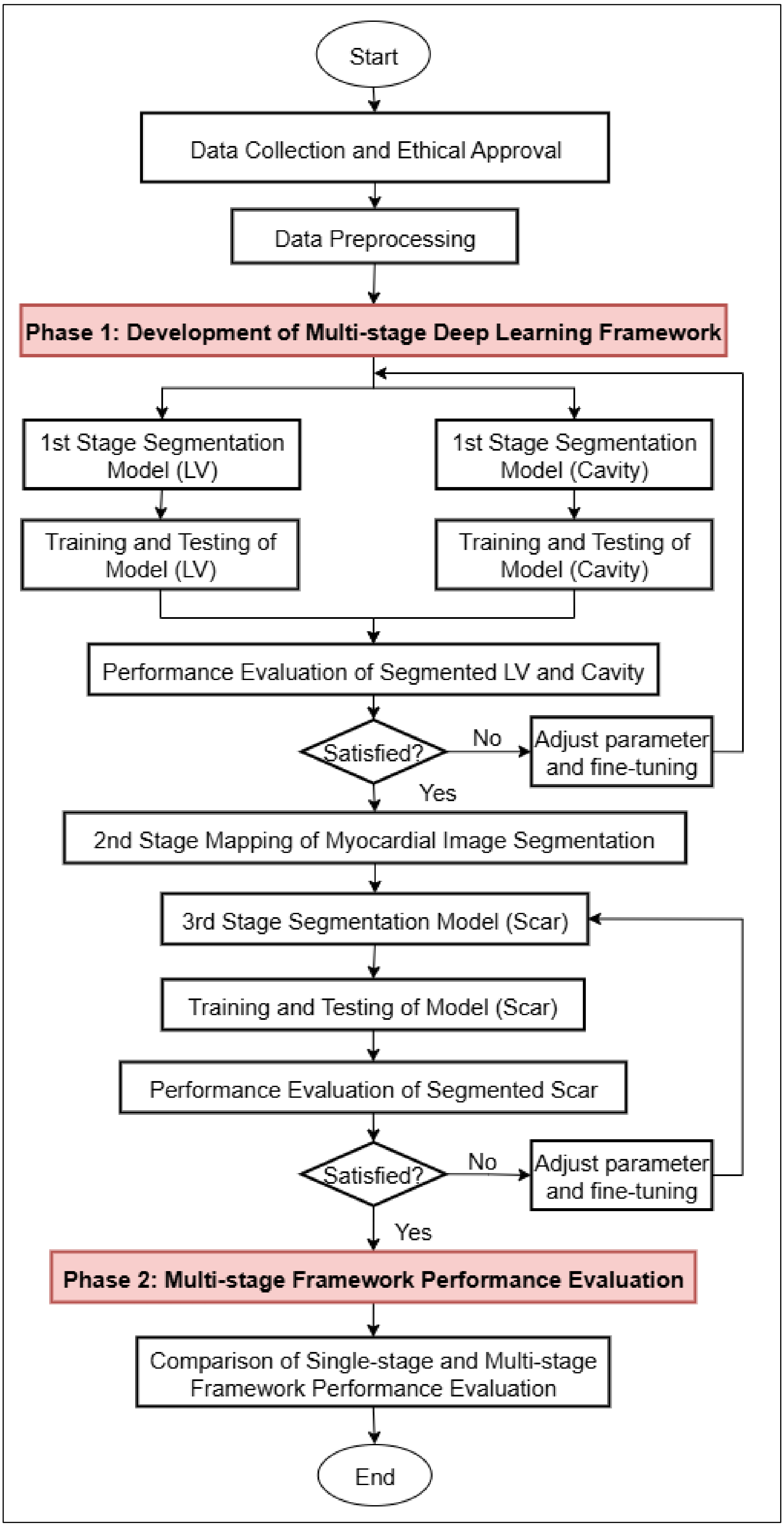

Figure 3.9 Flowchart of Multi-stage DeepLabV3+ Framework for Scar Segmentation

DeepLabV3+ was a CNN architecture widely recognised for its effectiveness in semantic image segmentation tasks. It was developed to improve segmentation accuracy by combining strong feature extraction with precise boundary refinement (Chen et al., 2023). The network adopts an encoder–decoder structure as shown in Fig 3.10, where the encoder captures important image features, and the decoder reconstructs detailed segmentation maps. The encoder uses a technique called Atrous Spatial Pyramid Pooling (ASPP), which applies several atrous (dilated) convolutions with different dilation rates to gather information from multiple scales. This approach enables the model to capture both global context and local stuctural details without reducing the image resolution.

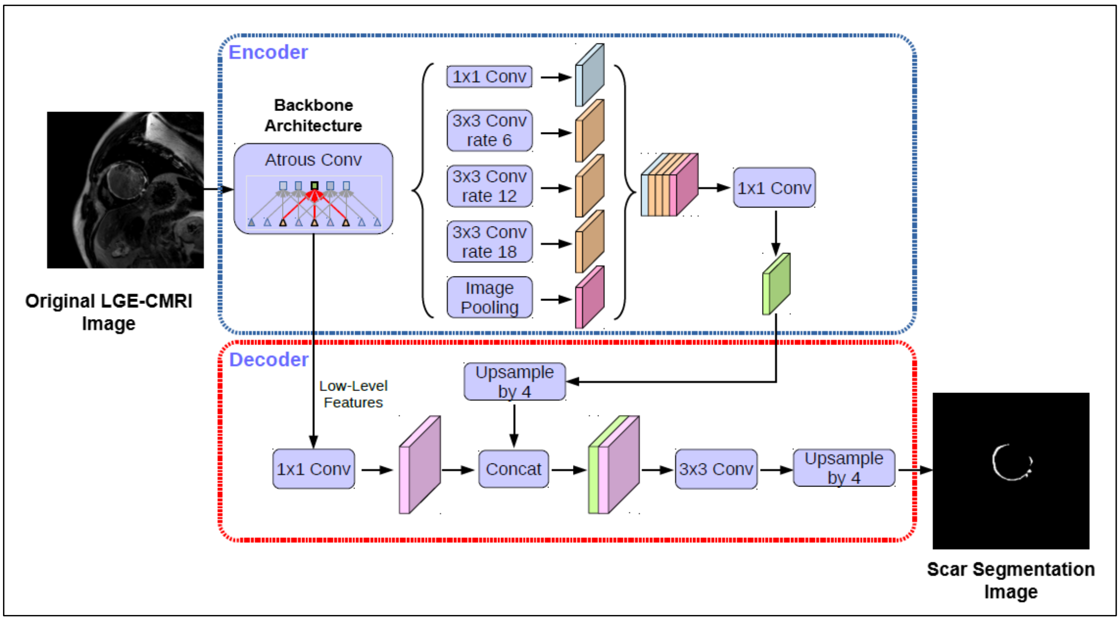

Figure 3.10 DeepLabV3+ Architecture

The decoder then refines the segmentation output by merging the high-level semantic features from the encoder with low-level spatial information, resulting in sharper and more accurate object boundaries. This combination of global and local feature learning allows DeepLabV3+ to perform well even in complex medical images, where accurate boundary detection was essential. Therefore, in this study, DeepLabV3+ is selected as the main segmentation model due to its proven ability to capture detailed cardiac structures and differentiate between healthy myocardium and scar tissue in LGE-CMRI images.

The training process of the DeepLabV3+ model was designed to ensure robust performance and generalisation across all three segmentation stages. The dataset used in this study was divided into training, validation, and testing subsets to enable fair and unbiased evaluation of the model's performance. During training, each model learned to accurately segment specific cardiac structures of the LV, the cavity, and the myocardium, based on its corresponding ground-truth labels. The optimisation process minimised a combined loss function that balanced both region overlap and pixel-wise classification accuracy.

The training parameters of the proposed deep learning segmentation model was carried out using the Adaptive Moment Estimation (Adam) optimisation algorithm, as shown in Table 3.3 which is widely adopted for training convolutional neural networks due to its ability to adaptively adjust learning rates for individual parameters. This adaptive behaviour is particularly beneficial when dealing with medical imaging data such as LGE-CMRI, where intensity distributions and feature scales vary across different regions of the image. The initial learning rate was fixed at 0.0001 to ensure stable and gradual updates of the network weights during the optimisation process (Hong & Zhang, 2023; Qi et al., 2021). A gradient decay factor (β) of 0.999 was employed to maintain a smooth exponential moving average of the squared gradients, which helps reduce sudden oscillations and promotes stable convergence (Vesal et al., 2020). The training process was executed for a maximum of 30 epochs, allowing the network sufficient exposure to the training data while avoiding prolonged training that could increase the likelihood of overfitting.

Table 3.3
Model Framework Training Parameters

Parameter	**Initialization**
Training algorithm	Adam
Initial learning rate, α	0.0001
Gradient decay factor, β	0.999
Maximum Epoch	30
Mini batch size	8
Validation Frequency	50
Execute environment	GPU

A mini-batch size of 8 was selected to balance memory usage and gradient estimation stability, particularly given the high spatial resolution of CMRI images (S. Wang et al., 2023). Throughout training, model performance was monitored at a validation frequency of 50 iterations to observe learning trends and ensure consistent optimisation behaviour. In order to improve the generalisation capability of the model, data augmentation techniques including image rotation, horizontal flipping, and slight intensity variations were applied during the training phase. These transformations were designed to simulate realistic variations in cardiac orientation, anatomical differences among patients, and acquisition-related intensity changes in LGE-CMRI data. By exposing the model to a wider range of image variations, the training process encouraged the learning of more robust and invariant feature representations. All training procedures were executed in a GPU-based computing environment to accelerate computation and enable efficient training of the proposed framework.

As illustrated in Fig 3.11, the proposed segmentation framework was divided into three primary stages. In the first stage, two independent DeepLabV3+ models were developed to segment the LV and cavity separately. Each model performs a binary segmentation task, distinguishing the target region from the background. By training each model independently, the model can specialise in learning the unique spatial and structural features of one specific region, rather than handling multiple overlapping classes simultaneously. This separation reduces class ambiguity and improves boundary precision for both the myocardial wall and the cavity region. The resulting LV and cavity segmentation serve as the anatomical foundation for subsequent myocardial mapping.

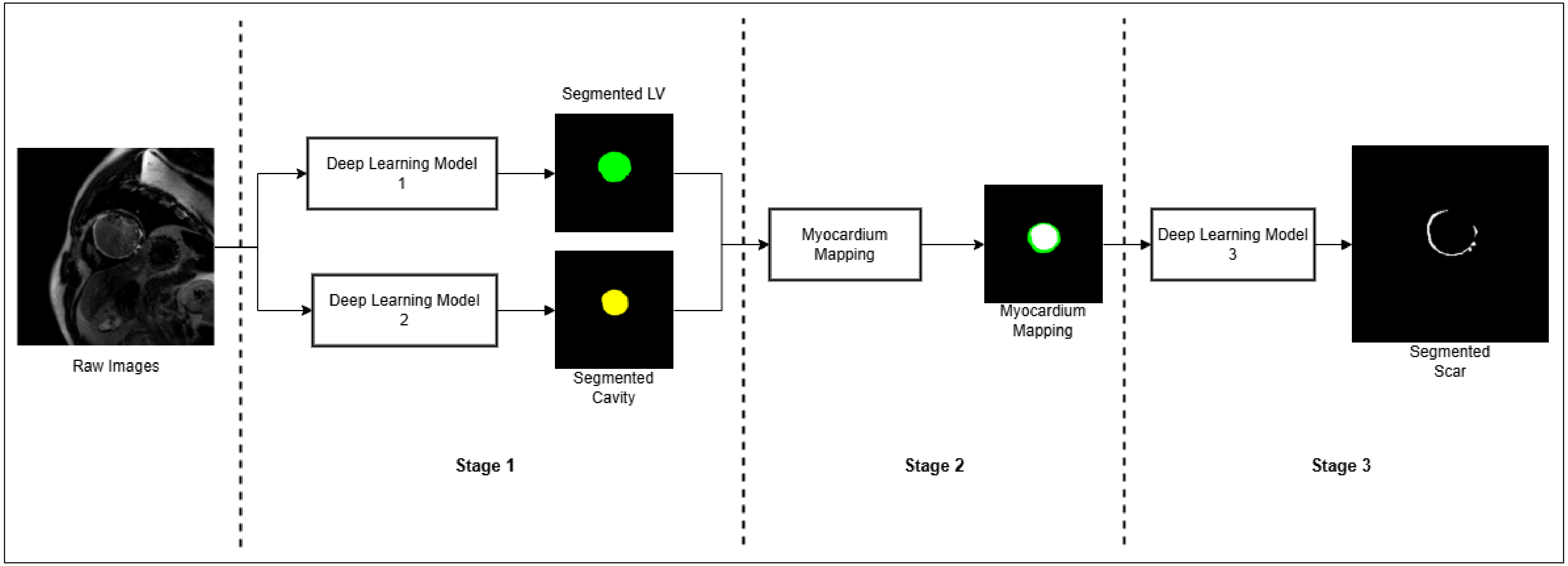

Figure 3.11 Multi-Stage DeepLabV3+ Image Segmentation Framework

In the second stage, the myocardial region was obtained using the segmentation results of the LV and cavity from Stage 1. The myocardium represents the muscular layer of the heart that lies between the LV boundary and the cavity. This step involves mapping LV and cavity segmented images to produce a myocardial segmented images that precisely defines the region of interest for subsequent analysis. Establishing these myocardial segmented images are essential because scars are exclusively located within this region. By restricting the focus to the myocardium, the following stage can learn and identify scar tissues more effectively while ignoring irrelevant areas. Furthermore, this mapping process helps reduce computational complexity by narrowing the segmentation focus to a smaller, anatomically relevant area. As a result, the segmentation performance was expected to become more stable, consistent, and clinically interpretable.

The third stage was dedicated to the segmentation of myocardial scars within the previously defined myocardial region. A separate DeepLabV3+ model was trained in this stage, using the myocardial images generated from Stage 2 as the primary input. By focusing exclusively on the myocardium, the model can learn discriminative features that distinguish fibrotic scar tissue from healthy myocardial tissue. This targeted learning approach improves segmentation precision by guiding the model's attention toward the most relevant anatomical region. The model processes the LGE-CMRI images and produces a binary scar mask that represents the distribution of scarred areas within the myocardium.

This stage benefits from the reduced search space and improved anatomical constraints established in the earlier stages. Since the model only analyses the myocardium, it minimizes false predictions outside the heart and enhances the reliability of scar localization. Overall, Stage 3 completes the multi-stage framework by translating the refined anatomical representation into a clinically meaningful segmentation of myocardial scar regions that can be used by radiologist in MI diagnosis through measurement of scar size and distribution.

In this study, three backbone architectures were examined to determine the most suitable feature extractor for the DeepLabV3+ framework used across all three segmentation stages. The backbone functions as the encoder within the model, responsible for learning hierarchical image representations that capture both global context and fine structural details. Selecting an appropriate backbone was essential, as it directly influences segmentation precision, computational efficiency, and model convergence behaviour. Three commonly adopted convolutional backbones were investigated in this work-ResNet-50, MobileNetV2, and Xception, each offering unique strengths in terms of feature representation and efficiency.

ResNet-50

ResNet-50 was employed in this study as a deep and high-capacity backbone to evaluate its effectiveness in learning complex feature representations from LGE-CMRI data. The architecture is based on residual learning, where identity skip connections enable information and gradients to bypass intermediate convolutional layers (de Giorgio et al., 2023). This structural design directly addresses optimisation difficulties commonly encountered in deep neural networks, particularly gradient attenuation during backpropagation (Heidari et al., 2024) as shown in Figure 3.12. In this research, the use of residual connections allowed the network to maintain stable convergence behaviour across training epochs, even when trained on high-resolution CMRI slices with substantial inter-slice variability.

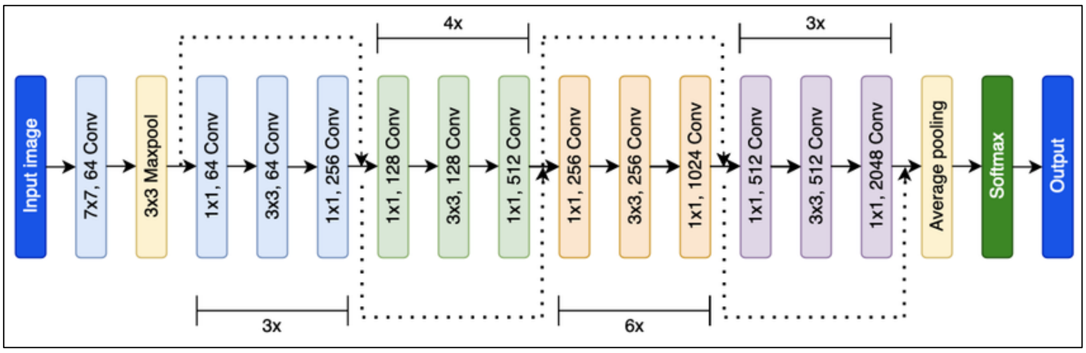

Figure 3.12 ResNet-50 Model Architecture (Oloruntoba et al., 2021)

From a feature learning perspective, ResNet-50 provides a balanced representation of low-level spatial details and high-level semantic context. Early layers capture intensity gradients, myocardial boundaries, and coarse anatomical structures, while deeper layers progressively encode contextual relationships between healthy myocardium, blood pool, and scar regions. This hierarchical feature extraction was particularly relevant for LGE-CMRI, where scar tissue may not always exhibit sharply defined borders and often appears as subtle hyper-intense regions embedded within normal myocardium. The depth of ResNet-50 enabled the network to integrate these subtle cues across multiple receptive field scales.

Within the proposed multi-stage segmentation framework, ResNet-50 demonstrated consistent performance across both anatomical and pathological segmentation tasks. Its capacity to preserve spatial coherence while extracting discriminative features made it suitable for downstream decoder stages that rely on accurate feature fusion. ResNet-50 was retained as a reference backbone in this study due to its robustness, representational strength, and reliability when dealing with complex myocardial tissue characteristics.

MobileNetV2

MobileNetV2 was incorporated as a lightweight backbone to investigate segmentation performance under reduced computational complexity. In Figure 3.13 shows the architecture that was built upon depthwise separable convolutions combined with inverted residual blocks and linear bottlenecks, significantly decreasing the number of parameters compared to conventional convolutional networks. This design enabled faster training and inference while maintaining stable optimisation behaviour, making MobileNetV2 suitable for scenarios where computational efficiency is a priority (Zhao et al., 2024).

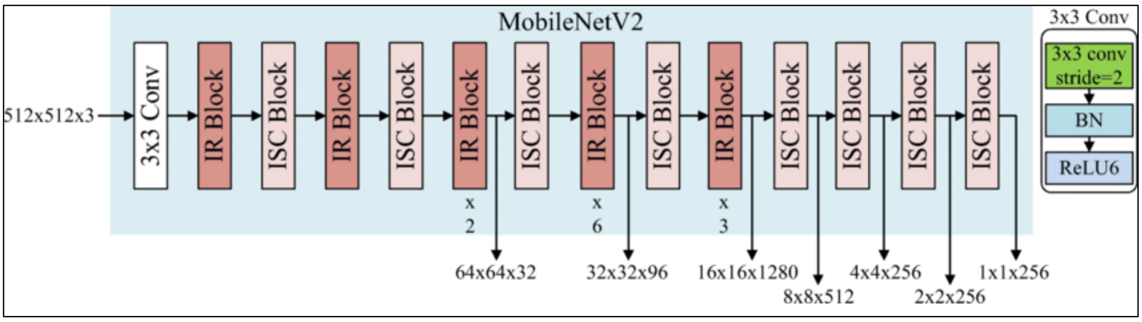

Figure 3.13 MobileNetV2 Model Architecture (Tsai & Su, 2022)

From a methodological standpoint, MobileNetV2 demonstrated adequate capability in extracting dominant anatomical features, particularly during early segmentation stages involving the left ventricle and cavity. These structures exhibit relatively high contrast and well-defined boundaries, allowing the compact feature representations of MobileNetV2 to remain sufficient. The reduced parameter counts also helped mitigate overfitting, which is a critical consideration when training on limited medical imaging datasets.

Xception

Xception was evaluated as a backbone that emphasises efficient yet expressive feature extraction through fully decoupled depthwise separable convolutions. Unlike MobileNetV2, which prioritises compactness, Xception focuses on maximising representational efficiency by separating spatial and channel-wise feature learning at every convolutional layer as shown in Figure 3.14. In this research, this design enabled the network to learn fine-grained spatial patterns while maintaining strong channel discrimination, which is advantageous for complex medical imaging data.

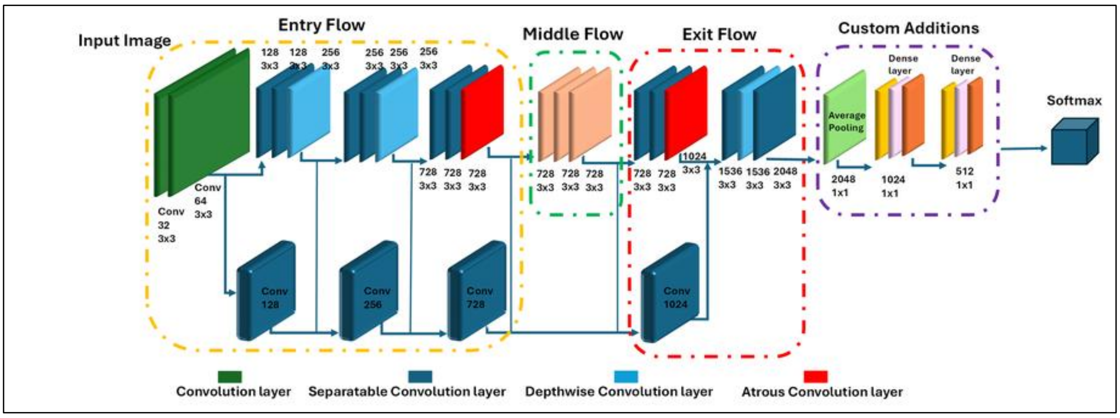

Figure 3.14 Xception Model Architecture (Cheraghi et al., 2025)

Within the proposed multi-stage segmentation framework, Xception was incorporated as the encoder backbone to extract hierarchical feature representations from LGE-CMRI images. The depthwise convolution layers were responsible for capturing spatial patterns such as myocardial contours, ventricular boundaries, and local intensity variations, while the pointwise convolutions modelled inter-channel dependencies to produce more abstract feature representations. This separation allows structured feature extraction across multiple scales, which is important for medical images that exhibit subtle intensity transitions and complex anatomical structures. The extracted feature maps were subsequently forwarded to the decoder stage for feature fusion and segmentation map reconstruction. Xception was included in this study to examine its suitability as a feature extraction backbone within the proposed segmentation framework. Its architectural design supports multi-level feature abstraction, enabling the modelling of both local textures and broader contextual information present in LGE-CMRI data. By integrating Xception into the encoder stage, the framework was able to generate deep feature embeddings intended to support accurate myocardial and scar region segmentation.

Overall, the use of the DeepLabV3+ framework in the proposed three-stage segmentation framework is expected to provides an effective and structured approach for myocardial segmentation. Each stage allows the model to concentrate on specific regions, which helps improve focus and segmentation accuracy. This staged learning was expected to reduces class imbalance and ensures more stable training results. Among the tested backbone model, the best performing model will be selected for the multi-stage segmentation framework. The combination of the multi-stage design and the selected backbone enhance the overall segmentation quality, enabling accurate and consistent delineation of myocardial regions and supporting reliable analysis for subsequent scar detection.

3.7 Proposed Hybrid Image Enhancement-Image Segmentation using Multi-Stage DeepLabV3+ Framework

The proposed hybrid image enhancement-multi-stage image segmentation using multi-stage DeepLabV3+ (Hybrid IE – IS) framework integrates the processes of image enhancement in Section 3.4 and image segmentation in Section 3.5 into a unified framework to achieve more accurate and reliable myocardial scar detection. In this study, the enhanced LGE-CMRI images generated from the best performing image enhancement method were utilized as the input for the multi-stage segmentation model based on the DeepLabV3+ framework. This integration enables the segmentation model to operate on images with improved contrast and reduced noise, resulting in clearer boundary delineation and more effective discrimination between healthy myocardium and the targeted scar regions. The overall hybrid workflow was illustrated in Figure 3.16.

Figure 3.15 Block Diagram of the Proposed Hybrid IE - IS Using Multi-Stage DeepLabv3+ Framework

The combination of these two processes addresses one of the primary limitations of conventional segmentation approaches, which often struggle with poor image quality and low contrast inherent in LGE-CMRI data. The enhancement stage refines the image intensity distribution, reduces artifacts, and highlights structural boundaries of the myocardium, thereby improving the visibility of fibrotic and viable regions. As a result, when the enhanced images are passed into the segmentation model, the model was expected to focus on learning meaningful spatial and textural features that correspond to pathological regions. This leads to improved accuracy, faster convergence, and more stable segmentation results across different patient data.

From a methodological perspective, the hybrid framework establishes a complementary relationship between enhancement and segmentation. The hybrid image enhancement component acts as a preparatory stage that improves the image contrast and overall visibility of critical regions, while the multi-stage segmentation model utilizes these refined visual cues to perform anatomically consistent myocardial and scar delineation. Each stage contributes distinct advantages - enhancement amplifies the data quality, and segmentation translates that visual improvement into precise structural interpretation. This complementary design bridges the gap between low-level visual refinement and high-level semantic understanding, ensuring that myocardial scars are accurately localized within the myocardium. The effectiveness of the proposed Hybrid Image Enhancement-Multistage Image Segmentation framework was quantitatively validated through comparative experiments.

Overall, the proposed hybrid IE – IS combined with multi-stage DeepLabV3+ framework is expected to effectively achieve superior myocardial scar detection performance. By providing the segmentation model with enhanced visual input, the framework was expected to ensure better feature extraction, improved tissue boundary definition, and anatomically consistent segmentation. This synergistic integration of enhancement and segmentation will establish a robust and efficient computational pipeline for accurate myocardial scar analysis in LGE-CMRI imaging.

3.8 Performance Evaluation

Performance evaluation was conducted to determine how effectively the proposed framework achieves accurate and reliable myocardial scar detection. Both quantitative and qualitative assessments were performed. Quantitative metrics provide objective evaluation of image quality and segmentation accuracy, while expert review ensures anatomical plausibility and clinical relevance. This dual approach allows a comprehensive assessment of the framework's performance.

3.8.1 Performance Evaluation for Image Enhancement

Mean Squared Error (MSE)

MSE measures the average squared difference between the enhanced image and its original reference. Lower MSE values indicate minimal distortion and preservation of anatomical details, which was important for ensuring that enhanced images retain critical myocardial structures. MSE is given by Equation (3.5):

$$\mathrm{MSE}=\frac{1}{n}\sum_{j=1}^{n}(I_j-K_j)^2 \tag{3.5}$$

where Ij is the ith observed value while Kj is the corresponding predicted value for Ij and n is the number of observations.

Peak Signal-to-Noise Ratio (PSNR)

PSNR quantifies the ratio between the maximum possible pixel intensity and the noise introduced by image enhancement. Higher PSNR values reflect better image fidelity and reduced distortion, supporting clearer visualization of myocardial boundaries. The PSNR is given by Equation 3.6:

$$\mathrm{PSNR}=10\cdot\log_{10}\left(\frac{\mathrm{MAX}_I^2}{\mathrm{MSE}}\right) \tag{3.6}$$

where MAXI2 is the maximum possible pixel intensity in the image and MSE is the mean squared error between original and enhanced image.

Structural Similarity Index Measure (SSIM)

SSIM evaluates the structural and perceptual similarity between the enhanced and reference images by considering luminance, contrast, and structural information. A value closer to 1 indicates that image enhancement has preserved important anatomical structures and overall tissue integrity. The SSIM is given by Equation 3.7:

$$\mathrm{SSIM}(x,y)=\frac{(2\mu_x\mu_y+C_1)(2\sigma_{xy}+C_2)}{(\mu_x^2+\mu_y^2+C_1)(\sigma_x^2+\sigma_y^2+C_2)} \tag{3.7}$$

where μ is the mean intensities of images x and y, σ2 are the variances, σxy is the covariance between x and y, and C are constants to stabilise the calculation.

Contrast Root Mean Square (CRMS)

CRMS quantifies the overall intensity variation of an image by measuring the square root of the mean of squared pixel values. Higher RMS values indicate greater contrast and improved visibility of myocardial structures after enhancement. It is calculated as in Equation 3.8:

$$\mathrm{CRMS}=\sqrt{\frac{1}{n}\sum_{i=1}^{n}x_i^2} \tag{3.8}$$

where $x_i$represents the intensity of the i-th pixel and $n$is the total number of pixels in the image.

Entropy

Entropy evaluates the amount of disorder or information content in an image. A higher entropy value suggests richer image details and better contrast enhancement, supporting clearer visualization of myocardial boundaries. It can be expressed as Equation (3.9):

$$\mathrm{Entropy}=-\sum_{i-0}^{L-1}p_i\log_2 p_i \tag{3.9}$$

where pi is the probability of the i-th gray level in the image and L is the total number of gray levels.

3.8.2 Performance Evaluation for Image Segmentation

Dice Similarity Coefficient (DSC)

The Dice coefficient measures the spatial overlap between predicted and ground-truth segmentation masks. A higher Dice value indicates better agreement and more accurate segmentation of myocardial regions. The DSC is given by Equation (3.10):

$$\text{Dice}=\frac{2TP}{2TP+FP+FN} \tag{3.10}$$

where TP is the number of true positive pixels, FP is false positive and FN is false negatives.

Intersection over Union (IoU)

IoU quantifies the ratio of the intersection to the union between predicted and reference masks. Higher IoU values indicate better localization and consistency in segmentation. The IoU is given by Equation (3.11):

$$\text{IoU}=\frac{TP}{TP+FP+FN} \tag{3.11}$$

where TP, FP and FN are defined as above.

Accuracy

Accuracy represents the proportion of correctly classified pixels (both positive and negative) relative to all pixels. Higher accuracy indicates the model's overall reliability in correctly segmenting myocardial tissue. It is calculated as Equation (3.12):

$$\text{Accuracy}=\frac{TP+TN}{TP+TN+FP+FN} \tag{3.12}$$

where TN refers to true negative.

3.9 Summary

This chapter has provided a comprehensive description of the methodology employed in this study, which integrates image enhancement, deep learning-based segmentation, and a hybrid multi-stage framework for myocardial scar detection in LGE-CMRI images. The methodology begins with image enhancement and sharpening, which improves contrast, reduces noise, and enhances structural details, thereby facilitating the extraction of relevant myocardial features. The enhanced images provide a more informative input for subsequent segmentation tasks, ensuring that subtle variations in myocardial tissue intensity are better captured.

The core of the segmentation methodology was a Multi-stage DeepLabV3+ framework. In Stage 1, independent models were trained to segment the left ventricular myocardium and cavity, allowing each model to specialise in a single anatomical structure and reduce class confusion. Stage 2 derives the myocardium region of interest (ROI), focusing the analysis on the tissue where scar regions are physiologically expected, thereby improving the spatial specificity of subsequent predictions. Stage 3 performs scar detection within the myocardial ROI, enabling the model to learn features exclusively from relevant regions, which improves segmentation. To ensure optimal performance, three backbone architectures which were ResNet-50, MobileNetV2, and Xception were systematically evaluated.

Performance evaluation was conducted using both quantitative and qualitative measures. Quantitative metrics such as MSE, PSNR, SSIM, Dice, IoU and accuracy provided objective assessment of enhancement and segmentation quality, while expert evaluation by cardiologists ensured anatomical plausibility and clinical relevance. The combination of these evaluations allows a thorough understanding of the framework's effectiveness, highlighting its ability to produce reliable and meaningful segmentation results for myocardial scar detection.

Overall, the methodology presented in this chapter establishes a robust and systematic framework that addresses the challenges of low contrast, intensity variability, and anatomical heterogeneity inherent in LGE-CMRI images. By combining advanced image enhancement with a multi-stage, anatomically guided deep learning segmentation approach, the study is expected to provides a reliable foundation for accurate myocardial scar detection, setting the stage for the experimental validation and analysis detailed in the subsequent chapters. The following chapter presents results and discussion of the proposed methodology in details.

CHAPTER 4
RESULTS AND DISCUSSION

4.1 Introduction

This chapter presents the experimental results obtained from the proposed LGE-CMRI image enhancement and image segmentation framework. The primary objective was to evaluate the performance of the methods described in Chapter 3 and to quantify the contribution of each processing stage toward improving myocardial scar tissue visibility. The results were structured following the research workflow, beginning with image pre-processing, followed by image enhancement techniques, image segmentation model framework, and concluding with the integrated evaluation of the hybrid enhancement–segmentation framework.

The chapter begins by presenting the outcomes of the image pre-processing stage, which includes both image augmentation and labelling. The chapter then discusses the performance of different image enhancement techniques, including contrast adjustment, image sharpening, and the proposed hybrid approach that combines both methods. Each method was quantitatively evaluated using metrics such as PSNR, SSIM, MSE, entropy, and contrast RMS, which collectively assess improvements in structural preservation, textural detail, and contrast enhancement.

Subsequently, the results of the multi-stage deep learning segmentation model were presented, focusing on accurate myocardial scar precise boundaries at each stage. Segmentation performance was assessed using standard metrics, including DSC, IoU and accuracy, complemented by qualitative visual inspection of the segmentation masks. Finally, the chapter examines the integrated impact of hybrid enhancement and multi-stage segmentation, demonstrating whether enhancement contributes measurable improvements to segmentation outcomes. Collectively, this chapter provides a comprehensive evaluation of the proposed system's effectiveness and forms the basis for in-depth discussion within this chapter.

4.2 Result of Image Pre-Processing

Image pre-processing was performed to ensure that the LGE-CMRI dataset was suitable for subsequent enhancement and segmentation analysis. The effectiveness of this stage was reflected in the improved dataset size, annotation consistency, and overall readiness of the data for deep learning–based processing. The original dataset comprised 463 LGE-CMRI slices, which was relatively limited considering the high variability in cardiac anatomy and image appearance across subjects. After the application of image augmentation, the dataset size increased significantly to 3,704 images, representing an eight-fold expansion.

The augmented images include variations in orientation through rotation and horizontal flipping, while preserving the underlying myocardial structure. Visual examples of the augmented images were presented in Figure 4.1, demonstrating that the applied augmentation process that maintain anatomical validity. This substantial increase in data enhances the diversity of myocardial appearances available during training, allowing the segmentation framework to better accommodate anatomical variability and complex myocardial textures. As a result, the augmented dataset provides a more robust representation of real-world LGE-CMRI conditions, contributing to improved generalisation performance in later enhancement and segmentation stages.

In addition to dataset expansion, accurate image labelling was achieved through the generation of pixel-level ground truth masks for the myocardial structure. Qualitative assessment of the labelled images, as illustrated in Figure 4.2, shows that the annotations closely follow myocardial boundaries despite challenges such as intensity inhomogeneity and unclear tissue contrast. The consistency of these labels across different slices ensures reliable supervision during network training. Overall, the pre-processing results demonstrate that the dataset was sufficiently enriched and accurately annotated, forming a stable foundation for the image enhancement experiments presented in Section 4.3 and the subsequent image segmentation and hybrid image enhancement – image segmentation frameworks discussed in Sections 4.4 and 4.5.

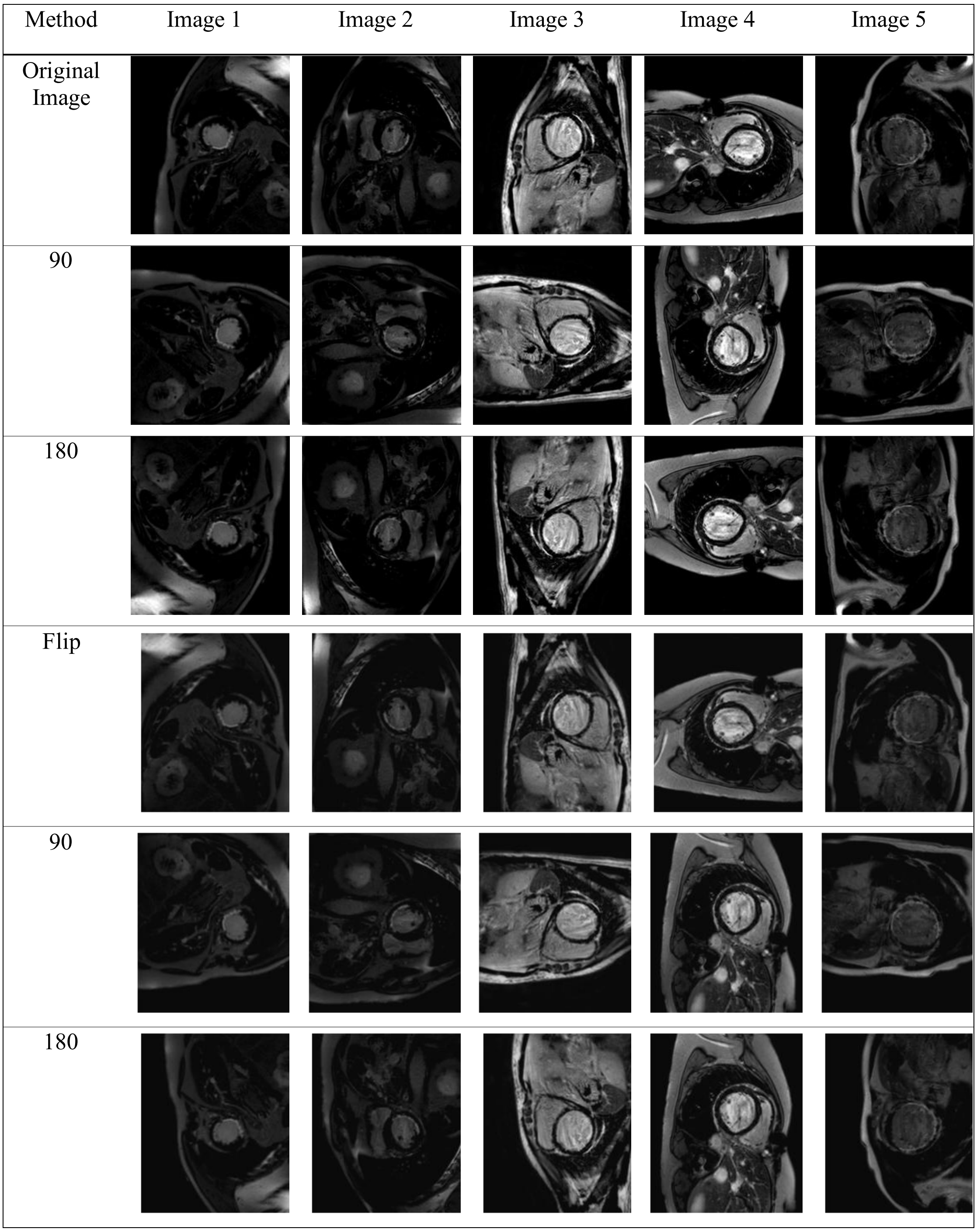

Figure 4.1 Example of Image Augmentation Process on LGE-CMRI Image Across Dataset

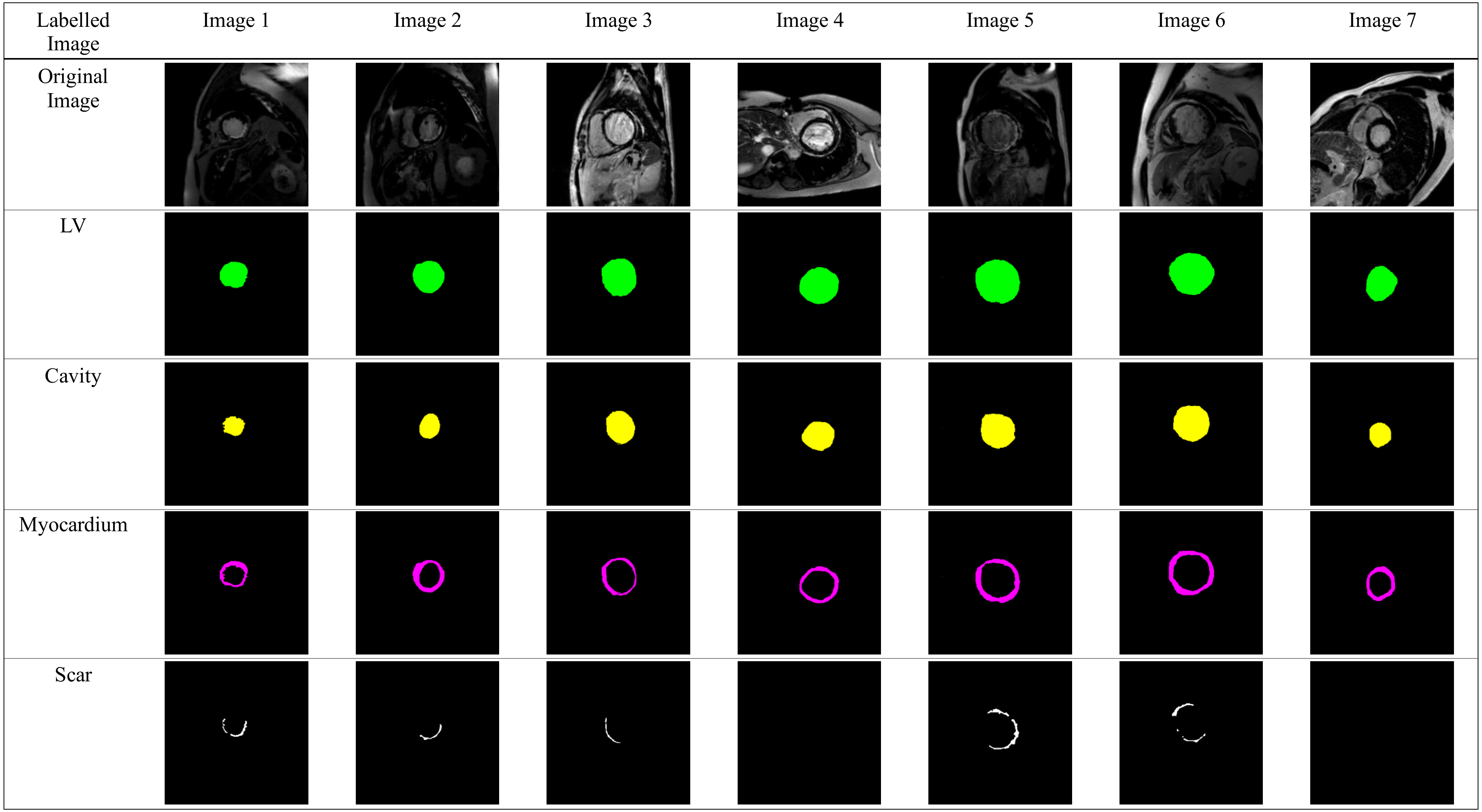

Figure 4.2 Example of Image Labelling Process on LGE-CMRI Image

4.3 Result of Proposed Image Enhancement

Image enhancement plays a crucial role in LGE-CMRI analysis, as the quality of input images directly influences the accuracy of automated image segmentation frameworks using multi-stage DeepLabV3+. In this study, image enhancement was conducted to improve the visibility of myocardial structures, enhance the differentiation between healthy and infarcted tissue, and sharpen myocardial boundaries. The enhancement process involved two main operations, namely contrast enhancement and image sharpening, which were integrated to form a proposed hybrid image enhancement approach. Both qualitative and quantitative analyses were performed, including visual inspection of myocardial boundaries and scar regions, as well as quantitative evaluation using PSNR, SSIM, MSE, entropy, and CRMS were used to evaluate the effectiveness of the techniques. A comparative assessment of individual enhancement techniques and the proposed hybrid method was carried out to identify the most effective strategy for improving image quality prior to segmentation.

4.3.1 Contrast Enhancement

LGE-CMRI images often exhibit low contrast and mild blurriness, making it challenging to clearly distinguish myocardial walls and potential scar regions. Improving image contrast was therefore essential to enhance visual clarity and support accurate observation of structural details. In this study, four enhancement techniques were applied to address these issues: HE, CLAHE, Type-II Fuzzy Set (F2FS), and Morphological Residual Processing (MRP). Each technique employs a different approach to enhancing either global or local intensity, providing a comprehensive evaluation of contrast improvement strategies for myocardial LGE-CMRI images. The discussion below focuses on the qualitative outcomes and highlights the differences observed among these methods based on the images obtained in this research.

The first technique used was HE as it was a standard global contrast enhancement technique that has been widely used in previous studies for MRI image enhancement, as it redistributes intensity values to improve overall visibility. Based on Figure 4.3, the HE technique enhanced the images appear significantly brighter compared to the original images, making the overall myocardial walls and general cardiac structures clearly visible. Regions that were previously difficult to perceive in the raw images, such as the outer layer wall of larger area boundaries and chambers, become more distinguishable. However, due to the global nature of HE, the contrast was increased across the entire image uniformly. As a result, some important subtle areas, such as scar regions, were over-brightened or partially lost, reducing their visibility. While HE provides a clear improvement for the overall structure, it cannot selectively enhance critical targeted low-contrast scar areas, limiting its usefulness for precise myocardial scar detection.

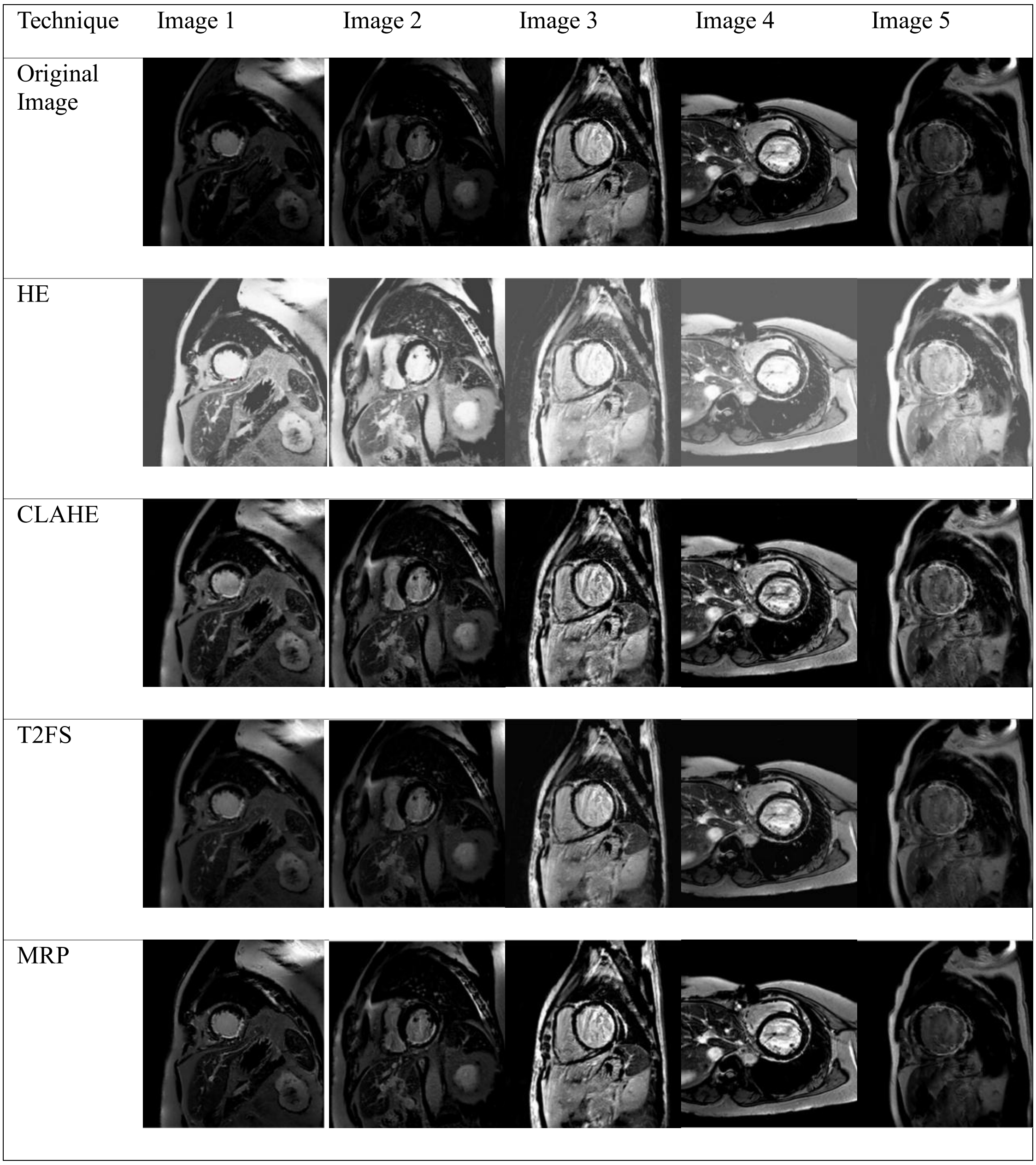

Figure 4.3 Visual Result Comparison of Contrast Enhancement Techniques Applied to LGE-CMRI Image

The second technique, CLAHE was applied to improve local contrast while avoiding over-brightening the entire image. Previous studies have proposed CLAHE as an improvement over HE, allowing better visualization of small or low-contrast regions in medical images. In Figure 4.3, the result of CLAHE enhanced images presents better myocardial walls contrasts compared to both the original and HE enhanced images. Regions that were over-enhance in HE images enhancement technique, were more visible using CLAHE technique. The localized processing preserves details in low-contrast areas without over-amplifying the high contrast regions. However, some areas still appear slightly higher contrast, especially on LV regions, creating minor inconsistencies across the myocardium. Despite these small limitations, CLAHE significantly improves the visibility of finer structures compared to HE and allows better observation of subtle myocardial variations.

Next, T2FS was applied to produce a more adaptive image enhancement by modelling uncertainty in contrast transitions. As shown in Figure 4.3, T2FS produces a smoother and more balanced image, where the differences between the cavity, LV, and myocardium area were easier to see. Compared to the original images, HE and CLAHE, T2FS allows both the main structures and small scar regions to be observed more clearly, improving overall perception of the heart's anatomy. The enhancement appears more natural, avoiding the abrupt brightness changes seen in HE, and however fine texture of myocardium boundaries seems to be slightly blurred. Overall, F2FS offers a balance between visual clarity and natural appearance, improving overall visibility without over-brightening, it may reduce edge sharpness and limit precise boundary of small infarcts, which was critical for segmentation accuracy.

Finally, MRP produces images with better contrast quality, which allows the LV cavity, myocardial walls, and particularly scar regions to be more clearly distinguished compared to the original images and the other enhancement techniques. As shown in Figure 4.3, the scar areas stand out more prominently against the surrounding myocardium, making them easier to observe and analyse. The improved brightness differences between the scar and myocardial tissue help reveal regions that were less visible in HE, CLAHE, or F2FS. This makes MRP particularly effective in highlighting small pathological features, which is important for image segmentation of myocardial scar using deep learning framework. However, in certain areas of the myocardium the fine texture of the LV, myocardium, and scar wall appears slightly blurred, which may reduce the visibility of very small structural details. Overall, MRP provides a better enhancing contrast between the myocardial structure areas, but its effects on fine details was low between the boundaries.

The quantitative results presented in Table 4.1 provide clear evidence of how contrast enhancement quality improves progressively across the applied techniques. The result were obtained from 463 original LGE-CMRI images and averaged. Compared to the original LGE-CMRI images, all four image enhancement technique increase contrast between the LV, cavity, myocardial walls, and scar regions, as resulted with higher PSNR and SSIM values and lower MSE.

Table 4.1
Performance Evaluation of Contrast Enhancement Technique on LGE-CMRI Images

Contrast Enhancement Technique	**Evaluation Metrics**				
	PSNR (dB)	**SSIM**	**MSE**	**CRMS**	**Entropy**
HE	11.94	0.348	0.064	0.092	4.617
CLAHE	21.47	0.727	0.007	0.121	5.021
T2FS	39.05	0.821	0.004	0.156	5.237
MRP	**45.08**	**0.971**	**0.003**	**0.178**	**5.521**

Based on Table 4.1, HE exhibits the lowest quantitative performance among the evaluated enhancement techniques, with a PSNR of 11.94 dB, SSIM of 0.348, and MSE of 0.064. Although HE increases overall brightness and improves global contrast, these values indicate that the enhancement is not well balanced. The low PSNR suggests limited signal quality improvement relative to noise, while the low SSIM reflects poor preservation of structural information, particularly in myocardial walls and scar regions. The high MSE further demonstrates uneven intensity changes across the image, which can distort fine anatomical details. Additionally, the low CRMS value of 0.092 and entropy of 4.617 support this observation, indicating weak intensity variation and limited information content. As a result, HE-enhanced images show poorly defined myocardial boundaries and scar regions, limiting their utility for both diagnostic interpretation and automated segmentation tasks.

CLAHE shows noticeable improvement over HE, achieving a PSNR of 21.47 dB, SSIM of 0.727, and MSE of 0.007. The higher PSNR indicates stronger separation between the LV cavity, myocardium, and scar tissue, while the improved SSIM suggests that structural relationships are better preserved compared to HE. The lower MSE reflects more uniform application of contrast enhancement across the image, reducing localized over- or under-enhancement. CLAHE also shows improved CRMS of 0.121 and entropy of 5.021, indicating increased contrast intensity and richer image information. These improvements result in clearer visualization of myocardial walls and scar regions. However, CLAHE may still introduce slight over-enhancement in some local regions, which could partially obscure subtle scar details, making it moderately effective but not optimal for high-precision segmentation.

T2FS further enhances image quality, achieving a PSNR of 39.05 dB, SSIM of 0.821, and MSE of 0.004. The PSNR demonstrates substantial improvement in signal fidelity and contrast separation between cardiac structures, while the SSIM indicates better preservation of anatomical structures compared to HE and CLAHE. The low MSE reflects smooth and consistent application of contrast across the image. Furthermore, T2FS achieves a CRMS of 0.156, indicating stronger contrast intensity, and an entropy of 5.237, reflecting richer texture and more informative images. These improvements allow better visualization of myocardial walls and scar regions, producing smoother transitions and maintaining tissue integrity. Nevertheless, slight blurring of fine myocardial and scar textures may still occur, suggesting that T2FS, while strong in overall enhancement, may lack the edge sharpness necessary for precise boundary delineation.

MRP demonstrates the highest quantitative performance, with a PSNR of 45.09 dB, SSIM of 0.971, and the lowest MSE of 0.003. The high PSNR indicates excellent signal quality with minimal noise, while the SSIM close to 1 demonstrates near-complete structural preservation. The very low MSE confirms that contrast enhancement is applied uniformly, with negligible distortion. The CRMS of 0.178 reflects strong contrast differentiation between tissue types, and the entropy of 5.521 indicates maximal information content and texture richness among all techniques. Together, these metrics translate to the clearest visualization of myocardial walls and scar regions. However, the aggressive enhancement may cause partial blurring of fine tissue details, especially along myocardial boundaries. Despite this, MRP provides the best balance between strong contrast, structural preservation, and information content, making it the most suitable enhancement method for LGE-CMRI myocardial segmentation.

HE improves global brightness but fails to preserve structural details, whereas CLAHE enhances local contrast and better preserve's structure, albeit with some over-enhancement in high-contrast regions. T2FS achieves smooth contrast enhancement with preserved textures and improved visualization of scars, though edge sharpness is slightly compromised. MRP maximizes all metrics, providing the clearest distinction between myocardial tissue and scar regions while maintaining structural fidelity. These observations demonstrate that systematic enhancement directly improves image quality and provides more reliable inputs for automated segmentation algorithms, supporting both clinical diagnosis and research analysis.

In summary, MRP emerges as the most effective contrast enhancement technique, offering the optimal balance between intensity improvement, structural preservation, and information content. T2FS provides smooth transitions and maintains tissue textures, but slightly less edge sharpness. CLAHE improves local contrast but may introduce minor over-enhancement, while HE enhances brightness but offers minimal structural preservation. Overall, MRP-enhanced images provide superior diagnostic and segmentation utility, making it the preferred preprocessing method for LGE-CMRI myocardial image segmentation analysis.

4.3.2 Result of Image Sharpening

Image sharpening enhances myocardial edges and fine details within infarcted regions, which was important for accurate delineation of scar boundaries. Five sharpening methods were evaluated: Unsharp Masking, High-Boost Filter, Laplacian Filter, Nimble Filter, and Adaptive Sharpening. These methods were chosen to compare traditional and adaptive approaches in preserving edge information which was particularly critical for automated image segmentation. Image sharpening resulted in a noticeable refinement of myocardial boundaries. As illustrated in Figure 4.4, the edges of the myocardium exhibit increased sharpness after image processing. This improvement was especially noticeable along the inner heart walls, where the boundaries between the myocardium and scar areas appear sharper and easier to differentiate compared to the original image.

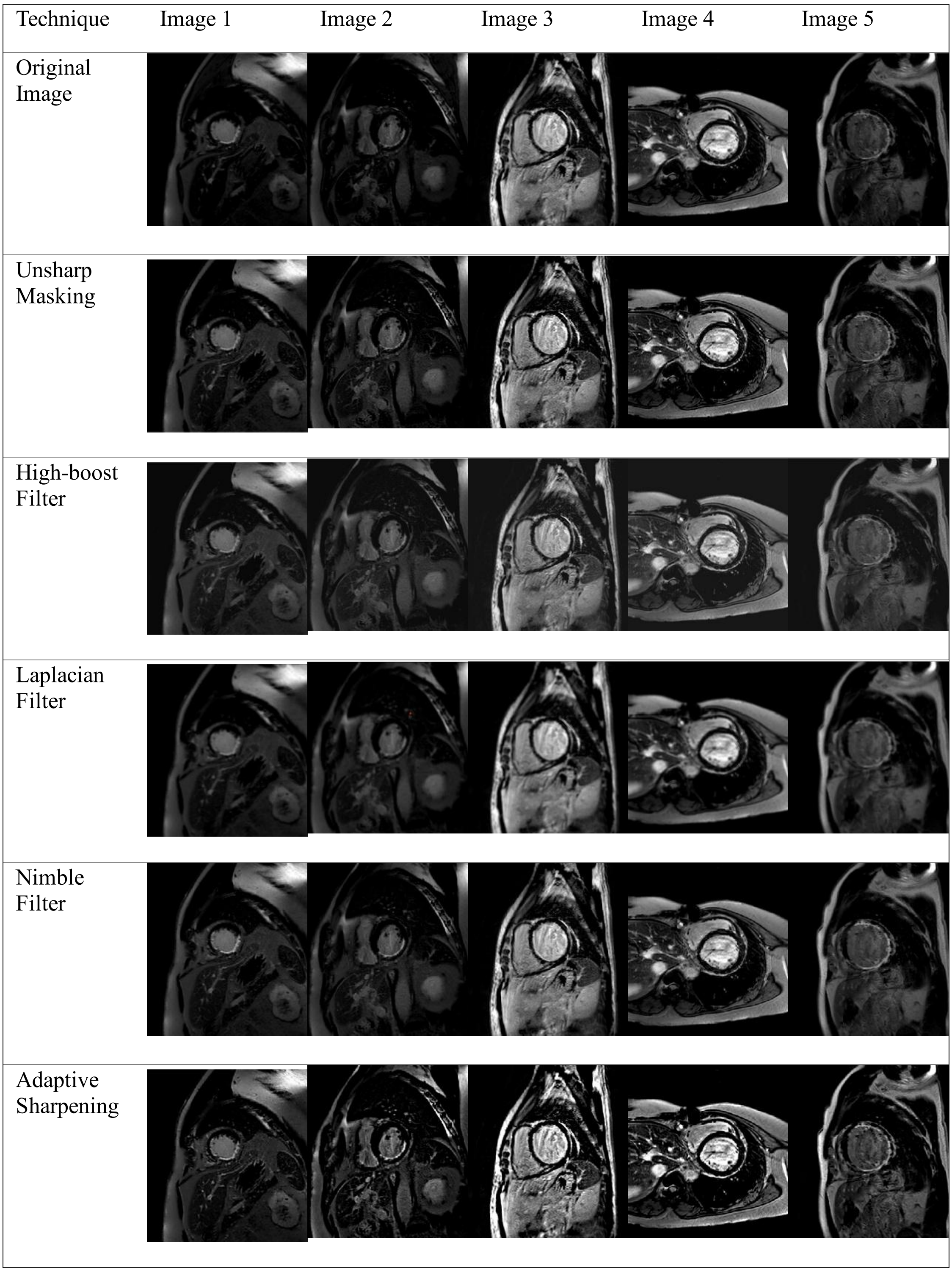

Figure 4.4 Visual Result Comparison of Image Sharpening Techniques Applied to LGE-CMRI Image

The images showed that Unsharp Masking and High-Boost Filter improved the visibility of the major myocardial contours, making the overall wall shape and thickness more noticeable such as LV and cavity. However, subtle scar regions remain poorly defined in the figure, suggesting that this method primarily enhances large-scale structures but was less effective in emphasizing small, low-contrast scar. In contrast, Laplacian Filter produced sharper edges in some areas, but most myocardial walls and parts of the cavity appeared blurry, especially in thin regions. Especially scar area seems to into the myocardium, indicating that although Laplacian filter sharpening strengthened global edges, it could not improve the clarity of fine structure. Therefore, this technique may compromise the accuracy of automated image segmentation of scar region.

Adaptive sharpening was designed to improve edge clarity, but the figure shows that some fine scar details remain slightly less defined compared to Nimble Filter. It shows the image was well sharpened on LV and background regions globally making some areas slightly clearer than Laplacian. However, parts of the cavity, myocardium and scar appeared sharpened however seem fragmented, and some small scar regions remained difficult to see. Nimble Filter provided a more balanced improvement, reducing blurriness across most myocardial walls and LV cavity regions and making scar areas somewhat more visible. Figure 4.4 illustrates that both major myocardial walls and subtle scar boundaries were well highlighted. Nevertheless, minor blur persisted in thin walls, and very small scar regions were still challenging to observe.

Overall, the comparison showed that image sharpening reduced blurriness in varying ways across the techniques. Unsharp Masking and High-Boost Filter were more effective in improving the clarity of larger structures, Laplacian Filter increased edge strength but left thin walls and some LV cavity areas blurriness, adaptive sharpening enhanced selected regions but caused fragmentation, and Nimble Filter gave a more even reduction of blur while some fine details remained unclear. Compared to other methods, it provides the clearest and most diagnostically useful images for subsequent segmentation by deep learning models, supporting more accurate delineation of myocardial and scar structures. These observations provided a clear visual comparison of the techniques and highlighted the importance of selecting a sharpening technique that balances edge sharpening for more reliable myocardial analysis.

The quantitative results in Table 4.2 provided further insight into how image sharpening affected image quality and blurriness in myocardial LGE-CMRI images. These metrics helped explain the visual differences observed in Figure 4.4, particularly in terms of edge clarity, structural preservation, and loss of texture in myocardial and LV cavity regions. The PSNR values showed clear differences in the level of distortion introduced by different image sharpening techniques. Higher PSNR values indicated that the sharpened images remained closer to the original image while reducing blurriness. Nimble Filter and Adaptive Sharpening recorded the highest PSNR values at 51.65 dB and 49.69 dB, suggesting that these techniques reduced blurriness without heavily altering the original myocardial structure. Unsharp Masking also achieved a relatively high PSNR of 43.57 dB, which explained why its visual output appeared comparable to High-Boost but with less severe degradation. In contrast, the low PSNR of 27.67 dB for High-Boost Filter indicated stronger image alteration, which was consistent with the observed unstable background and reduced clarity in some myocardial regions. An increase in RMS value after enhancement indicates improved contrast and intensity variation, which supports clearer visualization of myocardial boundaries. Increased entropy values suggest richer image details and improved information content, which are beneficial for subsequent myocardial segmentation.

Table 4.2
Performance Evaluation of Image Sharpening Technique on LGE-CMRI Images

Image Enhancement Technique	**Evaluation Metrics**				
	PSNR (dB)	**SSIM**	**MSE**	**CRMS**	**Entropy**
Unsharp Masking	43.57	0.997	0.702	0.175	5.639
High-boost Filter	27.67	0.6731	0.057	0.112	5.891
Laplacian Filter	38.92	0.9752	**0.001**	0.161	**6.079**
Nimble Filter	**51.65**	**0.9979**	0.152	**0.185**	5.721
Adaptive Sharpening	49.69	0.9933	**0.001**	0.182	5.184

Based on Table 4.2, Unsharp Masking demonstrates strong overall performance among the evaluated sharpening techniques, achieving a PSNR of 43.57 dB, SSIM of 0.997, and an MSE of 0.702. The high PSNR indicates that the sharpened images remain very close to the original in overall intensity distribution, minimizing noise relative to signal and preserving global image fidelity. The SSIM value near one confirms that structural features, particularly the myocardium and LV cavity, are maintained with high similarity to the original image. Meanwhile, the higher MSE suggests that the pixel-level adjustments are more pronounced, reflecting the technique’s emphasis on edge enhancement rather than uniform intensity correction. Its CRMS of 0.175 and entropy of 5.639 highlight that local contrast has been improved and image information content is enriched, supporting better delineation of myocardial walls and scar regions. Visually, Unsharp Masking enhances edges effectively, making the myocardial contours clearer and scar regions more distinguishable. However, very subtle or thin myocardial structures may still lack consistent sharpness, indicating that while Unsharp Masking improves edge visibility, it is not uniformly optimal across all tissue features.

High-Boost Filter exhibits lower quantitative performance, achieving a PSNR of 27.67 dB, SSIM of 0.673, and MSE of 0.057. Although this technique enhances the general edges of the image, making major myocardial contours more noticeable, the relatively low PSNR indicates that signal quality improvement relative to noise is limited, and the SSIM shows noticeable structural distortion in thin myocardial walls and subtle scar regions. The moderate MSE indicates uneven pixel adjustments across the image, which can lead to fluctuations in background intensity and reduce clarity in low-contrast regions. Its CRMS of 0.112 and entropy of 5.891 further reflect weak local contrast enhancement and only moderate image information content. Consequently, High-Boost Filter can sharpen broad edges but fails to consistently enhance fine myocardial or scar structures, producing images that are partially improved but with less reliable visualization for detailed analysis or automated segmentation.

Laplacian Filter provides a more balanced approach to sharpening, with a PSNR of 38.92 dB, SSIM of 0.975, and MSE of 0.001. The higher PSNR relative to High-Boost Filter indicates better overall fidelity to the original image while enhancing edge details. The SSIM demonstrates strong structural preservation across the myocardium and LV cavity, and the very low MSE reflects minimal pixel-level deviation from the original, reducing the likelihood of introducing artifacts. Its CRMS of 0.161 and entropy of 6.079 indicate moderate local contrast enhancement and richer texture content, which allows myocardial walls and scar regions to appear more defined and distinguishable. Despite these improvements, some very thin myocardial walls and subtle scar boundaries remain slightly blurred, showing that Laplacian sharpening, while effective at enhancing local edges, may not uniformly improve all fine tissue structures. The technique’s moderate enhancement suggests that it may be best suited when balanced sharpening with structural preservation is prioritized over maximal edge amplification.

Nimble Filter achieves the highest quantitative performance, with a PSNR of 51.65 dB, SSIM of 0.997, and MSE of 0.152. The very high PSNR demonstrates that the overall image intensity remains extremely close to the original, indicating minimal noise introduction, while the near-perfect SSIM reflects excellent structural fidelity throughout the myocardium, LV cavity, and scar regions. The MSE, slightly higher than that of Laplacian Filter, indicates purposeful pixel adjustments that enhance edge sharpness without compromising global structural integrity. Its CRMS of 0.185 and entropy of 5.72 show strong local contrast and enriched image details, contributing to the clear delineation of myocardial walls and scar tissue. Visually, Nimble Filter produces images with reduced blurriness, well-defined scar boundaries, and consistent myocardial wall thickness, demonstrating both effective edge enhancement and structural preservation.

Adaptive Sharpening also delivers strong quantitative and qualitative performance, achieving a PSNR of 49.69 dB, SSIM of 0.993, and an exceptionally low MSE of 0.001. The high PSNR and SSIM confirm minimal distortion and strong structural fidelity, while the very low MSE suggests that pixel-level changes are carefully applied to maintain image integrity. Its CRMS of 0.182 and entropy of 5.184 indicate that local contrast and texture richness are enhanced moderately, producing sharp myocardial walls and scar boundaries while preserving smooth transitions across the image. Although some very thin myocardial walls and subtle scar regions may appear less distinct than in Nimble Filter, Adaptive Sharpening strikes an effective balance between edge enhancement and smooth intensity transitions, reducing the risk of over-sharpening artifacts.

Overall, the comparison of these techniques highlights the nuanced effects of different sharpening approaches. High-Boost Filter improves broad edges but fails to enhance fine detail consistently, Laplacian Filter provides moderate edge enhancement with uneven performance in delicate structures, Unsharp Masking strengthens edges with moderate contrast enhancement but may overemphasize certain regions, Adaptive Sharpening balances sharpness with smoothness, and Nimble Filter consistently delivers the strongest combination of PSNR, SSIM, CRMS, and entropy values. The results indicate that Nimble Filter is the most effective technique for enhancing myocardial walls and scar regions in LGE-CMRI images, providing improved edge definition, richer image detail, and minimal blurring, all of which support both accurate diagnostic interpretation and precise automated segmentation.

4.3.3 Result of Proposed Hybrid Contrast Enhancement – Image Sharpening

Hybrid image enhancement was applied by combining the best-performing contrast enhancement technique, MRP with the best-performing image sharpening method, Nimble Filter, to simultaneously improve contrast and reduce blurriness in LGE-CMRI images. This approach aimed to integrate the strengths of both methods, addressing low contrast and unclear myocardial and scar structures while preserving tissue texture. Figure 4.5 shows the hybrid-image enhancement images, highlighting improvements in myocardial, LV, cavity, and scar regions compared with images enhanced using only contrast or sharpening methods.

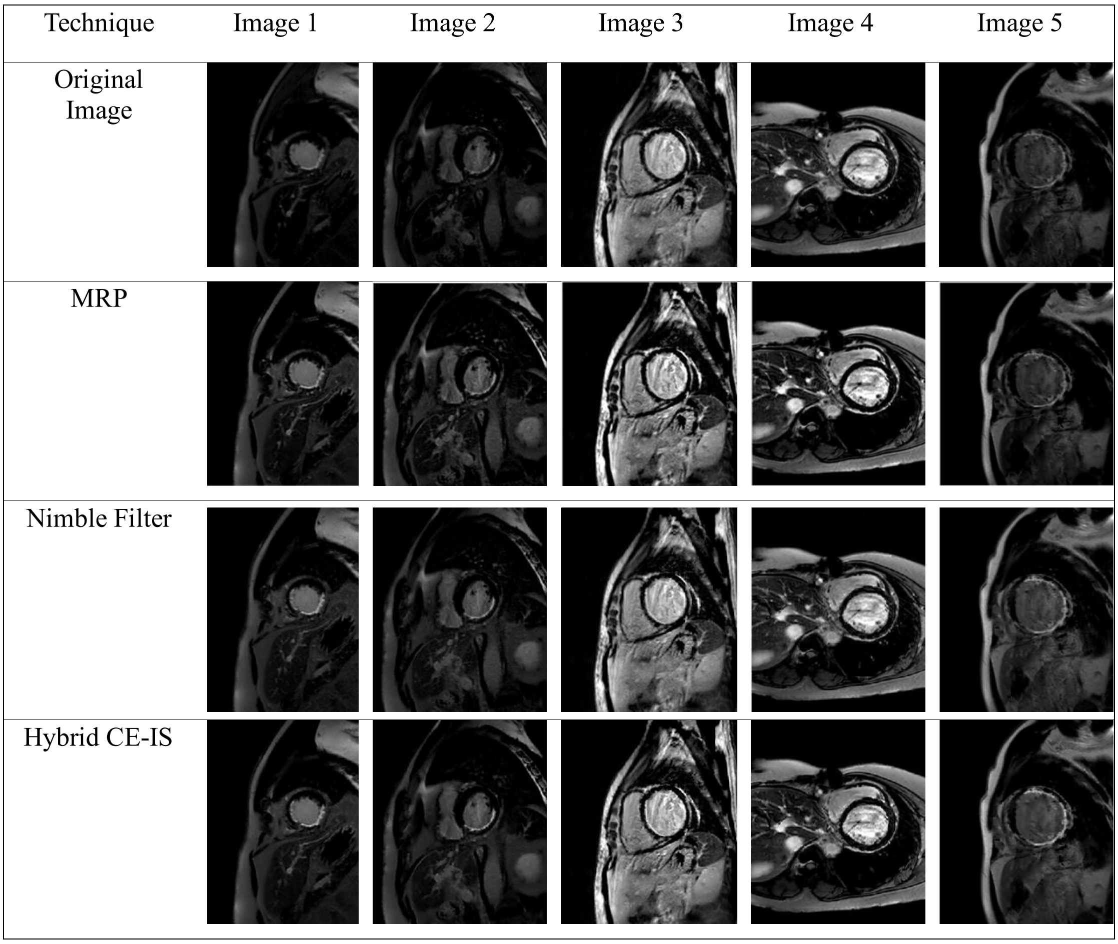

Figure 4.5 Visual Result Comparison of Hybrid Contrast Enhancement – Image Sharpening Method Applied to LGE-CMRI Image

As observed in Figure 4.5, the visual observations indicated that the hybrid method produced images where myocardial walls were more continuous, LV cavities were clearer, and scar regions were more visible. While MRP alone improved contrast, some fine myocardial textures and small scar boundaries were occasionally blurred. Nimble Filter sharpened edges and reduced general blurriness, but thin myocardial walls and small scars were sometimes less distinct or slightly broken. By combining these methods, the hybrid approach retained the contrast improvements from MRP while benefiting from the edge clarity provided by Nimble Filter, resulting in a more balanced enhancement across all regions. Hence, the hybrid method enhanced contrast enhancement and edge definition simultaneously, improving the interpretability of images for both human observers and hopefully for automated image segmentation.

The quantitative evaluation supported the qualitative observations regarding the hybrid CE-IS method. Based on Table 4.3, the hybrid approach achieved a PSNR of 56.33 dB and an SSIM of 0.989, surpassing the values obtained by Nimble Filter alone, which recorded a PSNR of 51.65 dB and SSIM of 0.997, as well as Laplacian Filter, which achieved a PSNR of 45.09 dB and SSIM of 0.971. These high PSNR and SSIM values indicate that the hybrid method preserved overall image fidelity while enhancing edge clarity and structural similarity, maintaining the integrity of myocardial walls, LV cavity, and scar regions. The mean squared error of 0.007 demonstrates that pixel-level deviations were minimal, suggesting that the hybrid approach improved contrast and visibility without significantly distorting tissue structures.

Table 4.3
Performance Evaluation of Hybrid CE-IS Technique on LGE-CMRI Images

Image Enhancement Technique	**Evaluation Metrics**				
	PSNR (dB)	**SSIM**	**MSE**	**CRMS**	**Entropy**
MRP	45.09	0.971	**0.003**	0.178	5.521
Nimble Filter	51.65	**0.997**	0.152	**0.185**	5.721
Hybrid CE-IS	**56.33**	0.989	0.007	0.128	**5.189**

In terms of local contrast and information content, the hybrid method recorded a CRMS of 0.128 and an entropy of 5.189. While the CRMS is slightly lower than that of Nimble Filter, indicating a more moderate local intensity variation, the entropy reflects sufficient image information to enhance subtle myocardial and scar features. This combination of metrics shows that the hybrid approach effectively balances edge sharpening, contrast enhancement, and structural preservation. Compared to Laplacian

Filter, which improved edges but left many regions blurry, and Nimble Filter, which enhanced sharpness but could not fully improve contrast in low-intensity regions, the hybrid CE-IS method produced more uniform enhancement.

The hybrid approach not only increased the visibility of myocardial walls, LV cavity, and scar regions but also maintained the natural tissue texture, preventing over-sharpening or artificial edge exaggeration. These results demonstrate that combining contrast enhancement and image sharpening in a hybrid framework leverages the strengths of individual techniques while mitigating their limitations, providing superior performance for both visual interpretation and automated segmentation of LGE-CMRI images.

Overall, both qualitative and quantitative results demonstrated that hybrid image enhancement achieved the most effective improvement in LGE-CMRI image quality. By integrating the best contrast and sharpening methods, the hybrid approach reduced blurriness, enhanced contrast, and preserved myocardial and scar textures, providing clearer and more diagnostically useful images for image segmentation of cardiac structures. Therefore, hybrid-image enhancement hopefully able to reduces misclassification and provides optimal input for the multi-stage DeepLabV3+ image segmentation framework as the optimal preprocessing strategy for image input.

4.4 Result of Proposed Multi-Stage Image Segmentation using DeepLabV3+

In this research, the performance of the proposed multi-stage image segmentation using DeepLabV3+ framework was discussed according to the structural of three segmentation stage: Stage 1 that consist of LV and cavity segmentation, followed by Stage 2 by myocardium mapping, and final Stage 3 of myocardial scar segmentation. This research continued by the proposed hybrid image enhancement–image segmentation multi-stage framework using DeepLabV3+. This section also discusses the segmentation results obtained for four regions of interest, namely LV, cavity, myocardium, and scar. The evaluation performance of this method was based on qualitative and quantitative evaluation by using the DSC, IoU and accuracy. In addition, the effectiveness of the multi-stage framework was analysed across different backbone architectures and compared with a conventional single-stage segmentation approach.

4.4.1 Stage 1 Multi-Stage Image Segmentation: LV and Cavity Segmentation

The first stage of the proposed multi-stage image segmentation framework focuses on segmenting the LV and cavity, which were the largest and most visually distinguishable cardiac structures in LGE-CMRI. This stage then was evaluated using three backbone architectures, namely ResNet-50, Xception, and MobileNetV2, to examine how backbone depth and feature representation influence segmentation behaviour on the testing dataset. The discussion in this section was based on the predicted segmentation masks and the corresponding performance values reported in the tables. These segmentation errors were further illustrated by the color-coded outputs. Regions highlighted in magenta represented false positive segmentation, where the model predicted targeted in areas without actual targeted tissue. This over-segmentation was mainly observed near myocardial boundaries and scar regions, suggesting confusion of complex myocardial anatomy. Meanwhile, regions shown in green indicated false negative segmentation, where true scar regions were present but were not successfully segmented.

The qualitative evaluation of LV segmentation, as illustrated in Figure 4.6, demonstrates the proposed multi-stage framework's ability to accurately delineate the left ventricle across different backbone architectures. ResNet-50 produced the most precise LV masks, with boundaries closely aligned to the reference contours. The color-coded visualization highlights only minor false negative regions along the ventricular edges, indicating minimal missed pixels in areas with subtle intensity transitions. The LV wall appeared continuous and well-defined, suggesting that ResNet-50's deep feature hierarchies successfully captured both global ventricular shape and local intensity variations. This precise boundary delineation is particularly important in regions where myocardial thickness varies or the intensity difference between myocardium and surrounding tissue is limited, allowing subsequent segmentation stages to have a reliable structural anchor.

MobileNetV2 also performed effectively in segmenting the LV, producing masks that broadly captured the overall structure. However, closer inspection revealed occasional minor false negative pixels along areas of gradual intensity change, particularly near thinner portions of the myocardium. These small inaccuracies indicate that MobileNetV2, with its shallower architecture, is slightly less sensitive to subtle edge cues compared to ResNet-50. Despite this, the predicted LV region remained continuous and correctly localized, demonstrating that the multi-stage framework provides sufficient contextual guidance to compensate for the lighter backbone's reduced feature extraction capacity. This highlights the balance between computational efficiency and segmentation reliability, where MobileNetV2 can achieve reasonable performance with lower computational cost.

Xception showed slightly higher segmentation errors along the LV boundaries, with scattered false positives and false negatives near complex anatomical features. While the overall LV shape was accurately identified, these localized misclassifications indicate that lightweight backbones may struggle to precisely capture edge details in areas of subtle contrast or myocardial heterogeneity. Nevertheless, Xception successfully established a coarse LV segmentation, sufficient for guiding subsequent myocardium and scar segmentation, confirming that even less computationally demanding backbones can provide meaningful anatomical localization when integrated into the multi-stage framework.

Across all backbones, the qualitative evaluation shows that the LV segmentation was consistently robust, producing closed, continuous, and anatomically plausible structures. The predicted masks effectively capture the general shape and orientation of the ventricle, providing a reliable foundation for the next stages of myocardial and scar segmentation. Notably, ResNet-50 stands out for its superior boundary precision and continuity, while MobileNetV2 offers a strong balance between accuracy and efficiency, and Xception provides an acceptable coarse LV delineation at reduced computational complexity. These observations confirm that the multi-stage framework successfully leverages backbone-specific strengths to produce anatomically consistent LV segmentation, which is critical for both visual assessment and automated downstream analysis.

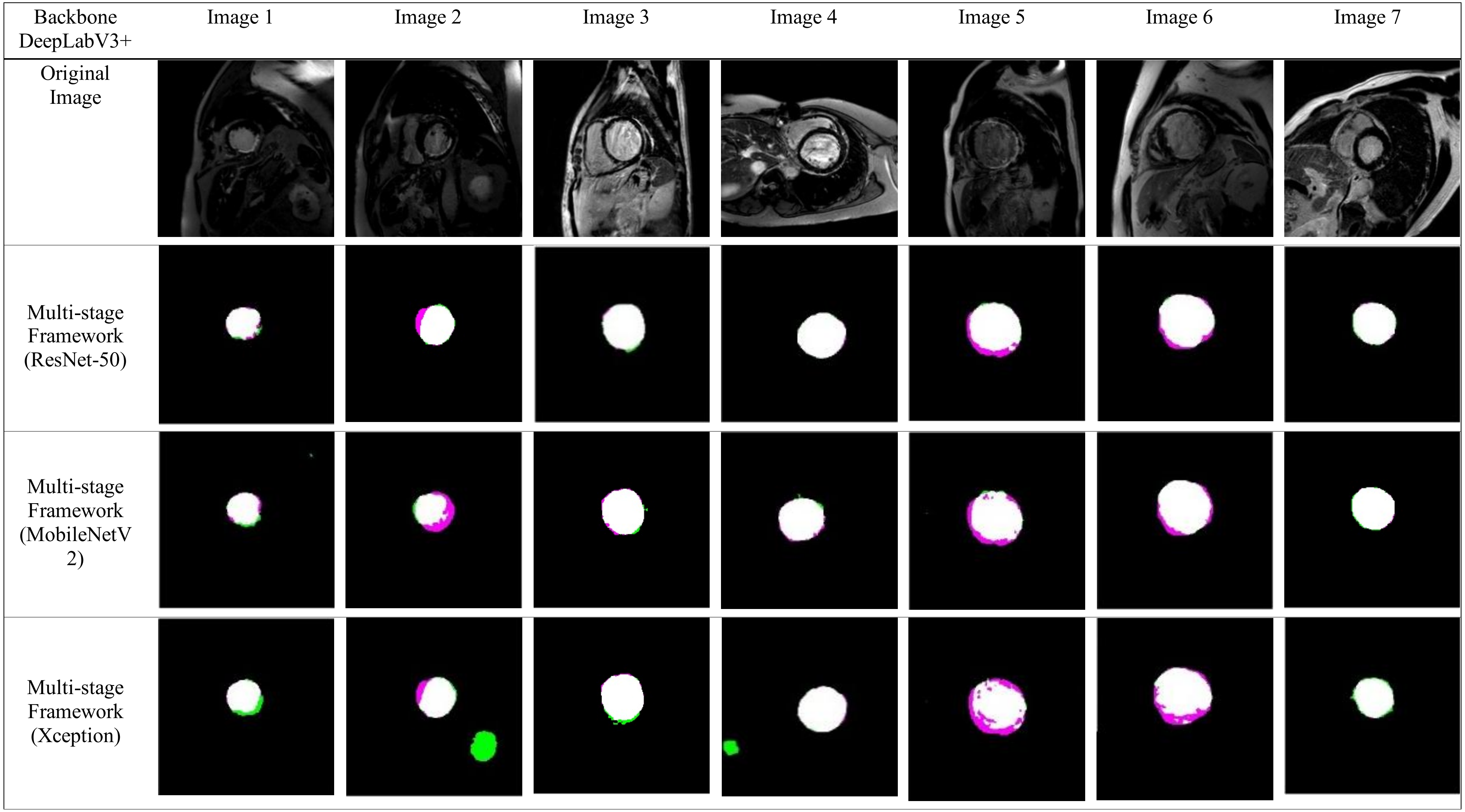

Figure 4.6 Visual Result on Stage 1 LV Image Segmentation Using DeepLabV3+ Framework

The qualitative evaluation of cavity segmentation, as shown in Figure 4.7, demonstrates that the proposed multi-stage framework reliably identifies the blood pool within the left ventricle across all backbone architectures. For the ResNet-50 backbone, the multi-stage framework produces highly accurate and consistent cavity masks across all seven images. The segmented blood pool demonstrates smooth and continuous boundaries that are fully enclosed within the LV, reflecting both the global shape and local intensity variations of the cavity. Only minimal areas of false negative pixels are observed along the lower edges in a few slices, suggesting very slight under-segmentation. Despite these minor imperfections, the masks retain excellent structural fidelity, capturing the circularity and uniformity of the LV cavity. This consistency across multiple slices indicates that ResNet-50 is particularly effective at integrating spatial context and capturing high-contrast boundaries, making it a reliable backbone for downstream myocardial tissue and scar segmentation. The smooth transitions and continuity of the cavity boundary highlight the model's capacity to preserve anatomical correctness even in areas with subtle intensity variations, where segmentation can often be challenging.

MobileNetV2 also successfully identifies the LV cavity in all images; however, the masks exhibit more subtle irregularities compared to ResNet-50. Small areas along the lower and lateral edges show minor over-segmentation, with the predicted cavity slightly extending into adjacent myocardial tissue. Despite these imperfections, the masks remain largely continuous and fully enclosed, demonstrating that MobileNetV2 captures the overall cavity structure effectively while offering a lightweight and computationally efficient alternative. The observed deviations suggest that while MobileNetV2 adequately represents the general morphology of the cavity, it is slightly less precise in delineating thin or curved boundaries, particularly in slices with lower contrast or complex anatomical variations. Nonetheless, the framework still provides sufficient spatial context to maintain the overall structural integrity of the segmented cavity.

In contrast, Xception exhibits a higher presence of both false positive and false negative regions along the LV cavity boundary. The segmentation masks show noticeable irregularities, with portions of the blood pool either missing or erroneously extended into the surrounding myocardium. These inconsistencies are particularly evident in images where the cavity boundary transitions are sharp or where intensity gradients are subtle. Although Xception successfully identifies the general location of the cavity, the reduced sensitivity to fine edge details results in masks that are less smooth and less anatomically consistent. This highlights a limitation of the Xception backbone in capturing precise anatomical edges, suggesting that it may be more suitable for coarse localization tasks rather than fine-grained segmentation of high-contrast cardiac structures.

Overall, the visual evaluation across the seven MRI slices confirms that the ResNet-50 backbone within the multi-stage framework achieves the highest level of precision and anatomical plausibility in LV cavity segmentation. MobileNetV2 provides a balanced trade-off between efficiency and accuracy, producing reasonably continuous and enclosed cavity masks with minor deviations. Xception, while capable of coarse cavity localization, demonstrates increased boundary irregularities and misclassifications. These results underscore the importance of backbone selection in multi-stage segmentation frameworks: deeper, more expressive networks like ResNet-50 are particularly effective for delineating high-contrast cardiac structures such as the LV cavity, whereas lightweight architectures may require additional post-processing or refinement strategies to achieve comparable anatomical accuracy.

Figure 4.8 visually illustrates the qualitative comparison of left ventricular (LV) and cavity segmentation results produced by the multi-stage DeepLabV3+ framework using three different backbone architectures: ResNet-50, MobileNetV2, and Xception. The figure presents the original LGE-CMRI images alongside the corresponding ground truth and predicted segmentation masks for both the LV and its cavity. It highlights how each backbone captures the anatomical structure, with ResNet-50 showing the smoothest and most consistent cavity boundaries, MobileNetV2 providing reasonably accurate but slightly irregular masks, and Xception exhibiting more pronounced boundary deviations and segmentation artifacts. This visual comparison reinforces the quantitative findings by clearly demonstrating the differences in boundary precision, continuity, and anatomical plausibility among the three backbone models.

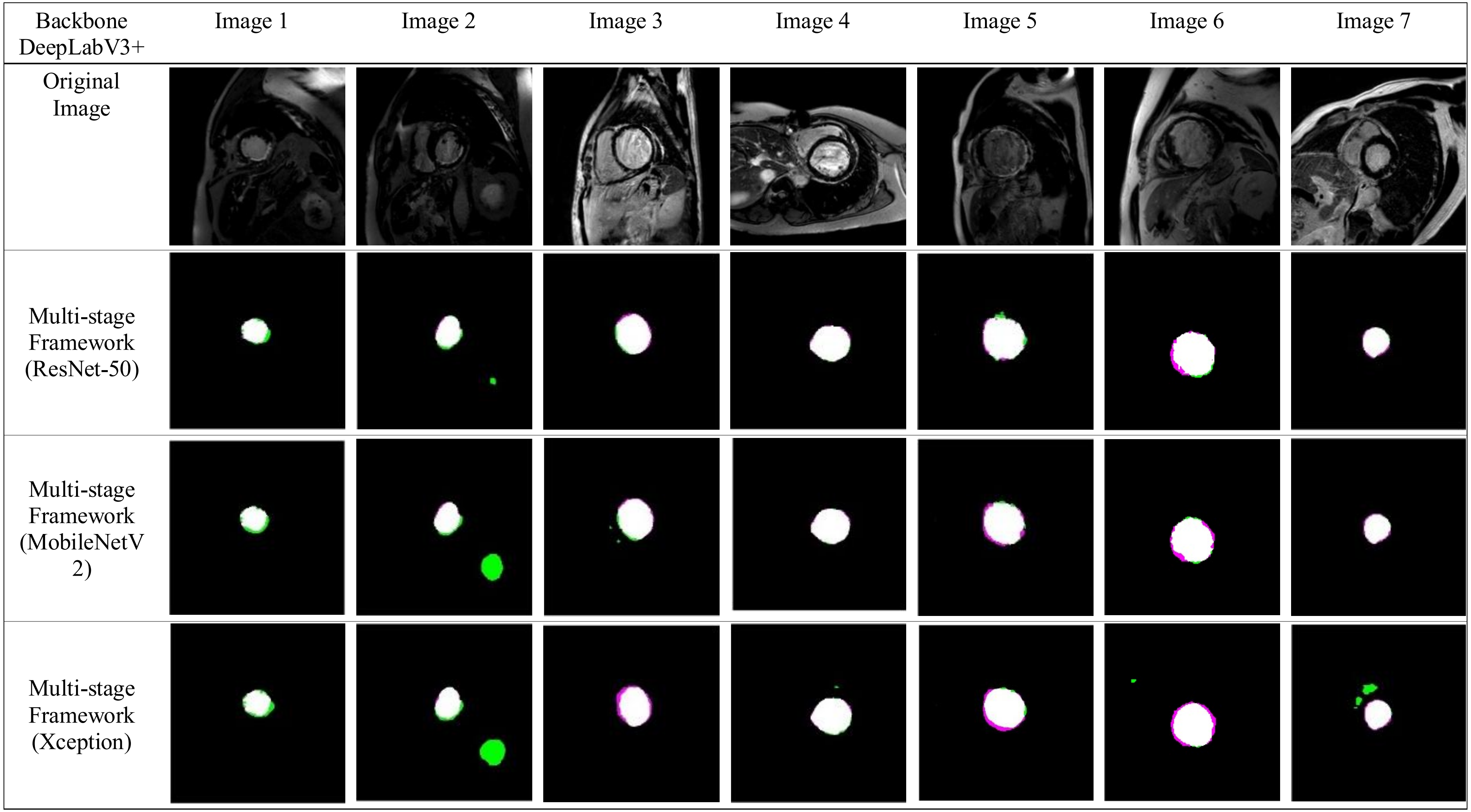

Figure 4.7 Visual Result on Stage 1 Cavity Image Segmentation Using DeepLabV3+ Framework

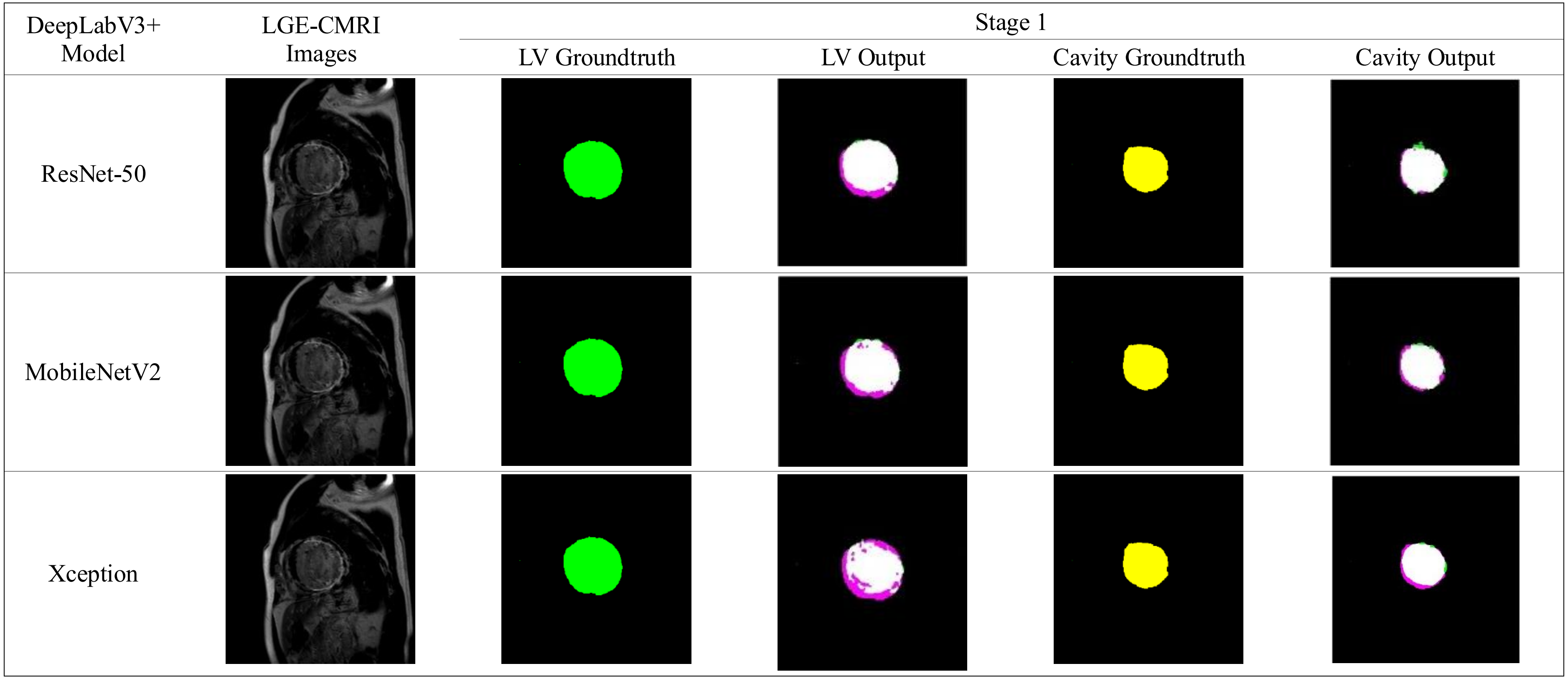

Figure 4.8 Visual Comparison Between 3 Backbone of LV and Cavity Image Segmentation

The performance evaluation results presented in Table 4.4 demonstrate that the multi-stage DeepLabV3+ framework is highly effective for LV segmentation across all tested backbone architectures. Among the three, ResNet-50 achieved the highest mean DSC of 96.98 %, indicating a nearly perfect overlap between the predicted and ground truth LV regions. This superior performance can be attributed to the depth and residual connections in ResNet-50, which facilitate the learning of both high-level contextual features and fine-grained structural details. These residual pathways mitigate the vanishing gradient problem, allowing the network to propagate detailed spatial information through multiple layers, which is critical for accurately delineating the LV boundaries, especially in regions with low contrast between the myocardium and adjacent structures.

MobileNetV2, while a lighter and more computationally efficient backbone, achieved a comparable mean DSC of 96.55 %, only slightly lower than ResNet-50. This demonstrates that even lightweight architectures can capture essential LV features when integrated within a multi-stage framework that emphasizes progressive refinement of segmentation masks. The smaller gap in performance suggests that the framework's design-comprising multiple stages that iteratively refine feature maps and boundary predictions-plays a significant role in stabilizing segmentation accuracy, effectively compensating for the reduced representational capacity of MobileNetV2.

Xception, with a mean DSC of 94.27 %, performed slightly lower than the other two backbones. Despite its depthwise separable convolutions offering efficient feature extraction, it appears less capable of capturing subtle LV boundary variations, particularly in areas of low contrast between the LV wall and surrounding tissues. Nevertheless, the DSC remains high, showing that the multi-stage framework can support different backbone complexities while maintaining strong performance. Similar trends are reflected in mean Intersection over Union (IoU) and pixel-wise accuracy metrics, where ResNet-50 consistently outperforms the others, followed by MobileNetV2 and Xception. This consistency across multiple evaluation metrics reinforces the conclusion that deeper backbones excel at refining LV boundaries, whereas the framework ensures robust segmentation even with less complex architectures.

Table 4.4
Performance Evaluation of Stage 1 of Multi-Stage Image Segmentation of LV and Cavity

Multi-stage Image Segmentation DeepLabV3+ Backbone	Evaluation Metrics			
	Targeted Region	Mean DSC (%)	Mean IoU (%)	Mean Accuracy (%)
ResNet-50	LV	**96.98**	**89.63**	**95.17**
	Cavity	**95.48**	**89.26**	**94.51**
MobileNetV2	LV	94.27	89.03	93.51
	Cavity	94.01	88.76	88.64
Xception	LV	93.18	81.09	83.72
	Cavity	92.07	79.12	74.82

Image segmentation performance evaluation for cavity shows a similar pattern but with slightly lower values compared to LV segmentation, as shown in Table 4.4. ResNet-50 again achieves the highest mean DSC at 95.48 %, highlighting its ability to accurately segment the blood pool region within the LV. This indicates that residual learning not only benefits the identification of thick myocardial walls but also enables precise delineation of the cavity, where pixel intensity differences may be subtler and more prone to partial volume effects in MRI scans.

MobileNetV2 achieved a mean DSC of 94.01 %, which is only marginally lower than ResNet-50. The relatively small performance gap underscores that the multi-stage framework successfully reinforces the segmentation of high-contrast internal structures such as the LV cavity. By progressively refining predictions across stages, the network is able to reduce false positives and negatives, even with a lightweight backbone. This is particularly important for cavity segmentation, as minor inaccuracies along the boundaries can significantly impact volumetric assessments used in clinical diagnostics.

Xception demonstrates a larger drop in performance for cavity segmentation, with a mean DSC of 92.07 %, accompanied by lower IoU and pixel-wise accuracy values of 79.12 % and 74.82 %, respectively. This indicates that while Xception captures general cavity features, it struggles to precisely define the full extent of the blood pool, likely due to less effective learning of local boundary variations and small-scale structures. The performance differences across backbones highlight that deeper or more sophisticated architectures can better manage subtle intensity transitions within the cavity, whereas lighter networks benefit more from the multi-stage refinement to maintain acceptable performance. The accuracy exceeds 94 % across all backbones, further demonstrating that the majority of pixels were correctly classified. ResNet 50 slightly outperforms MobileNetV2 and Xception, suggesting that deeper feature hierarchies better capture subtle intensity variations and structural patterns, even in high-contrast regions. Xception's slightly lower performance indicates that while lightweight backbones were efficient, they may be less robust under anatomical variability or imaging artefacts.

The segmentation results show that the LV region was consistently extracted as a closed and continuous structure, while the cavity was clearly separated from the surrounding myocardial tissue. The predicted masks closely follow the expected ventricular shape, indicating that the network was able to capture the overall heart anatomical structure at this stage. When the LV and cavity were examined separately, the LV segmentation appears more stable than the cavity. This was mainly because the LV wall occupies a larger area and presents clearer contrast against the background. The cavity, although generally well extracted, shows minor boundary inconsistencies in regions where the intensity difference between blood pool and myocardium was less obvious. Despite this, the cavity remains fully enclosed within the LV in most cases, which was important for guiding the following segmentation stages. Nevertheless, Stage 1 successfully establishes a coarse but reliable spatial reference, which constrains subsequent stages and narrows the search space for the myocardium and scar segmentation.

4.4.2 Stage 2 Multi-Stage Image Segmentation: Myocardium Mapping

Stage 2 refines the segmentation to focus on the myocardium, which presents greater challenges due to its thin, continuous structure and intensity overlap with the cavity and surrounding tissue. In Stage 2, the segmentation focuses on the myocardium, which presents greater challenges due to its thin, continuous structure and intensity overlap with the cavity and surrounding tissue. Myocardium segmentation was performed by mapping the segmentation outputs obtained from Stage 1 both LV and cavity as shown in Figure 4.9. The myocardium region was obtained by subtracting the cavity mask from the LV area, allowing the myocardial wall to be identified based on the natural anatomical structure of the heart. This approach ensures that the myocardium was always located between the cavity and the outer LV boundary, which helps maintain anatomical correctness.

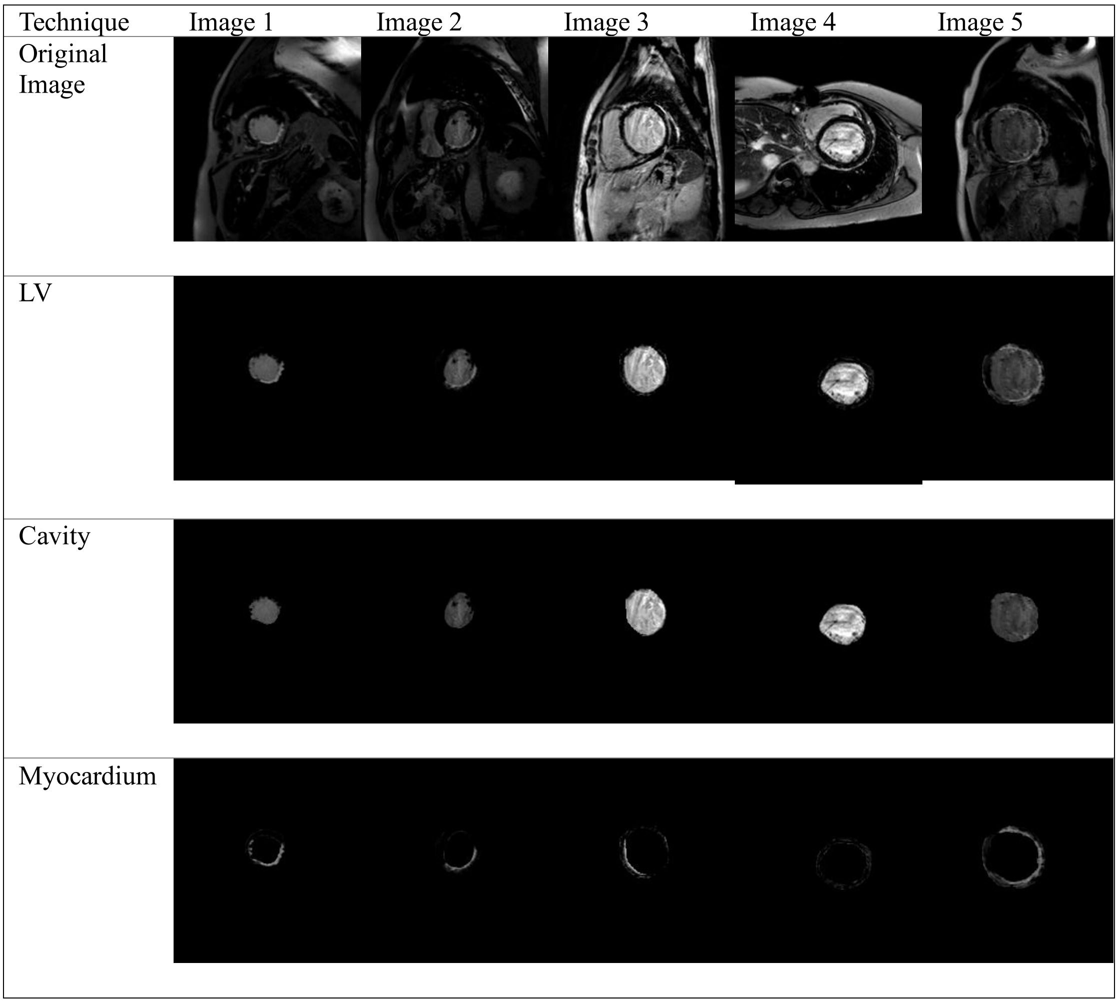

Figure 4.9 Visual Result of Myocardium Mapping from LV and Cavity

Figure 4.9 illustrates the myocardium mapping results produced using this method. The resulting myocardium masks generally form clear and continuous ring-shaped structures that closely follow the reference annotations. The myocardium was consistently positioned around the LV cavity and remains well separated from the background regions. This indicates that the mapping process was effective in preserving the overall shape and location of the myocardial wall, even without additional refinement steps. Despite the generally stable results, some limitations can still be observed. Minor discontinuities and uneven boundaries appear in very thin myocardial regions, particularly in slices where the LV or cavity segmentation from Stage 1 was less accurate. Since the myocardium mask was directly derived from these earlier outputs, any over-segmentation or under-segmentation at Stage 1 propagates into Stage 2. As a result, small gaps or irregular contours may form along the myocardial wall.

Overall, the Stage 2 myocardium mapping process provides a simple and reliable way to extract the myocardial. However, the accuracy and smoothness of the mapped myocardium remain highly dependent on the robustness of the segmentation results obtained in Stage 1, emphasising the importance of accurate LV and cavity segmentation for subsequent stages.

4.4.3 Stage 3 Multi-Stage Image Segmentation: Scar Segmentation

The final stage focuses on myocardial scar segmentation, which was the most challenging task due to the small size, irregular shape, and low contrast of scar regions that introduced a higher false positive and false negative in the segmentation output result. The segmentation results show that the network was able to identify major infarcted areas within the myocardium, although increased variation was observed compared to previous stages. Scar regions were generally detected within the myocardial boundaries, indicating that the spatial constraints from earlier stages effectively restrict the segmentation area. However, faint scars with low intensity were sometimes partially detected or missed, leading to fragmented predictions. This was expected, as scar tissue often appears subtle and varies significantly between patients.

As illustrated in Figure 4.10, the predicted scar masks reveal that the proposed framework was able to identify infarcted regions within the myocardial wall, although the segmentation behaviour varies notably across backbone architectures. The qualitative assessment of myocardial scar segmentation across the three backbone architectures, ResNet-50, MobileNetV2, and Xception was illustrated in Figure 4.10, which presents seven representative LGE-CMRI images. Scar tissue presents unique challenges due to its small size, irregular shape, and heterogeneous intensity, often blending subtly with surrounding myocardium. Across all slices, differences in boundary precision, structural continuity, and anatomical plausibility are clearly visible, highlighting the influence of backbone depth and feature extraction capability within the multi-stage framework.

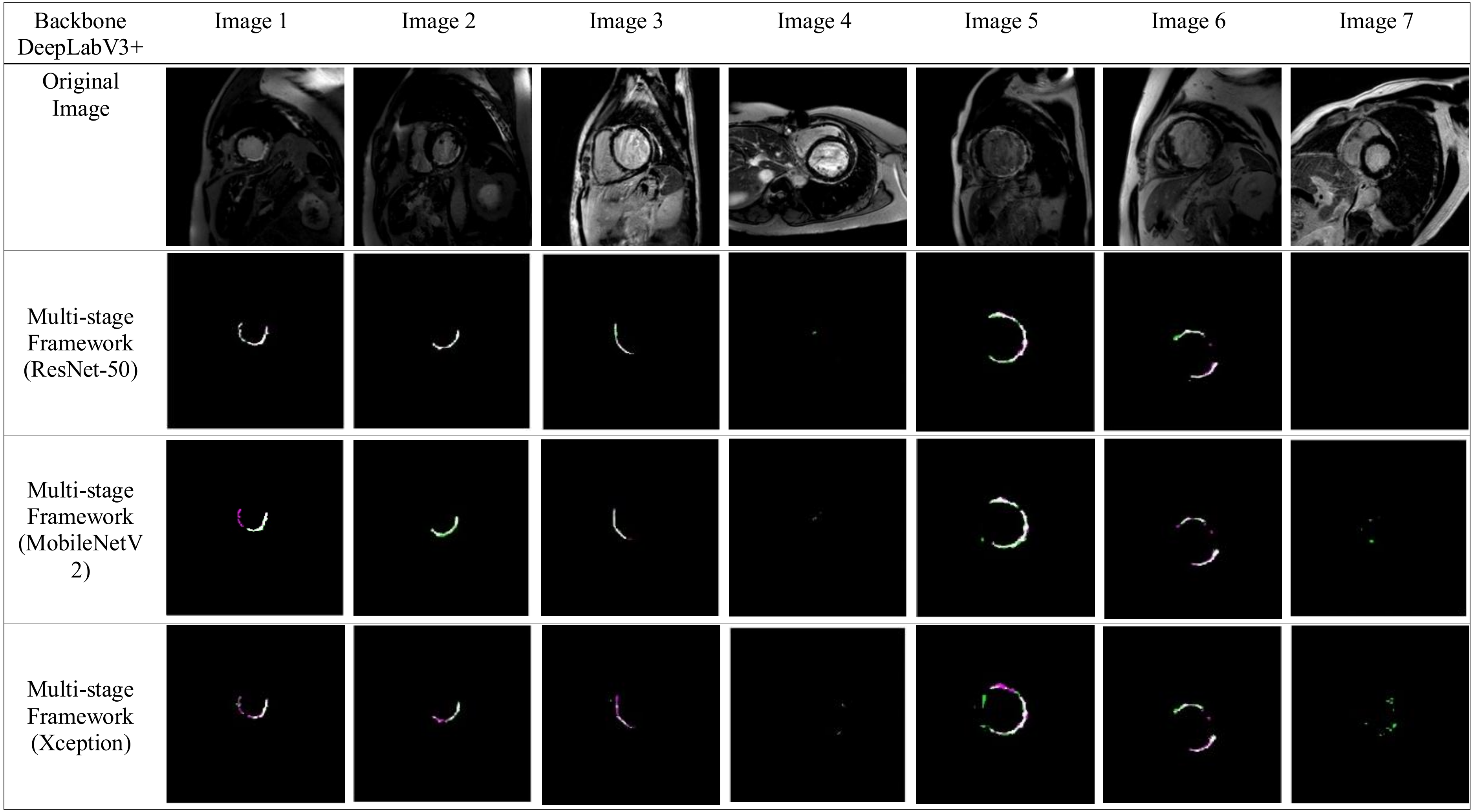

Figure 4.10 Visual Result on Stage 3 Scar Image Segmentation Using DeepLabV3+ Framework

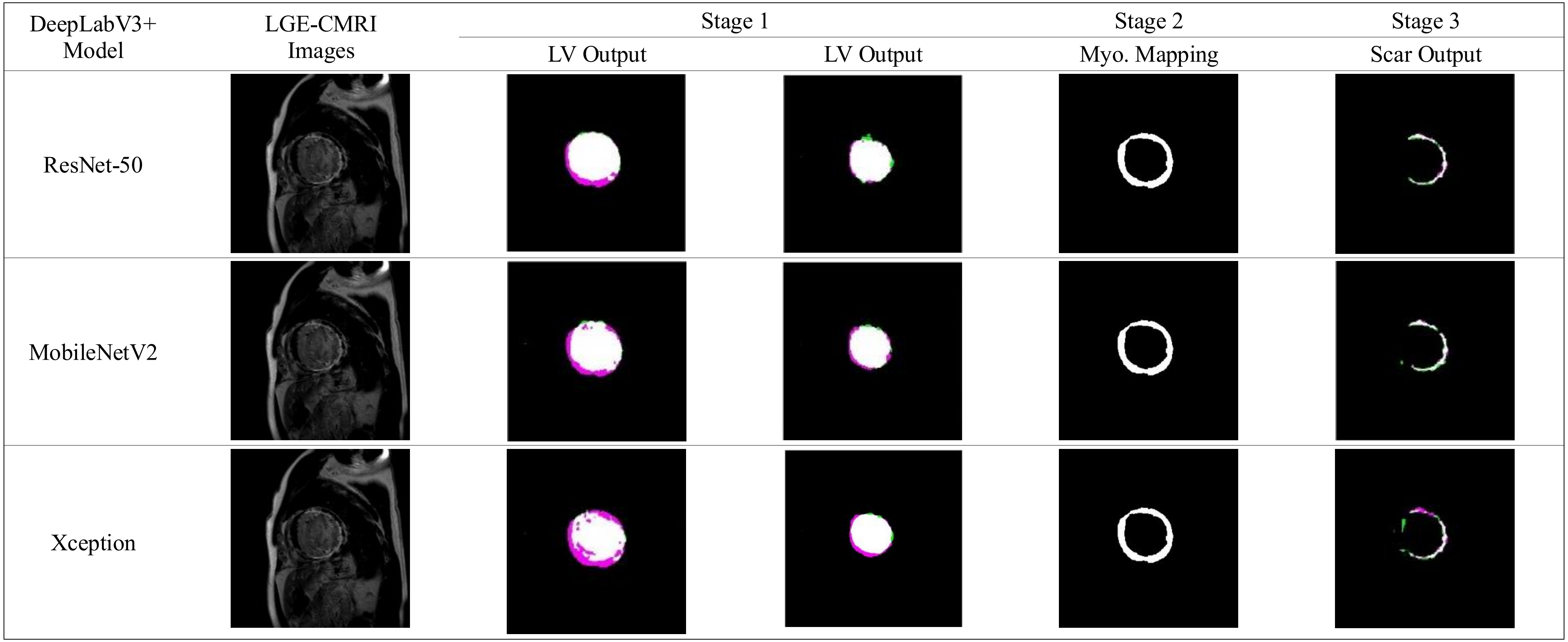

Figure 4.11 Comparison Between 3 Backbone for Scar Image Segmentation Using DeepLabV3+ Framework

For the ResNet-50 backbone, the predicted scar masks are generally well localized and follow the approximate shape and extent of the ground truth regions. Fine-scale boundary details are effectively captured, particularly in areas where scars are adjacent to the LV cavity or myocardial wall. Some minor under-segmentation is observed in thin or fragmented scar regions, reflecting the inherent difficulty of distinguishing subtle intensity gradients from healthy myocardium. Nevertheless, the masks exhibit smooth contours and coherent scar clusters, corresponding to the high mean DSC of 68.49 % and IoU of 48.49 %. These results indicate that the deep residual connections in ResNet-50 facilitate effective propagation of both local and global features, allowing accurate identification of small and irregular scar structures.

MobileNetV2 produces scar masks that correctly capture the general location of scar tissue, but small boundary irregularities are evident in several slices. Fragmentation occurs in thin scar regions, and occasional over-segmentation extends the predicted mask slightly into healthy myocardium. Despite these minor inaccuracies, the multi-stage framework's progressive refinement helps correct some misclassifications, maintaining the overall structural integrity of the segmented scars. This aligns with the moderate mean DSC of 56.96 % and IoU of 36.91 %, demonstrating that MobileNetV2 can still achieve reasonable scar localization despite its lightweight architecture.

Xception exhibits the greatest challenges in scar segmentation. Predicted masks are often discontinuous or fragmented, with higher occurrences of both false negatives and false positives. Thin scars are frequently missed, and some small healthy tissue regions are incorrectly classified as scar. The lower mean DSC of 54.65 % and IoU of 29.68 % reflect these qualitative inconsistencies, emphasizing the difficulty of detecting small, irregular structures with reduced feature granularity.

Overall, the seven-slice qualitative evaluation in Figure 4.10 confirms that scar segmentation is substantially more challenging than LV or cavity segmentation due to the small and fragmented nature of scar tissue. ResNet-50 achieves the most reliable performance, balancing localization accuracy and boundary fidelity. MobileNetV2 maintains moderate accuracy with some fragmentation, while Xception, although capable of coarse localization, struggles with anatomical continuity. These observations underscore the importance of both backbone selection and the multi-stage refinement strategy for detecting subtle cardiac abnormalities.

Figure 4.11 presents an overview of the multi-stage framework, showing the sequential refinement from Stage 1 of LV and cavity image segmentation through

Stage 3 scar segmentation. This figure highlights how the framework leverages high-contrast structures in early stages to provide spatial context for more challenging targets. LV and cavity masks are delineated accurately in Stage 1, establishing a structural foundation that supports Stage 2 myocardium segmentation and Stage 3 scar delineation.

The segmentation of myocardial scar tissue, as shown in Table 4.5, presents a more challenging task compared to LV and cavity segmentation. Scar tissue typically occupies a smaller region, exhibits heterogeneous intensity patterns, and often has low contrast relative to the surrounding healthy myocardium. These characteristics inherently increase the difficulty of automated detection, which is reflected in the lower performance metrics across all backbones.

Table 4.5
Performave Evaluation of Stage 3 of Multi-Stage Image Segmentation Using DeepLabV3+

DeepLabV3+'s backbone	**Performance of Deep Learning Model**			
	Targeted Region	**Mean DSC (%)**	**Mean IoU (%)**	**Mean Accuracy (%)**
Multi-stage Framework (ResNet-50)	LV	**96.98**	**89.63**	**95.17**
	Cavity	**95.48**	**89.26**	**94.51**
	Myo	**83.32**	**75.34**	**80.46**
	Scar	**68.49**	**48.49**	**61.33**
Multi-stage Framework (MobileNetV2)	LV	94.27	89.03	93.51
	Cavity	94.01	88.76	88.64
	Myo	77.19	72.14	74.52
	Scar	56.96	36.91	50.13
Multi-stage Framework (Xception)	LV	93.18	81.09	83.72
	Cavity	92.07	79.12	74.82
	Myo	79.81	73.28	73.54
	Scar	54.65	29.68	50.07

ResNet-50, as part of the multi-stage framework, achieved the highest mean DSC of 68.49 % for scar segmentation, with a corresponding IoU of 48.49 % and pixel-wise accuracy of 61.33 %. While these values are notably lower than those obtained for LV and cavity segmentation, they still indicate that the network is able to identify a significant proportion of scar pixels correctly. The depth and residual connections of ResNet-50 likely contribute to its superior performance by enabling the extraction of both global contextual cues and subtle local intensity variations, which are essential for distinguishing scar tissue from healthy myocardium. The multi-stage framework also plays a critical role, as progressive refinement at each stage allows the network to correct initial misclassifications, especially along complex scar boundaries.

MobileNetV2 achieved a mean DSC of 56.96 % for scar segmentation, with IoU and accuracy values of 36.91 % and 50.13 %, respectively. Despite being a lightweight architecture with fewer, MobileNetV2 demonstrates moderate capability in detecting scar regions. However, its reduced representational capacity limits its ability to capture fine structural and intensity differences inherent in scar tissue, resulting in more false negatives and less precise boundary delineation. Nevertheless, the multi-stage framework mitigates some of these limitations by iteratively refining predictions, helping even a smaller network achieve reasonable performance.

Xception recorded the lowest performance for scar segmentation, with a mean DSC of 54.65 %, IoU of 29.68 %, and pixel-wise accuracy of 50.07 %. Although Xception can efficiently extract features through depthwise separable convolutions, it appears less effective in capturing the subtle, heterogeneous characteristics of scar tissue compared to ResNet-50. The low IoU indicates that Xception struggles with precise spatial overlap between predicted and true scar regions, highlighting the challenge of segmenting small, irregular structures.

When comparing scar segmentation to LV and cavity segmentation, it is evident that scar tissue is significantly more difficult to segment due to its smaller size, variable appearance, and proximity to both healthy myocardium and the blood pool. These results underscore the importance of both backbone complexity and the multi-stage refinement process: deeper architectures like ResNet-50 offer better feature representation for small, low-contrast regions, while the multi-stage framework consistently improves segmentation stability, particularly for challenging targets like scar tissue.

Overall, the findings indicate that while automated scar segmentation remains less accurate than LV and cavity segmentation, the proposed multi-stage DeepLabV3+ framework enables meaningful detection across different backbone architectures, providing a strong foundation for further enhancement through advanced post-processing, attention mechanisms, or data augmentation strategies tailored to small, irregular structure.

4.5 Result of Proposed Hybrid Image Enhancement-Image Segmentation Multi-Stage Framework using DeepLabV3+

The proposed hybrid approach combined hybrid image enhancement, which integrates MRP and Nimble Filter, with multi-stage DeepLabV3+ segmentation to improve LGE-CMRI segmentation results. The hybrid image enhancement addressed issues of low contrast and blurriness, producing clearer images that highlighted myocardial walls, LV cavity, and scar regions. These enhanced images were then processed by the multi-stage DeepLabV3+ segmentation network, which was designed to handle challenges such as intensity inhomogeneity, anatomical variations, and complex myocardial and scar textures. Figure 4.12 shows the resulting segmented images after applying the hybrid approach, illustrating improved continuity of myocardial walls, clearer LV cavity structures, and more visible scar regions compared with segmentation performed on original or singly enhanced images.

Based on the visual results shown in Figure 4.14, the differences in segmentation performance between single-stage image segmentation, multi-stage image segmentation, and the proposed hybrid image enhancement–image segmentation framework can be clearly observed. The figure illustrated that image quality played an important role in influencing segmentation accuracy, particularly for regions affected by low contrast, blurriness, and complex texture such as the myocardium and scar regions. For the single-stage image segmentation approach. Figure 4.13 showed that all target regions, including the LV cavity, myocardium, and scar, were segmented in a single output. While the LV cavity was generally visible due to its larger size and clearer intensity difference, the segmentation of myocardium and scar regions appeared less reliable. Some myocardial and cavity areas, although relatively large, were incorrectly segmented, that indicates both false positive and false negative while scar regions were often partially detected or completely missed as a false negative. This limitation was more evident in areas with intensity inhomogeneity and weak contrast, indicating that handling multiple anatomical regions with varying sizes and intensities in a single stage was challenging, especially for small and low-contrast scar areas.

When compared to single-stage segmentation, the multi-stage image segmentation framework produced more structured outputs, as different regions were segmented separately in a dedicated stage (D. Chen et al., 2022). This reduced interference between regions and improved the segmentation consistency for the myocardium and LV cavity. As shown in Figure 4.14, the LV cavity segmentation appeared more stable, and myocardial boundaries were clearer in most cases than single-stage with smaller false positive and false negative. However, segmentation errors were still observed in images affected by blurriness, intensity inhomogeneity, and complex myocardial texture. Scar segmentation, in particular, remained challenging due to its small size and low contrast relative to the surrounding myocardium.

The proposed hybrid IE-IS framework demonstrated improved segmentation consistency across scar segmentation. As shown in Figure 4.14, a clear comparison between the hybrid and multi-stage frameworks showed that while both approaches achieved reasonable segmentation for the LV cavity and myocardium, the hybrid framework produced more stable outputs segmentation for scar regions. This indicated that fewer false positive and false negative regions were observed, indicating reduced segmentation errors compared to both the single-stage and standard multi-stage approaches. By applying image enhancement before segmentation, the input images showed reduced blurriness and clearer separation between tissue regions. The scar regions appeared more continuous and less fragmented compared to both single-stage and multi-stage approaches, even in images with complex texture and intensity variation.

Overall, Figure 4.14 confirmed that single-stage image segmentation was limited in handling multiple regions simultaneously, particularly in challenging LGE-CMRI images. Multi-stage segmentation improved region separation but remained sensitive to image quality variations. The hybrid image enhancement–image segmentation framework provided the most consistent segmentation results by reducing image quality limitations prior to segmentation. These observations were consistent with findings reported in previous studies, where enhanced image quality prior to segmentation was shown to improve model robustness and segmentation accuracy in LGE-CMRI analysis.

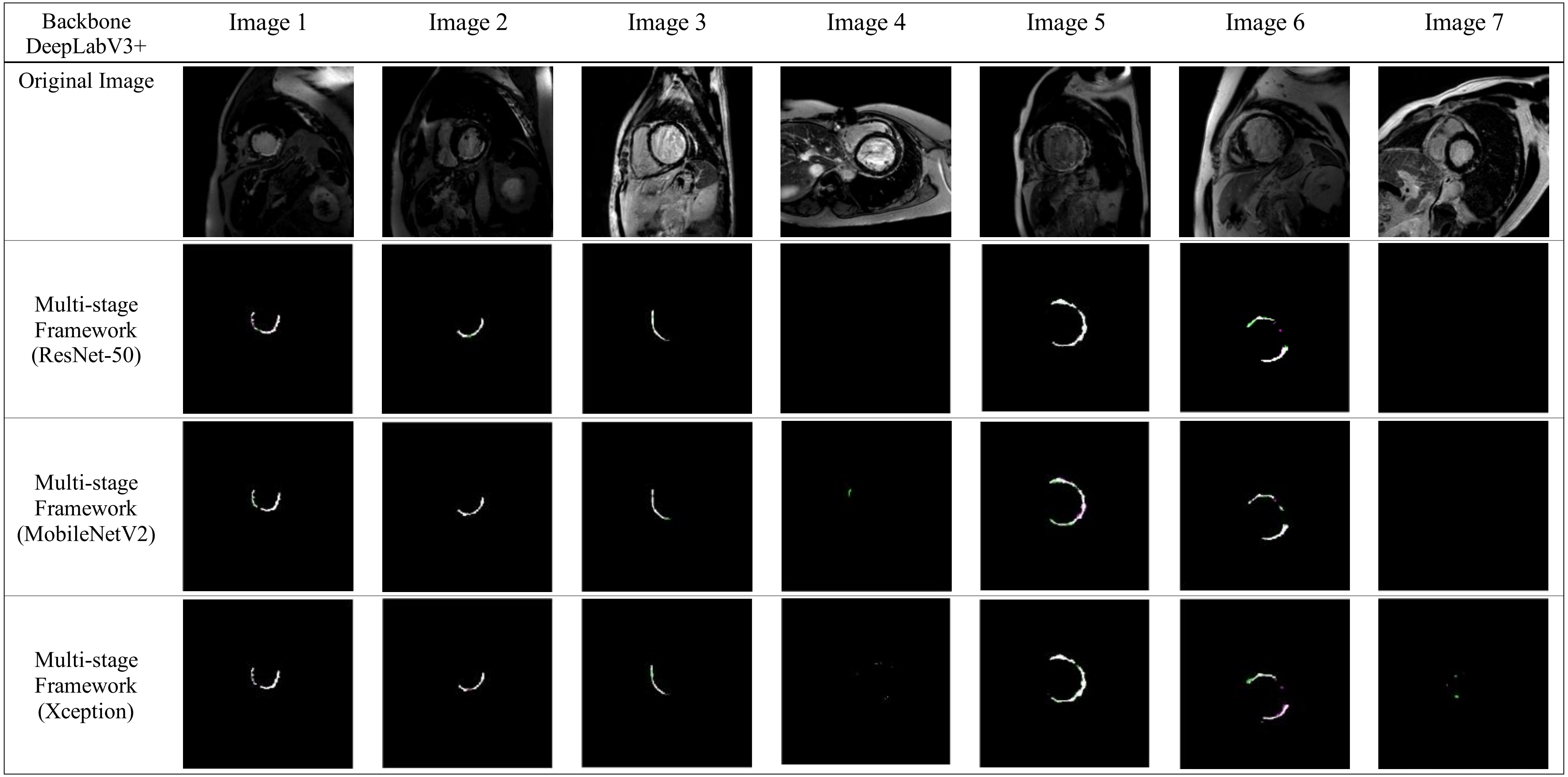

Figure 4.12 Visual Result on Hybrid Image Enhancement – Image Segmentation Using DeepLabV3+ Framework

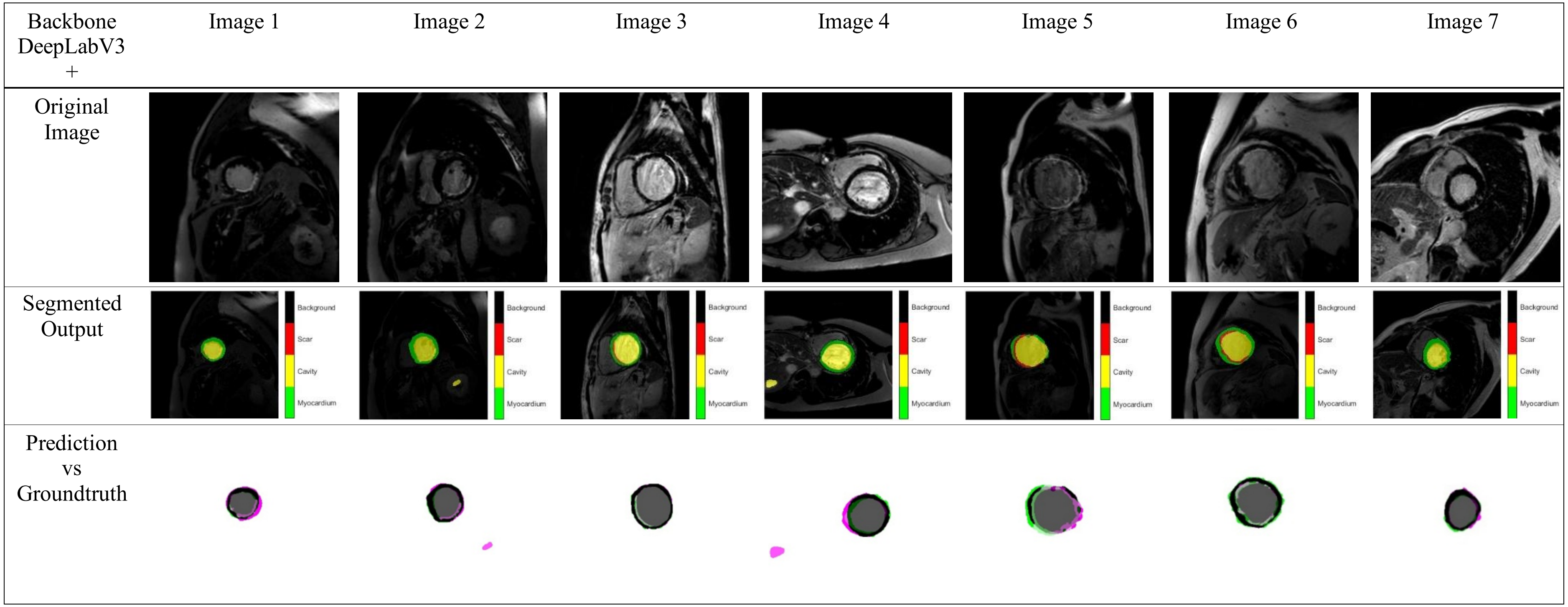

Figure 4.13 Single-Stage Image Segmentation Result and Comparison with Predicted Result Using Single-Stage DeepLabV3+ Framework

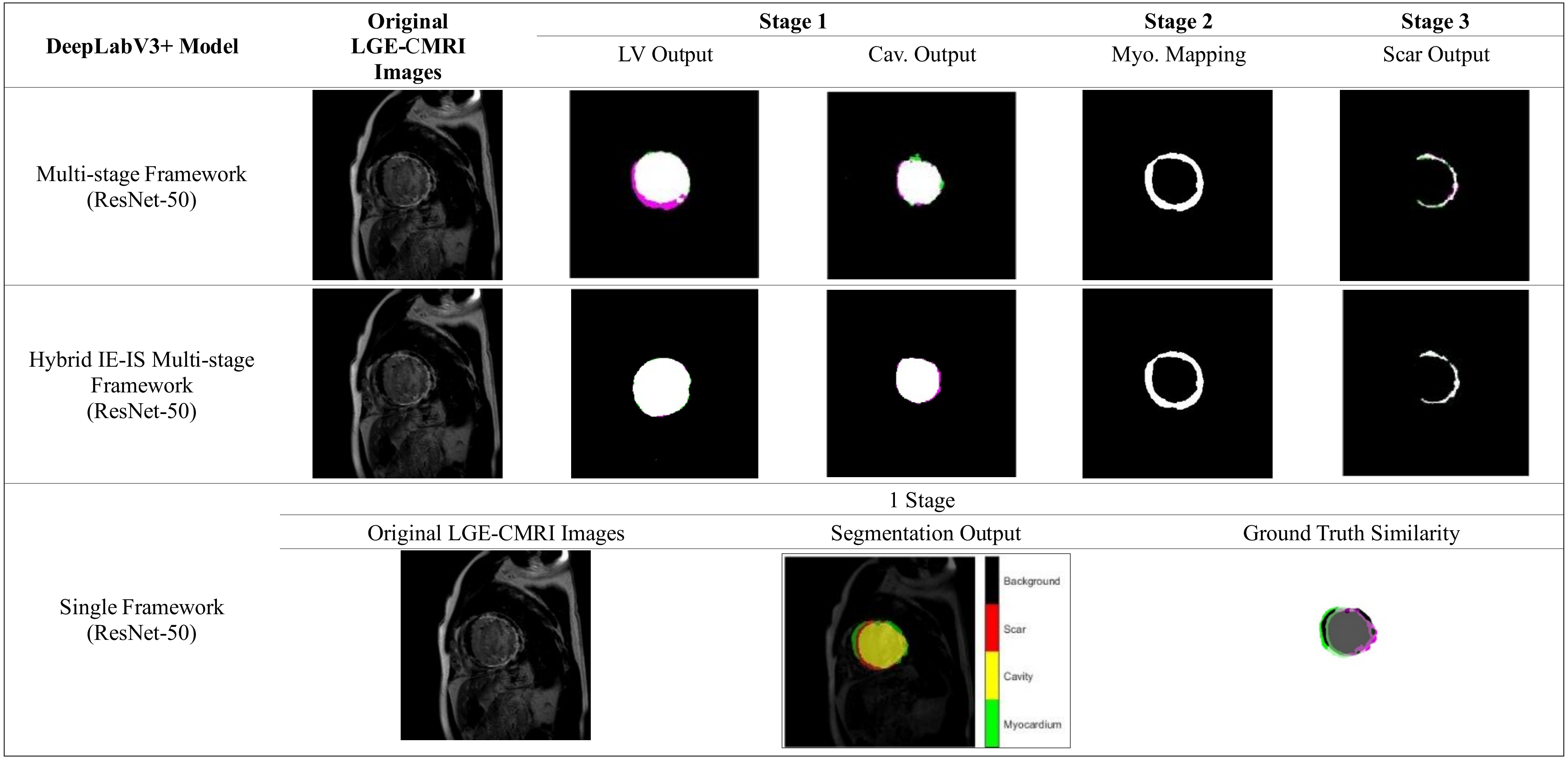

Figure 4.14 Image Segmentation Comparison Between Single-Stage, Multi-Stage and Hybrid Multi-Stage Image Segmentation Using DeepLabV3+ Framework with Resnet-50 Backbone

Table 4.6 presents a comparative evaluation of the segmentation performance across three different frameworks: single-stage DeepLabV3+, multi-stage DeepLabV3+, and a hybrid image enhancement–image segmentation framework. The metrics considered, mean DSC, mean IoU and mean accuracy, highlight the advantages of progressive refinement and image enhancement in improving segmentation quality across multiple cardiac structures, including the left ventricle, cavity, myocardium, and scar tissue.

Table 4.6
Performance Evaluation Comparison Across Single-Stage, Multi-Stage and Hybrid IE – IS using DeepLabV3+ Framework

DeepLabV3+'s backbone	**Performance of Deep Learning Model**			
	Targeted Region	**Mean DSC (%)**	**Mean IoU (%)**	**Mean Accuracy (%)**
Single Framework (ResNet-50)	LV	91.47	85.06	93.15
	Cavity	93.10	88.12	91.49
	Myo	12.38	56.44	67.75
	Scar	53.63	13.52	17.25
Multi-stage Framework (ResNet-50)	LV	96.98	89.63	95.17
	Cavity	95.48	89.26	94.51
	Myo	83.32	75.34	80.46
	Scar	68.49	48.49	61.33
Hybrid IE-IS using Multi-stage Framework (ResNet-50)	LV	**98.22**	**91.67**	**96.57**
	Cavity	**97.78**	**93.75**	**95.85**
	Myo	**85.15**	**75.68**	**83.54**
	Scar	**70.88**	**62.37**	**65.21**

The single-stage framework demonstrates the lowest overall performance, particularly for myocardium and scar segmentation. While left ventricle and cavity segmentation achieve moderate accuracy with mean DSC values of 91.47 percent and 93.10 percent, myocardium and scar segmentation are severely underperforming, with mean DSC values of only 12.38 percent and 53.63 percent, and extremely low IoU for scar at 13.52 percent. This indicates that single-stage networks struggle to capture small, low-contrast structures without the benefit of intermediate refinement or contextual information. The disparity between high-contrast regions such as the left ventricle and cavity and low-contrast targets such as myocardium and scar underscores the limitation of applying a single-stage network directly to complex CMRI data.

The multi-stage framework significantly improves performance across all targeted regions. Left ventricle and cavity segmentation metrics are already high with mean DSC values of 96.98 percent and 95.48 percent, reflecting the framework's ability to refine predictions progressively and preserve structural continuity. Notably, myocardium segmentation improves to a mean DSC of 83.32 percent, and scar segmentation reaches 68.49 percent, demonstrating that iterative refinement allows the network to capture smaller and lower-contrast regions more effectively. These results suggest that the multi-stage design, by progressively leveraging information from high-contrast structures in early stages, provides contextual guidance that enhances the accuracy of downstream segmentation tasks.

The hybrid image enhancement–image segmentation framework further improves performance over the multi-stage network. Left ventricle and cavity segmentation achieve mean DSC values of 98.22 percent and 97.78 percent, showing that contrast and detail enhancement of the input images increases boundary clarity and structural definition. Myocardium segmentation improves to 85.15 percent, while scar segmentation reaches 70.88 percent, accompanied by a notable increase in IoU to 62.37 percent and accuracy to 65.21 percent. The enhancement stage effectively amplifies subtle intensity differences in low-contrast tissues, enabling the network to better delineate fragmented or irregular scar regions. These improvements demonstrate that the combination of image preprocessing with multi-stage segmentation allows for more precise extraction of both high-contrast and low-contrast structures, achieving a balance between sensitivity and boundary fidelity.

Overall, the results in Table 4.6 clearly indicate a performance hierarchy from single-stage to multi-stage to hybrid image enhancement and segmentation. While high-contrast regions such as the left ventricle and cavity can be segmented effectively even in simpler frameworks, progressive refinement and image enhancement are critical for low-contrast structures like myocardium and scar tissue. The hybrid framework provides the most robust and anatomically plausible segmentation, validating the benefit of integrating preprocessing enhancement with multi-stage network design for comprehensive cardiac tissue analysis.

4.6 Conclusion

This chapter presents and discusses the experimental results of the proposed methodology, covering image preprocessing, image enhancement, image segmentation, and the hybrid enhancement–segmentation framework. The study began with image preprocessing, as described in Section 4.2, which prepared the CMRI images for further analysis. Preprocessing standardized the image intensity and improved the clarity of anatomical structures, providing a solid foundation for subsequent enhancement and segmentation. This step was important to ensure that the later stages could accurately highlight myocardial walls, the LV cavity, and scar regions without being affected by variations in the original images.

Image enhancement, detailed in Section 4.3, was conducted in three stages: contrast enhancement, image sharpening, and hybrid image enhancement. Contrast enhancement was applied to improve the visibility of myocardial walls, LV cavity, and scar regions, addressing the low contrast inherent in CMRI images. Visual observations showed that while contrast enhancement made major structures more visible, some areas remained slightly blurry, particularly small scar regions. Image sharpening was then applied to improve the edges of myocardial structures. Image sharpening increased the distinction between different regions, making myocardial walls and the LV cavity clearer. However, some sharpening methods produced slight blurriness in the cavity or misrepresented small scar regions, highlighting the limitations of using sharpening alone. The hybrid image enhancement combined the best-performing contrast enhancement and image sharpening technique. This combination produced images with improved contrast and clearer edges, allowing myocardial walls, LV cavity, and scar regions to be more distinguishable. The hybrid approach addressed the main image enhancement problems which are low contrast and blurry LGE-CMRI image in order to provide more reliable input for image segmentation.

Next, image segmentation was performed using the multi-stage DeepLabV3+ framework, which is presented in Section 4.4. By separating the image segmentation task into dedicated stages for the LV, cavity, myocardium, and scar regions, the framework produced more consistent and accurate results. Visual observations revealed that myocardial walls and LV cavity were clearly segmented, and scar regions, which were small and low contrast, were captured more accurately than in previous single-stage segmentation approaches. Incorrectly segmented regions, where scar or myocardium were wrongly classified, were reduced, and boundaries appeared more continuous. The hybrid enhancement prior to segmentation in Section 4.5 further improved the performance by increasing the clarity of edges and contrast, allowing the network to handle intensity inhomogeneity, anatomical variation, and complex textures more effectively. Compared to single-stage segmentation, which struggles to separate multiple regions simultaneously, the hybrid framework produced outputs with fewer errors and better overall consistency.

Overall, the results, summarized in Section 4.6, confirmed that each stage in the proposed methodology contributed to improved segmentation performance. Contrast enhancement improved visibility but could not fully resolve blurriness, and image sharpening clarified edges but had limitations for subtle structures. Hybrid image enhancement successfully combined these advantages, producing clearer and more informative images. When integrated with multi-stage segmentation, this approach yielded the most consistent and reliable segmentation of myocardial walls, LV cavity, and scar regions, effectively addressing all five problem statements identified in this research. The observations and results demonstrate that enhancing image quality before segmentation is essential for accurate and reliable analysis of CMRI images.

CHAPTER 5
CONCLUSION

5.1 Conclusion

This research has successfully developed a hybrid framework that integrates image enhancement with multi-stage deep learning segmentation for automated myocardial scar detection from LGE-CMRI. The study was guided by three main objectives: to enhance CMRI images using image processing techniques to improve image quality and segmentation accuracy, to develop a deep learning-based model with a multi-stage segmentation approach for accurate scar segmentation, and to evaluate the performance of the enhancement and segmentation model using both qualitative and quantitative methods. The findings of this study demonstrate that these objectives have been successfully achieved, providing strong evidence of the effectiveness, reliability, and clinical relevance of the proposed framework.

In the first objective, the study proposed to enhance LGE-CMRI images to improve image quality and facilitate more accurate myocardial scar segmentation. To achieve this, a hybrid Image Enhancement–Image Sharpening (IE-IS) method was developed, combining contrast enhancement techniques such as Morphological Residual Processing (MRP) and Type-II Fuzzy Set enhancement with sharpening techniques, including the Nimble Filter, Unsharp Masking, High-Boost Filter, and Laplacian Filtering. This hybrid approach was specifically designed to address the inherent challenges of LGE-CMRI data, which are characterized by low contrast and subtle myocardial scar boundaries, making conventional enhancement techniques insufficient to reveal fine structural details. The CI-IS method selectively enhanced low-contrast regions while preserving high-intensity structures, emphasizing intensity transitions, and improving the visibility of myocardial tissue and scar regions, which are critical for subsequent segmentation.

The application of the proposed Hybrid IE-IS method achieved notable improvements in objective image quality metrics, demonstrating its effectiveness in both contrast enhancement and detail preservation. The enhanced images reached a PSNR of 56.33 dB, indicating high fidelity to the original image, while the SSIM of 0.989 confirmed excellent structural similarity. The method also reduced reconstruction error, as reflected by a low MSE of 0.007, and improved intensity differentiation, with Contrast RMS reaching 0.128. Furthermore, the Entropy of 5.189 suggested that the enhanced images contained richer information and finer textural details, enabling clearer visualization of myocardial and scar boundaries.

In the second objective, the study proposed a multi-stage DeepLabv3+ segmentation framework with a ResNet-50 backbone to accurately delineate the LV, myocardium, cavity, and myocardial scar regions. This multi-stage design enabled progressive feature refinement, first capturing coarse anatomical structures and then resolving subtle myocardial scar details. The framework demonstrated excellent performance, with the LV segmented at a mean DSC of 96.98%, mean IoU of 89.63%, and mean accuracy of 95.17%, and the cavity at a mean DSC of 95.48%, mean IoU of 89.26%, and mean accuracy of 94.51%. The myocardium segmentation achieved a mean DSC of 83.32%, mean IoU of 75.34%, and mean accuracy of 80.46%, while myocardial scar regions were captured with a mean DSC of 68.49%, mean IoU of 48.49%, and mean accuracy of 61.33%. These results confirm that the multi-stage framework effectively extracted discriminative features, maintained spatial coherence, and accurately segmented both prominent anatomical structures and subtle scar regions.

For comparison, the Hybrid IE-IS approach integrated within the same multi-stage framework achieved slightly higher segmentation performance for myocardial and scar regions, indicating that while the hybrid enhancement improved overall feature visibility and edge clarity, the multi-stage segmentation strategy alone was not sufficient to achieve excellent delineation of major anatomical structures. The LV and cavity achieved near-complete overlap and high reliability, with DSC values of 98.22% and 97.78%, respectively, while the myocardium and scar achieved DSC values of 85.15% and 70.88%. The corresponding IoU and accuracy metrics followed a similar trend, confirming the strong capability of the multi-stage framework in challenging LGE-CMRI datasets.

In the third objective, the study evaluated the effectiveness of the multi-stage framework across different backbone architectures, comparing ResNet-50, MobileNetV2, and Xception. ResNet-50 was retained as the primary backbone due to its balance of depth, capacity, and ability to capture hierarchical features, which was critical for handling the subtle intensity variations of myocardial scar regions. MobileNetV2 offered a lightweight alternative, suitable for faster computation but with slightly lower segmentation accuracy for fine structures. Xception, with its depthwise separable convolutions, provided efficient feature extraction with strong channel-wise discrimination, but the overall performance remained comparable to ResNet-50 for most myocardial targets. This evaluation confirmed that the proposed multi-stage framework is robust and adaptable, capable of maintaining high segmentation accuracy across different backbone architectures while providing flexibility for deployment based on computational constraints.

In conclusion, the research successfully achieved its objectives. The proposed hybrid IE-IS method enhanced image quality, as reflected by improvements in PSNR, SSIM, MSE, Contrast RMS, and Entropy. The multi-stage DeepLabv3+ framework effectively segmented LV, myocardium, cavity, and scar regions with high accuracy, and the comparative evaluation of backbones demonstrated robustness and adaptability for LGE-CMRI datasets. Together, these findings highlight the strength of combining advanced image enhancement with a carefully designed multi-stage segmentation framework, providing a reliable foundation for automated myocardial scar analysis and potential clinical applications.

5.2 Research Contribution

This research contributes to the overall process of automated myocardial scar segmentation and detection using image enhancement and deep learning techniques. Based on the objectives of this study, the contributions of this research are listed as follows:

i) The study successfully developed advanced image enhancement techniques called Hybrid CE-IS for LGE-CMRI images that substantially improve image quality and clarity. Deep learning-based contrast and detail enhancement were applied to highlight low-contrast regions such as myocardium and scar tissue while preserving the structural integrity of high-contrast regions like the left ventricle and cavity. These enhancements enabled the segmentation network to extract more meaningful features, allowing for improved differentiation between healthy and pathological tissue. This contribution is significant as it addresses one of the main challenges in cardiac imaging, where subtle scar regions can be difficult to detect in raw LGE-CMRI images due to low contrast and noise.

ii) A multi-stage DeepLabV3+ segmentation framework was designed and implemented to accurately detect and delineate myocardial scars. The multi-stage approach allows the network to refine predictions progressively, reducing errors from initial segmentation stages and improving the accuracy of final masks. This design ensures precise segmentation of both high-contrast structures such as the left ventricle and cavity, and low-contrast regions such as myocardium and scars. The framework produces smooth, continuous, and anatomically coherent segmentation outputs, demonstrating its ability to capture complex cardiac structures and subtle scar regions that are often challenging to identify. This approach enhances the reliability of automated cardiac analysis, supporting potential clinical applications such as scar quantification and risk assessment.

iii) By integrating image enhancement with multi-stage segmentation, a hybrid framework was developed that outperforms both conventional single-stage and standard multi-stage networks. The combination of enhanced input images and progressive refinement across multiple segmentation stages allows for more accurate and complete masks, particularly in cases with fragmented or irregular scars. This hybrid approach improves boundary delineation, reduces false positive and false negative predictions, and maintains structural continuity, demonstrating the synergistic effect of combining image enhancement and multi-stage learning for cardiac segmentation tasks.

iv) The framework, including the image enhancement component, was rigorously evaluated using both qualitative and quantitative methods to assess its effectiveness and robustness. Metrics including Dice Similarity Coefficient, Intersection over Union, and pixel-wise accuracy, together with visual inspection, confirmed the superiority of the hybrid approach over conventional segmentation models. Evaluation highlighted the contribution of the image enhancement process itself, showing that enhanced visibility of subtle myocardial and scar regions significantly improved segmentation performance. Furthermore, comparison across multiple backbone architectures demonstrated that deeper networks such as ResNet-50 provided the optimal balance between segmentation accuracy, anatomical plausibility, and computational efficiency, while lighter networks could maintained speed and efficiency with slightly reduced precision. These evaluations validate the framework's robustness, adaptability, and potential for application to real-world clinical LGE-CMRI datasets.

5.3 Recommendation for Future Work

This research has successfully shown that integrating image enhancement with multi-stage segmentation improves the detection and delineation of myocardial scars from LGE-CMRI. However, several opportunities exist to further enhance and expand this work. One potential direction is to explore more advanced image enhancement techniques that are specifically tailored for LGE-CMRI. Deep learning-based contrast and detail enhancement could be applied not only as a preprocessing step but also progressively during each stage of segmentation. This would allow the network to better distinguish low-contrast scar and myocardium regions from surrounding tissues while preserving the integrity of high-contrast structures such as the left ventricle and cavity. By improving feature representation in this way, the framework could achieve more accurate and coherent segmentation masks, particularly for small or fragmented scar regions. Furthermore, integrating enhancement methods that adapt to variations in intensity, noise, or imaging artifacts could make the framework more robust across different LGE-CMRI scanners and acquisition protocols.

A further recommendation is to develop an automated image enhancement model that can dynamically adjust enhancement parameters based on the input LGE-CMRI slice. Currently, enhancement is applied uniformly or manually tuned, which may not optimally reveal subtle pathological features in all images. An automated model could learn to highlight critical features while preserving normal tissue structures, making the hybrid framework more adaptive and robust across diverse LGE-CMRI datasets. This would also reduce reliance on manual preprocessing, enabling a fully automated pipeline from raw image acquisition to final segmentation. Coupling the automated enhancement with real-time feedback from the segmentation stages could allow the system to iteratively refine the input image, further improving scar and myocardium delineation.

Finally, future work should aim to improve generalizability and clinical applicability. Techniques such as data augmentation, domain adaptation, and transfer learning could enable the model to perform consistently across different patient populations, scanners, and imaging protocols. Lightweight and efficient network designs could facilitate real-time implementation in hospitals or resource-limited clinical settings. Additionally, integrating the segmentation outputs with downstream clinical applications such as scar quantification, risk assessment, or therapy planning would provide actionable insights for patient management. Future studies could also explore linking segmentation results to functional cardiac metrics, combining anatomical and functional information to improve overall cardiac assessment. Collectively, these directions could transform the hybrid image enhancement and multi-stage segmentation framework into a robust, automated, and clinically useful tool for LGE-CMRI analysis.

REFERENCES

Abbas, S., Ojo, S., Krichen, M., Alamro, M. A., Mihoub, A., & Vilcekova, L. (2024). A novel deep learning approach for myocardial infarction detection and multi-label classification. *IEEE Access, 12*, 76003–76021. https://doi.org/10.1109/ACCESS.2024.3401744

Abduvaitov, A., Shavkatovich Buriboev, A., Sultanov, D., Buriboev, S., Yusupov, O., Jasur, K., & Choi, A. J. (2025). Enhancing medical image segmentation and classification using a fuzzy-driven method. *Sensors, 25*(18), 5931.

Al-Ameen, Z. (2018). Sharpness improvement for medical images using a new nimble filter. *3D Research, 9*. https://doi.org/10.1007/s13319-018-0164-0

Al-Ameen, Z. (2021). Contrast enhancement of digital images using an improved Type-II fuzzy set-based algorithm. *Traitement du Signal, 38*, 39–50. https://doi.org/10.18280/ts.380104

Almajmaie, L. K. A., Raheem, A. R., Mahmood, W. A., & Albawi, S. (2022). MRI image segmentation using machine learning networks and level set approaches. *International Journal of Electrical and Computer Engineering, 12*(1), 793–801. https://doi.org/10.11591/ijece.v12i1.pp793-801

Almas, M. A., & Sharma, V. (2020). Efficient iterative noise filtering method using high boost filter. *Solid State Technology, 63*, 16931–16937.

Avard, E., Shiri, I., Hajianfar, G., Abdollahi, H., Kalantari, K. R., Houshmand, G., Kasani, K., Bitarafan-Rajabi, A., Deevband, M. R., Oveisi, M., & Zaidi, H. (2022). Non-contrast cine cardiac magnetic resonance image radiomics features and machine learning algorithms for myocardial infarction detection. *Computers in Biology and Medicine, 141*, Article 105145. https://doi.org/10.1016/j.compbiomed.2021.105145

Bansal, A., & Singh, N. (2020). Image enhancement techniques: A review. *Asian Journal of Convergence in Technology, 6*, 7–11. https://doi.org/10.33130/AJCT.2020v06i02.002

Benz, D. C., Kaufmann, P. A., von Felten, E., Benetos, G., Rampidis, G., Messerli, M., Giannopoulos, A. A., Fuchs, T. A., Gräni, C., Gebhard, C., Pazhenkottil, A. P., Flammer, A. J., Kaufmann, P. A., & Buechel, R. R. (2021). Prognostic value of quantitative metrics from positron emission tomography in ischemic heart failure. *JACC: Cardiovascular Imaging, 14*(2), 454–464. https://doi.org/10.1016/j.jcmg.2020.05.033

Blomqvist, L., Nordberg, G. F., Nurchi, V. M., & Aaseth, J. O. (2022). Gadolinium in medical imaging-Usefulness, toxic reactions and possible countermeasures: A review. *Biomolecules, 12*(6), 742. https://doi.org/10.3390/biom12060742

Bogdan, V., Bonchiş, C., & Orhei, C. (2024). An image sharpening technique based on dilated filters and 2D-DWT image fusion.

Brouki, Y. (2023, February 7). *Cardiology internalmedicine foamed* [LinkedIn post]. LinkedIn. https://www.linkedin.com/posts/younes-brouki-122a9657_cardiology-internalmedicine-foamed-activity-7424708372802859008-iYzk

Chen, C., Qin, C., Qiu, H., Tarroni, G., Duan, J., Bai, W., & Rueckert, D. (2020). Deep learning for cardiac image segmentation: A review. *Frontiers in Cardiovascular Medicine, 7*, 25. https://doi.org/10.3389/fcvm.2020.00025

Chen, D., Bhopalwala, H., Dewaswala, N., Arunachalam, S. P., Enayati, M., Farahani, N. Z., Pasupathy, K., Lokineni, S., Bos, J. M., Noseworthy, P. A., Arsanjani, R., Erickson, B. J., Geske, J. B., Ackerman, M. J., Araoz, P. A., & Arruda-Olson, A. M. (2022). Deep neural network for cardiac magnetic resonance image segmentation. *Journal of Imaging, 8*(5), 149. https://doi.org/10.3390/jimaging8050149

Chen, Z., Pawar, K., Ekanayake, M., Pain, C., Zhong, S., & Egan, G. F. (2023). Deep learning for image enhancement and correction in magnetic resonance imaging-State-of-the-art and challenges. *Journal of Digital Imaging, 36*(1), 204–230. https://doi.org/10.1007/s10278-022-00721-9

Chen, Z., Shi, J., Pommier, T., Cottin, Y., Salomon, M., Decourselle, T., Lalande, A., & Couturier, R. (2022). Prediction of myocardial infarction from patient features with machine learning. *Frontiers in Cardiovascular Medicine, 9*, Article 754609. https://doi.org/10.3389/fcvm.2022.754609

Cheraghi, H., López-Escobar, L., Rino, J., Figueiredo, L., & Szabo, B. (2025). Classification of *Trypanosoma brucei* mammalian life cycle stages using deep learning algorithms. *PLOS Neglected Tropical Diseases, 19*. https://doi.org/10.1371/journal.pntd.0013298

Chollet, F. (2017). Xception: Deep learning with depthwise separable convolutions. In *Proceedings of the IEEE Conference on Computer Vision and Pattern Recognition* (pp. 1251–1258).

Clinical Imaging Systems. (2026, March 2). *Philips Achieva 3.0T MRI scanner*. https://clinicalimagingsystems.com/product/philips-achieva-3-0t-mri-scanner/

Curiale, A. H., Colavecchia, F. D., Kaluza, P., Isoardi, R. A., & Mato, G. (2017, September 4–8). Automatic myocardial segmentation by using a deep learning network in cardiac MRI. In *2017 XLIII Latin American Computer Conference (CLEI)*.

Damit, D., Sulaiman, S., Osman, M., A. Karim, N., & Setumin, S. (2024). Automated DeepLabV3+ based model for left ventricle segmentation on short-axis late gadolinium enhancement-magnetic cardiac resonance imaging images. *International Journal of Electrical and Computer Engineering, 14*, 3362–3371. https://doi.org/10.11591/ijece.v14i3.pp3362-3371

de Giorgio, A., Cola, G., & Wang, L. (2023). Systematic review of class imbalance problems in manufacturing. *Journal of Manufacturing Systems, 71*, 620–644. https://doi.org/10.1016/j.jmsy.2023.10.014

Deepika, S., & Jaisankar, N. (2024). Detecting and classifying myocardial infarction in echocardiogram frames with an enhanced CNN algorithm and ECV-3D network. *IEEE Access, 12*, 51690–51703. https://doi.org/10.1109/ACCESS.2024.3385787

Degerli, A., Zabihi, M., Kiranyaz, S., Hamid, T., Mazhar, R., Hamila, R., & Gabbouj, M. (2021). Early detection of myocardial infarction in low-quality echocardiography. *IEEE Access, 9*, 34442–34453. https://doi.org/10.1109/ACCESS.2021.3059595

Deng, G., Galetto, F., Al-Nasrawi, M., & Waheed, W. (2021). A guided edge-aware smoothing-sharpening filter based on patch interpolation model and generalized gamma distribution. *IEEE Open Journal of Signal Processing, 2*, 119–135. https://doi.org/10.1109/OJSP.2021.3063076

Dhaene, A., Loecher, M., Wilson, A., & Ennis, D. (2023). Myocardial segmentation of tagged magnetic resonance images with transfer learning using generative cine-to-tagged dataset transformation. *Bioengineering, 10*, 166. https://doi.org/10.3390/bioengineering10020166

Ding, W., Li, L., Qiu, J., Wang, S., Huang, L., Chen, Y., Yang, S., & Zhuang, X. (2023). Aligning multi-sequence CMR towards fully automated myocardial pathology segmentation. *IEEE Transactions on Medical Imaging, 42*(12), 3474–3486. https://doi.org/10.1109/TMI.2023.3288046

E, R. B., V, S., S, M. K., & Shilen, N. (2025, January 9–10). An improved nimble filter for medical image sharpening. In *2025 Fifth International Conference on Advances in Electrical, Computing, Communication and Sustainable Technologies (ICAECT)*.

El-Taraboulsi, J., Cabrera, C. P., Roney, C., & Aung, N. (2023). Deep neural network architectures for cardiac image segmentation. *Artificial Intelligence in the Life Sciences, 4*, Article 100083. https://doi.org/10.1016/j.ailsci.2023.100083

Fahmy, A. S., Rowin, E. J., Chan, R. H., Manning, W. J., Maron, M. S., & Nezafat, R. (2021). Improved quantification of myocardium scar in late gadolinium enhancement images: Deep learning based image fusion approach. *Journal of Magnetic Resonance Imaging, 54*(1), 303–312. https://doi.org/10.1002/jmri.27555

Gautam, N., Saluja, P., Malkawi, A., Rabbat, M. G., Al-Mallah, M. H., Pontone, G., Zhang, Y., Lee, B. C., & Al'Aref, S. J. (2022). Current and future applications of artificial intelligence in coronary artery disease. *Healthcare, 10*(2), 232. https://doi.org/10.3390/healthcare10020232

Gavirni, R., Gupta, D., Mishra, D., Gupta, A., & Viswamitra, S. (2023). Clinically relevant myocardium segmentation in cardiac magnetic resonance images. *IEEE Journal of Biomedical and Health Informatics, 27*(5), 2423–2431. https://doi.org/10.1109/JBHI.2023.3250429

Hasny, M., Demirel, O. B., Amyar, A., Faghihroohi, S., & Nezafat, R. (2024). Myocardial scar enhancement in LGE cardiac MRI using localized diffusion. In *International Conference on Medical Image Computing and Computer-Assisted Intervention*.

He, K., Zhang, X., Ren, S., & Sun, J. (2016). Deep residual learning for image recognition. In *Proceedings of the IEEE Conference on Computer Vision and Pattern Recognition* (pp. 770–778).

Heidari, M., Ding, L., Kheshti, M., Bao, W., Zhao, X., Popov, M., & Terzija, V. (2024). A review on application of machine learning-based methods for power system inertia monitoring. *International Journal of Electrical Power & Energy Systems, 162*, Article 110279. https://doi.org/10.1016/j.ijepes.2024.110279

Hong, Q., & Zhang, C. (2023, August 12–13). Multimodal RU-Net: A segmentation network based on multimodal cardiac CMR images. In *2023 IEEE 9th International Conference on Cloud Computing and Intelligent Systems (CCIS)*.

Ingkanisorn, W., Bandettini, W., Shanbhag, S., Mancini, C., McGuirt, D., Kellman, P., Xue, H., Henry, J., Lowery, M., Thein, S., Chen, M., & Campbell-Washburn, A. (2020). A comparison of cine CMR imaging at 0.55 T and 1.5 T. *Journal of Cardiovascular Magnetic Resonance, 22*. https://doi.org/10.1186/s12968-020-00618-y

Jacobson, L. E. O., Bader-El-Den, M., Maurya, L., Hopgood, A. A., Tamma, V., Masum, S. K., Prendergast, D. J., & Osborn, P. (2026). Prostate MR image segmentation using a multi-stage network approach. *International Urology and Nephrology, 58*(4), 1201–1229. https://doi.org/10.1007/s11255-025-04763-0

Jafari, M., Shoeibi, A., Khodatars, M., Ghassemi, N., Moridian, P., Delfan, N., Alizadehsani, R., Khosravi, A., Ling, S., Zhang, Y., Wang, S.-H., Gorriz, J., Rokny, H., & Acharya, U. R. (2022). *Automated diagnosis of cardiovascular diseases from cardiac magnetic resonance imaging using deep learning models: A review*. arXiv. https://doi.org/10.48550/arXiv.2210.14909

Jenista, E. R., Wendell, D. C., Azevedo, C. F., Klem, I., Judd, R. M., Kim, R. J., & Kim, H. W. (2023). Revisiting how we perform late gadolinium enhancement CMR: Insights gleaned over 25 years of clinical practice. *Journal of Cardiovascular Magnetic Resonance, 25*(1), 18. https://doi.org/10.1186/s12968-023-00925-0

Jian, J.-Z., Ger, T.-R., Lai, H.-H., Ku, C.-M., Chen, C.-A., Abu, P. A. R., & Chen, S.-L. (2021). Detection of myocardial infarction using ECG and multi-scale feature concatenate. *Sensors, 21*(5).

Jiang, Y., Cui, L., Jiang, B., Zhao, X., & Chai, S. (2024, July 28–31). Cardiac MRI image enhancement based on GAN network. In *2024 43rd Chinese Control Conference (CCC)*.

Karim, R., Bhagirath, P., Claus, P., James Housden, R., Chen, Z., Karimaghaloo, Z., Sohn, H.-M., Lara Rodríguez, L., Vera, S., Albà, X., Hennemuth, A., Peitgen, H.-O., Arbel, T., Gonzàlez Ballester, M. A., Frangi, A. F., Götte, M., Razavi, R., Schaeffter, T., & Rhode, K. (2016). Evaluation of state-of-the-art segmentation algorithms for left ventricle infarct from late gadolinium enhancement MR images. *Medical Image Analysis, 30*, 95–107. https://doi.org/10.1016/j.media.2016.01.004

Ko, S. M. (2024). Current status of cardiac CT for nuclear medicine professionals: Coronary artery disease evaluation. *Nuclear Medicine and Molecular Imaging, 58*(7), 418–430. https://doi.org/10.1007/s13139-024-00859-0

Kolandaivelu, A., Bruce, C. G., Seemann, F., Yildirim, D. K., Campbell-Washburn, A. E., Lederman, R. J., & Herzka, D. A. (2024). Evaluation of 12-lead electrocardiogram at 0.55T for improved cardiac monitoring in magnetic resonance imaging. *Journal of Cardiovascular Magnetic Resonance, 26*(1), 101009. https://doi.org/10.1016/j.jocmr.2024.101009

Lechien, T., Dehaerne, E., Dey, B., Blanco, V., De Gendt, S., & Meert, W. (2023). *Automated semiconductor defect inspection in scanning electron microscope images: A systematic review*. arXiv. https://arxiv.org/abs/2308.08376

Lepcha, D., Goyal, B., Dogra, A., Wang, S.-H., & Chohan, J. (2022). Medical image enhancement strategy based on morphologically processing of residuals using a special kernel. *Expert Systems*. https://doi.org/10.1111/exsy.13207

Li, L., Wu, F., Wang, S., & Zhuang, X. (2024). Multi-modality cardiac image analysis with deep learning. In *Deep learning for medical image analysis* (pp. 299–335). Elsevier.

Liu, Q., Lu, Q., Chai, Y., Tao, Z., Wu, Q., Jiang, M., & Pu, J. (2023). Radiomics-based quality control system for automatic cardiac segmentation: A feasibility study. *Bioengineering, 10*(7), 791.

Liu, X., Song, L., Liu, S., & Zhang, Y. (2021). A review of deep-learning-based medical image segmentation methods. *Sustainability, 13*(3).

Luo, C., Shi, C., Li, X., & Dongrui, G. (2020). Cardiac MR segmentation based on sequence propagation by deep learning. *PLOS ONE, 15*, e0230415. https://doi.org/10.1371/journal.pone.0230415

Department of Statistics Malaysia. (2023). *Statistics on causes of death, Malaysia, 2023*. Department of Statistics Malaysia. https://www.dosm.gov.my/uploads/release-content/file_20231030112043.pdf

Mandoli, G. E., D'Ascenzi, F., Vinco, G., Benfari, G., Ricci, F., Focardi, M., Cavigli, L., Pastore, M. C., Sisti, N., De Vivo, O., Santoro, C., Mondillo, S., & Cameli, M. (2021). Novel approaches in cardiac imaging for non-invasive assessment of left heart myocardial fibrosis. *Frontiers in Cardiovascular Medicine, 8*. https://doi.org/10.3389/fcvm.2021.614235

Marquis, H., Willowson, K. P., & Bailey, D. L. (2023). Partial volume effect in SPECT and PET imaging and impact on radionuclide dosimetry estimates. *Asia Ocean Journal of Nuclear Medicine and Biology, 11*(1), 44–54. https://doi.org/10.22038/aojnmb.2022.63827.1448

Michaelis, A., Gunaga, S., McKechnie, T., Baroff, B., & Shafiq, Q. (2020). Three lives at stake: A case of acute myocardial infarction in a patient with twin pregnancy. *Case Reports*, 51. https://scholarlycommons.henryford.com/merf2020caserpt/51

Moafi, A., Moafi, D., Mirkes, E. M., McCann, G. P., Alatrany, A. S., Arnold, J. R., & Mehdipour Ghazi, M. (2026). Robust deep learning for myocardial scar segmentation in cardiac MRI with noisy labels. In *Medical Image Computing and Computer-Assisted Intervention – MICCAI 2025*. Springer.

Mosquera-Rojas, G., Ouadah, C., Hadadi, A., Lalande, A., & Leclerc, S. (2023). Automatic myocardium segmentation in delayed-enhancement MRI with pathology-specific data augmentation and deep learning architectures. *Algorithms, 16*, 488. https://doi.org/10.3390/a16100488

Mukaida, M., Ueda, Y., & Suetake, N. (2023). Low-light image enhancement method using a modified gamma transform and gamma filtering-based histogram specification for convex combination coefficients. *IEICE Transactions on Fundamentals of Electronics, Communications and Computer Sciences, E106.A*(11), 1385–1394. https://doi.org/10.1587/transfun.2023SMP0003

Mustafa, A., Mansour Alzyat, A., Mohammad Abdelmonem, A., & Hegazy, A. (2022). Myocardial infarction: Risk factors, pathophysiology, classification, assessment and management. *Cardiology Research and Reports, 4*. https://doi.org/10.31579/2692-9759/056

National Heart, Lung, and Blood Institute. (n.d.). *Heart attack: Causes*. https://www.nhlbi.nih.gov/health/heart-attack/causes

Oloruntoba, I., Nguyen, T., Ge, Z., Vestergaard, T., & Mar, V. (2021). Assessing generalizability of deep learning models trained on standardized and nonstandardized images and their performance against teledermatologists. *iProceedings, 6*, e35391. https://doi.org/10.2196/35391

World Health Organization. (2021). *Cardiovascular diseases (CVDs) fact sheet*. https://www.who.int/news-room/fact-sheets/detail/cardiovascular-diseases-(cvds)

Papetti, D. M., Van Abeelen, K., Davies, R., Menè, R., Heilbron, F., Perelli, F. P., Artico, J., Seraphim, A., Moon, J. C., Parati, G., Xue, H., Kellman, P., Badano, L. P., Besozzi, D., Nobile, M. S., & Torlasco, C. (2023). An accurate and time-efficient deep learning-based system for automated segmentation and reporting of cardiac magnetic resonance-detected ischemic scar. *Computer Methods and Programs in Biomedicine, 229*, 107321. https://doi.org/10.1016/j.cmpb.2022.107321

Prabhakararao, E., & Dandapat, S. (2020). Automated detection of posterior myocardial infarction from VCG signals using stationary wavelet transform based features. *IEEE Sensors Letters, 4*(6), 1–4. https://doi.org/10.1109/LSENS.2020.2992760

Pradeep Kundur, S., Malik, A., & Sivalokanathan, S. (2025). The utility of nuclear imaging in hypertrophic cardiomyopathy: A narrative review. *Journal of Clinical Medicine, 14*(7), 2183.

Prastaro, M., Pirozzi, E., Gaibazzi, N., Paolillo, S., Santoro, C., Savarese, G., Losi, M. A., Esposito, G., Perrone Filardi, P., Trimarco, B., & Galderisi, M. (2017). Expert review on the prognostic role of echocardiography after acute myocardial infarction. *Journal of the American Society of Echocardiography, 30*(5), 431–443.e432. https://doi.org/10.1016/j.echo.2017.01.020

Qi, H., Qian, P., Tang, L., Chen, B., An, D., & Wu, L.-M. (2024). Predicting late gadolinium enhancement of acute myocardial infarction in contrast-free cardiac cine MRI using deep generative learning. *Circulation: Cardiovascular Imaging, 17*(9), e016786. https://doi.org/10.1161/CIRCIMAGING.124.016786

Qi, Y., Yang, Z., Sun, W., Lou, M., Lian, J., Zhao, W., Xiang-yu, D., & Ma, Y. (2021). *A comprehensive overview of image enhancement techniques*.

Qiu, J., Li, L., Wang, S., Zhang, K., Chen, Y., Yang, S., & Zhuang, X. (2022). *MyoPS-Net: Myocardial pathology segmentation with flexible combination of multi-sequence CMR images*. arXiv. https://doi.org/10.48550/arXiv.2211.03062

Rajput, K. S. C., Kumar, M., Kodipalli, A., R, B. R., Rao, T., & P, V. (2023, June 22–23). Prediction of myocardial infraction using machine learning algorithms. In *2023 International Conference on Computational Intelligence for Information, Security and Communication Applications (CIISCA)*.

Rayed, M. E., Islam, S. M. S., Niha, S. I., Jim, J. R., Kabir, M. M., & Mridha, M. F. (2024). Deep learning for medical image segmentation: State-of-the-art advancements and challenges. *Informatics in Medicine Unlocked, 47*, 101504. https://doi.org/10.1016/j.imu.2024.101504

Rehman, S. A., Jeffrey, Z., Sun, Y., & Simpson, O. (2024, May 8–10). Image enhancement using modified Laplacian filter, CLAHE and adaptive thresholding. In *2024 International Conference on Intelligent Systems and Computer Vision (ISCV)*.

Safdar, M. F., Nowak, R. M., & Pałka, P. (2024). Pre-processing techniques and artificial intelligence algorithms for electrocardiogram (ECG) signals analysis: A comprehensive review. *Computers in Biology and Medicine, 170*, 107908. https://doi.org/10.1016/j.compbiomed.2023.107908

Sahu, G., & Ray, K. C. (2022). An efficient method for detection and localization of myocardial infarction. *IEEE Transactions on Instrumentation and Measurement, 71*, 1–12. https://doi.org/10.1109/TIM.2021.3132833

Schulz-Menger, J., Bluemke, D. A., Bremerich, J., Flamm, S. D., Fogel, M. A., Friedrich, M. G., Kim, R. J., von Knobelsdorff-Brenkenhoff, F., Kramer, C. M., Pennell, D. J., Plein, S., & Nagel, E. (2020). Standardized image interpretation and post-processing in cardiovascular magnetic resonance-2020 update. *Journal of Cardiovascular Magnetic Resonance, 22*(1), 19. https://doi.org/10.1186/s12968-020-00610-6

Shaaf, Z., Jamil, M., & Ambar, R. (2023). Convolutional neural network model to segment myocardial infarction from MRI images. *International Journal of Online and Biomedical Engineering, 19*, 150–162. https://doi.org/10.3991/ijoe.v19i02.36607

Sharma, R., & Kamra, A. (2023, September 14–16). A review on CLAHE based enhancement techniques. In *2023 6th International Conference on Contemporary Computing and Informatics (IC3I)*.

Sharma, U. C., Zhao, K., Mentkowski, K., Sonkawade, S. D., Karthikeyan, B., Lang, J. K., & Ying, L. (2021). Modified GAN augmentation algorithms for the MRI-classification of myocardial scar tissue in ischemic cardiomyopathy. *Frontiers in Cardiovascular Medicine, 8*. https://doi.org/10.3389/fcvm.2021.726943

Sheikhjafari, A., Krishnaswamy, D., Noga, M., Ray, N., & Punithakumar, K. (2023). Deep learning based parameterization of diffeomorphic image registration for cardiac image segmentation. *IEEE Transactions on NanoBioscience, 22*(4), 800–807. https://doi.org/10.1109/TNB.2023.3276867

Shi, K. (2025). Comparison of image enhancement algorithms based on denoising and edge detection. *Applied and Computational Engineering, 133*, 174–184. https://doi.org/10.54254/2755-2721/2025.20700

Sinha, S., Denney, T., Zhou, Y., & Zheng, J. (2020, December 14–17). Automated semantic segmentation of cardiac magnetic resonance images with deep learning. In *2020 19th IEEE International Conference on Machine Learning and Applications (ICMLA)*.

Smith, T. B., Zhang, S., Erkanli, A., Frush, D., & Samei, E. (2021). Variability in image quality and radiation dose within and across 97 medical facilities. *Journal of Medical Imaging, 8*(5), 052105. https://doi.org/10.1117/1.JMI.8.5.052105

Song, Y., Li, C., Xiao, S., Xiao, H., & Guo, B. (2022). Unsharp masking image enhancement: The parallel algorithm based on cross-platform. *Scientific Reports, 12*(1), 20175. https://doi.org/10.1038/s41598-022-21745-9

Srinivas, K., Bhandari, A. K., & Singh, A. (2020). Low-contrast image enhancement using spatial contextual similarity histogram computation and color reconstruction. *Journal of the Franklin Institute, 357*(18), 13941–13963. https://doi.org/10.1016/j.jfranklin.2020.10.013

Tsai, C.-Y., & Su, Y.-K. (2022). MobileNet-JDE: A lightweight multi-object tracking model for embedded systems. *Multimedia Tools and Applications, 81*, 1–23. https://doi.org/10.1007/s11042-022-12095-9 van der Velde, N., Hassing, H. C., Bakker, B. J., Wielopolski, P. A., Lebel, R. M., Janich, M. A., Kardys, I., Budde, R. P. J., & Hirsch, A. (2021). Improvement of late gadolinium enhancement image quality using a deep learning–based reconstruction algorithm and its influence on myocardial scar quantification. *European Radiology, 31*(6), 3846–3855. https://doi.org/10.1007/s00330-020-07461-w

Vesal, S., Maier, A., & Ravikumar, N. (2020). Fully automated 3D cardiac MRI localisation and segmentation using deep neural networks. *Journal of Imaging, 6*(7), 65. https://doi.org/10.3390/jimaging6070065

Wallis, A., Manghat, N., & Hamilton, M. (2012). The role of coronary CT in the assessment and diagnosis of patients with chest pain. *Clinical Medicine, 12*(3), 222–229. https://doi.org/10.7861/clinmedicine.12-3-222

Wang, G., Luo, X., Gu, R., Yang, S., Qu, Y., Zhai, S., Zhao, Q., Li, K., & Zhang, S. (2023). PyMIC: A deep learning toolkit for annotation-efficient medical image segmentation. *Computer Methods and Programs in Biomedicine, 231*, 107398. https://doi.org/10.1016/j.cmpb.2023.107398

Wang, K.-N., Yang, X., Miao, J., Li, L., Yao, J., Zhou, P., Xue, W., Zhou, G.-Q., Zhuang, X., & Ni, D. (2022). AWSnet: An auto-weighted supervision attention network for myocardial scar and edema segmentation in multi-sequence cardiac magnetic resonance images. *Medical Image Analysis, 77*, 102362. https://doi.org/10.1016/j.media.2022.102362

Wang, L., Huang, J., Xing, X., Wu, Y., Rajakulasingam, R., Scott, A. D., Ferreira, P. F., Silva, R. D., Nielles-Vallespin, S., & Yang, G. (2023, November 15–17). Style transfer and self-supervised learning powered myocardium infarction super-resolution segmentation. In *2023 19th International Symposium on Medical Information Processing and Analysis (SIPAIM)*.

Wang, S., Abdelaty, A. M. S. E. K., Parke, K., Arnold, J. R., McCann, G. P., & Tyukin, I. Y. (2023). MyI-Net: Fully automatic detection and quantification of myocardial infarction from cardiovascular MRI images. *Entropy, 25*(3).

Wojnicki, M., Wojtaszek, K., Tokarski, T., Csapó, E., Knutelska, J., Bednarski, M., Skórkowska, A., Pomierny-Chamioło, L., & Kotańska, M. (2024). Synergistic enhancement of diagnostic imaging: Synthesis and preliminary safety evaluation of gadolinium-doped carbon quantum dots as dual-contrast agent. *Molecules, 29*(17). https://doi.org/10.3390/molecules29174075

Wong, T. C., Piehler, K. M., Zareba, K. M., Lin, K., Phrampus, A., Patel, A., Moon, J. C., Ugander, M., Valeti, U., Holtz, J. E., Fu, B., Chang, C. C., Mathier, M., Kellman, P., Butler, J., Gheorghiade, M., & Schelbert, E. B. (2013). Myocardial damage detected by late gadolinium enhancement cardiovascular magnetic resonance is associated with subsequent hospitalization for heart failure. *Journal of the American Heart Association, 2*(6), e000416. https://doi.org/10.1161/JAHA.113.000416

Woods, J. W. (2012). Chapter 7: Image enhancement and analysis. In J. W. Woods (Ed.), *Multidimensional signal, image, and video processing and coding* (2nd ed., pp. 223–256). Academic Press. https://doi.org/10.1016/B978-0-12-381420-3.00007-2

Wu, Y., Tang, Z., Li, B., Firmin, D., & Yang, G. (2021). Recent advances in fibrosis and scar segmentation from cardiac MRI: A state-of-the-art review and future perspectives. *Frontiers in Physiology, 12*, 709230. https://doi.org/10.3389/fphys.2021.709230

Xing, J., Wang, S., Bilchick, K. C., Patel, A. R., & Zhang, M. (2023, April 18–21). Joint deep learning for improved myocardial scar detection from cardiac MRI. In *2023 IEEE 20th International Symposium on Biomedical Imaging (ISBI)*.

Xiong, J., Po, L.-M., Cheung, K. W., Xian, P., Zhao, Y., Rehman, Y. A. U., & Zhang, Y. (2021). Edge-sensitive left ventricle segmentation using deep reinforcement learning. *Sensors, 21*(7), 2375.

Xiong, P., Lee, S. M.-Y., & Chan, G. (2022). Deep learning for detecting and locating myocardial infarction by electrocardiogram: A literature review. *Frontiers in Cardiovascular Medicine, 9*, 860032.

Yu, X., Bo, L., & Xin, C. (2022). Low light combining multiscale deep learning networks and image enhancement algorithm. *Modern Innovations, Systems and Technologies, 2*, 0215–0232. https://doi.org/10.47813/2782-2818-2022-2-4-0215-0232

Zafar, K., Siddiqui, H. U. R., Majid, A., Saleem, A. A., Raza, A., Rustam, F., & Dudley, S. (2023). Deep learning-based feature engineering to detect anterior and inferior myocardial infarction using UWB radar data. *IEEE Access, 11*, 97745–97757. https://doi.org/10.1109/ACCESS.2023.3312948

Zamir, S. W., Arora, A., Khan, S., Hayat, M., Khan, F. S., Yang, M.-H., & Shao, L. (2021). Multi-stage progressive image restoration. In *Proceedings of the IEEE/CVF Conference on Computer Vision and Pattern Recognition* (pp. 14821–14831).

Zhang, J., Liu, M., Xiong, P., Du, H., Yang, J., Xu, J., Hou, Z., & Liu, X. (2023). Automated localization of myocardial infarction from vectorcardiographic signals via tensor decomposition. *IEEE Transactions on Biomedical Engineering, 70*(3), 812–823. https://doi.org/10.1109/TBME.2022.3202962

Zhang, W., Li, X., & Wang, Z. (2023, October 8–11). Segmentation of the left ventricle by SDD double threshold selection and CHT. In *2023 IEEE International Conference on Image Processing (ICIP)*.

Zhang, Z., Wang, Z., Wang, X., Wang, K., Yuan, Y., & Li, Q. (2024). A novel network with enhanced edge information for left atrium segmentation from LGE-MRI. *Frontiers in Physiology, 15*, 1478347. https://doi.org/10.3389/fphys.2024.1478347

Zhao, D., Zhang, W., & Wang, Y. (2024). Research on personnel image segmentation based on MobileNetV2 H-Swish CBAM PSPNet in search and rescue scenarios. *Applied Sciences, 14*(22), 10675.

Zhao, Z., Howes, A., & Zhang, X. (2025). *MultiTaskVIF: Segmentation-oriented visible and infrared image fusion via multi-task learning*. arXiv. https://arxiv.org/abs/2505.06665

Zhou, Z., Shi, Z., & Ren, W. (2023). Linear contrast enhancement network for low-illumination image enhancement. *IEEE Transactions on Instrumentation and Measurement, 72*, 1–16. https://doi.org/10.1109/TIM.2022.3232641

APPENDICES

APPENDIX 1

Ethical Approval

UNIVERSITI SAINS MALAYSIA

Jawatankuasa Etika Penyelidikan Manusia USM (JEPeM)

Human Research Ethics Committee USM (HREC)

Universiti Sains Malaysia
Kampus Kesihatan
16150 Kubang Kerian, Kelantan, Malaysia.
Tel. : +609 - 767 3000/2354/2362
Fax. : + 609 - 767 2351
Email : jepem@usm.my
Laman Web : www.jepem.kk.usm.my
www.usm.my

22nd December 2023

Assoc. Prof. Ir. Ts. Dr. Siti Noraini Sulaiman
School of Electrical Engineering
Universiti Teknologi Mara Cawangan Pulau Pinang
Kampus Permatang Pauh
13500 Permatang Pauh, Pulau Pinang

JEPeM USM Code: USM/JEPeM/21090623
Study Protocol Title: An Automated Segmentation of Left Ventricular Scar from Cardiac MR Images Based on Deep Convolutional Neural Networks for Myocardial Infarction Diagnosis

Dear Assoc. Prof. Ir. Ts. Dr. Siti Noraini,

We wish to inform you that the Jawatankuasa Etika Penyelidikan Manusia, Universiti Sains Malaysia (JEPeM-USM) acknowledged receipt of the Continuing Review Application dated 13th December 2023.

Upon review of JEPeM-USM Form 3(B) 2021: Continuing Review Application Form, the committee **AGREED** for the **EXTENSION OF APPROVAL (commencing from 5th February 2024 to 4th February 2025)**. The document is included in the protocol file.

Thank you for your continuing compliance with the requirements of JEPeM-USM.

"MALAYSIA MADANI"

"BERKHIDMAT UNTUK NEGARA"

Sincerely,

ASSOC. PROF. DR. HASLINA HAROON
Deputy Chairperson
Jawatankuasa Etika Penyelidikan (Manusia), JEPeM
Universiti Sains Malaysia

c.c Secretary
Jawatankuasa Etika Penyelidikan (Manusia), JEPeM
Universiti Sains Malaysia

JEPeM
JAWATANKUASA ETIKA PENYELIDIKAN MANUSIA

APPENDIX 2

Anonymized CMRI Radiology Report Samples from AMDI

Minimal increase in basal anteroseptal wall thickness, 11.5 cm.
Normal mass index.
The inferomedial papillary muscle is hypoplastic.
No aneurysmal formation.

Right ventricle:
Normal end diastolic and end systolic volumes with low normal ejection fraction.
TAPSE 1.8 cm.
No aneurysmal formation.

Atria:
Normal bi-atrial size; RA 11 cm? and LA 20 cm?.

Valves:
All valves appear competent by visual assessment under scan condition. Please correlate with echocardiography.

Post-gadolinium:
Early phase - No intracardiac thrombus.
Late phase - Transmural hyperenhancement of mid to apical anterior and anteroseptal wall as well as inferior wall; basal to apical inferolateral walls; and apex. Subendocardial hyperenhancement of basal to mid anterolateral walls, basal inferior wall and mid inferoseptal wall.

Thoracic great vessels:
Thoracic aorta and pulmonary artery are normal in size.
Normal systemic and pulmonary venous return.

Pericardium:
Normal pericardial thickness. No pericardial effusion.

Title	EDV	ESV	SV	EDV	MASS INDEX
LEFT VENTRICLE	226 ml	174 ml	52 ml	23 %	80 g/m?
= 126 ml/m?	= 98 ml/m?				
RIGHT VENTRICLE	99 ml	52 ml	47 ml	48 %	-
[88-227]	[23-105]	[52-138]	[47-74]		

Impression:
1. Dilated LV with poor ejection fraction, LVEF 23%.
2. Normal RV size with low normal ejection fraction, RVEF 48%.
3. Transmural infarction of mid-apical anterior and anteroseptal wall as well as inferior wall; basal-apical inferolateral walls; and apex.
4. Subendocardial infarction of basal-mid anterolateral walls, basal inferior wall and mid inferoseptal wall.
5. No myocardial infiltration or inflammation.

Features are of ischaemic dilated cardiomyopathy.
LAD: 5 segments are non-viable. Only 2 segments are viable and hibernating.
LCx: 3 segments are non-viable. 2 segments are viable with subendocardial infarct.
RCA: 2 segments are non-viable. 3 segments are viable (1 segment is hibernating, 2 segments with subendocardial infarct)
(see myocardial viability map for summary)

AUTHOR'S PROFILE

Nur 'Ulya Nasuha binti Zakaria obtained Bachelor of Engineering (Hons.) Electrical and Electronic Engineering in 2024 from Universiti Teknologi MARA (UiTM). Her final year project focused on the detection of semiconductor wafer defects in lithography images using YOLOv8, where she developed skills in deep learning, computer vision, Python programming, and image preprocessing. Currently, she is pursuing her Master's degree focusing on magnetic resonance image enhancement and segmentation for myocardial scar detection using deep learning, and she is interested in applying AI and machine learning techniques in biomedical and engineering applications.

LIST OF PUBLICATION

PROCEEDING:

Abdul Morad, N. U., Awang Damit, D. S., Osman, M. K., Zakaria, N. U. N., Sulaiman, S. N., Nor Kamal, N. A. Z., Ahmad, K. A., & Karim, N. K. A., Improving visual quality of LGE-CMRI myocardial scar detection using deep convolutional neural networks. 2026 IEEE 16th Internation Conference on Control System, Computing and Engineering (ICCSCE), 27-28 June 2026, Penang, Malaysia (Accepted for publication)

Zakaria, N. N., Osman, M. K., Sulaiman, S. N., Damit, D. S. A., Hussain, Z., Kamal, N. A. Z. N., Isa, N. A. M., & Karim, N. K. A. (2025, 26-28 Aug. 2025). Magnetic Resonance Image Segmentation for Myocardial Scar Detection using Multi-stage DeepLabV3+ Framework with Comparative Backbone Analysis. 2025 IEEE

International Conference on Artificial Intelligence in Engineering and Technology (IICAIET)

Zakaria, N. N., Osman, M. K., Sulaiman, S. N., Damit, D. S. A., Isa, N. A. M., Karim, N. K. A., & Hussain, Z. (2025, 22-23 Aug. 2025). Comparison of Image Enhancement and Sharpening Technique for Magnetic Resonance Image Quality Improvement. 2025 IEEE 15th International Conference on Control System, Computing and Engineering (ICCSCE)

JOURNAL

1. Nor Kamal, N. A. Z., Osman, M. K., Awang Damit, D. S., Sulaiman, S. N., Zakaria, N. U. N., Ahmad, K. A., & A Karim, N. K. (2026). Two-stage deep learning framework for myocardial infarction segmentation in late-gadolinium enhancement magnetic resonance imaging images. Journal of Electrical and Electronic Systems Research (JEESR), 28(1), 97-108
2. Zakaria, N. U. N., Osman, M. K., Sulaiman, S. N., Awang Damit, D. S., Isa, N. A. M., Hussain, Z., Nor Kamal, N. A. Z., & Karim, N. K. A. (2026). A hybrid contrast enhancement-image sharpening for improving visual quality scar in LGE-CMRI images. International Journal of Integrated Engineering. (Submitted for review)

LIST OF COPYRIGHT:

1. Automated Classification of Left Ventricle and Non-Left Ventricle Segment in Late Gadolinium Enhancement Cardiac MRI using Deep Convolutional Neural Network – No. LY2022P05193 (2022), Intellectual Property Corporation of Malaysia (MyIPO).
2. SCAR NET-MS: A Multi-Stage Magnetic Resonance Image Segmentation for Myocardial Scar Detection Using Deep Learning – No. CRLY2025P02133 (2025), Intellectual Property Corporation of Malaysia (MyIPO).